AN UPPER CARBONIFEROUS SHELF-TO-BASIN TRANSECT: NANSEN AND HARE FIORD FORMATIONS, NW ELLESMERE ISLAND

by

Colleen Sherry

A Thesis

Submitted to the School of Graduate Studies and Research

in Partial Fulfillment of the Requirements for the

Degree of Master of Science

in Geology

Ottawa-Carleton Geoscience Centre

Department of Geology

University of Ottawa

Ottawa, Ontario

ISBN 0-612-15673-7

UNIVERSITÉ D'OTTAWA
UNIVERSITY OF OTTAWA

ACKNOWLEDGMENTS

I would like to express my sincere gratitude to Dr. André Desrochers, my thesis supervisor, and to Dr. Benoît Beauchamp, the individual who introduced me to the Canadian Arctic . Their support and guidance both in the field and throughout the remainder of the study have been invaluable. Drs. Sylvie Pinard and Rui Lin are also thanked for providing comprehensive biostratigraphic information. I am also grateful to the following scientists, technicians and field assistants for their help: Pierre Bertrant, Karen Besemann, Lorraine Bloom, Frank Brunton, Greg Cain, George Dix, Owen Dixon, Debbie Guilfoyle, Edward Hearn, Charles Henderson, Carmen Lee, John Loop, Bernard Mamet, Ian McIlreath, Dale McInroy, George Mrazek, Pierrette Paroz, Stephan Ruest, Rémi Simard, Jean-François Tardif, Pierre Thériault and Vivianne Wasiuta. Last, but certainly not least, thanks to my friends and relatives for their encouragement, patience and understanding, especially through the tough times: Brian Eddie, Tim Grover, Melanie Kells, Kevin Kirley, Glen McCrimmon, Beata Olchowy, Sue Schaan, Donn Sherry, Kathleen Sherry, Madeleine Sherry, Natalie Sweet and Kevin Williams.

Financial and logistical field support was provided by the following organizations: American Association of Petroleum Geologists' Grant-in-Aid, Canadian Society of Petroleum Geologists' Graduate Scholarship in Petroleum Geology and Marine Geoscience, Geological Survey of Canada (Institute of Sedimentary and Petroleum Geology), Natural Sciences and Engineering Research Council of Canada (Grants to Dr. Desrochers), PanCanadian Petroleum Limited and Polar Continental Shelf Project.

ABSTRACT

An ancient transition from shallow marine platform to deep basin is preserved in the Upper Carboniferous strata of the Sverdrup Basin on northwestern Ellesmere Island. The shelf break is delineated by an approximately 200 km long discontinuous reef tract extending from Audhild Bay to the head of Hare Fiord within the Nansen Formation. The reef tract is marked by a series of massive, coalesced shelf edge buildups which developed during a major second order regression within the Sverdrup Basin. The shelf edge buildups are largely composed of phylloid alga-rich boundstones with abundant early marine synsedimentary cement. Fenestellid bryozoans, however, dominate buildups that grew in deeper slope settings. Shoreward of the reef tract lie cyclic, shallowing-upward carbonate shelf deposits, also of the Nansen Formation. The outer shelf deposits include bedded oolitic and foraminiferal grainstones representing a shallow water sand apron located immediately behind the reef tract. On the mid-shelf, small reefal buildups and shoals dominated commonly by a single taxon (i.e. chaetetids, beresellid algae, dasycladacean algae) occur sporadically within mixed crinoid-bryozoan, foraminiferal and peloidal deposits. Basinward of the shelf edge reef tract lie correlative slope-to-basin rhythmic mixed deposits of the Hare Fiord Formation. The upper slope deposits are dominated by fine grained calcisiltites while the lower slope/basin facies comprise calcisiltites, siltstones and shales interbedded with abundant turbidites and debrites.

The massive prograding shelf edge buildups reach stratigraphic thicknesses up to 1 km in the study area. The Nansen reef tract appears to be a reef complex in which the reefal rim, rather than being near sea level, remained relatively deeply submerged, but still within the photic zone, through much of its growth. Depth preference of the dominant reef builder (i.e. phylloid algae) was controlled by wave energy which inhibited vertical buildup to sea level. This extensive reef tract with a deep rim was an uncommon scenario in the geological record, especially during Late Carboniferous time when most buildups occurred as small mounds on slopes, ramps and inner parts of platforms.

The cyclic shelf deposits were strongly affected by fluctuating relative sea level within the Sverdrup Basin. The inner to mid-shelf was periodically exposed during relative sea level lowstands allowing some siliciclastic sediment influxes across the remaining submerged shelf. Otherwise the shelf maintained open marine conditions within the photic zone.

The rhythmic slope deposits also record the effects of fluctuating relative sea level but episodic deposits (turbidites and debris flows), along with the regressive nature of the succession, make more difficult the recognition of individual cycles. The upper slope was relatively steep and largely bypassed by gravity-displaced shelf sediment. As the incline decreased into the lower slope/basin region the gravity-flow sediments accumulated more readily, forming a base-of-slope apron.

The carbonate buildups on the shelf, shelf edge and slope all represent potential petroleum-bearing stratigraphic traps within the Sverdrup Basin. If these occur in the subsurface they would be likely exploration targets but unfortunately within the study area little porosity remains. Where the buildups are extensively dolomitized, higher porosity and permeability create excellent potential hydrocarbon reservoirs.

RÉSUMÉ

Le passage d'une ancienne plate-forme marine peu profonde à un bassin profond est bien exposé dans les strates du Carbonifère Supérieur dans le Bassin de Sverdrup au nord de l'Île d'Ellesmere. La marge de cette plate-forme est représentée par une étroite ceinture récifale qui se trouve à l'intérieur de la Formation de Nansen et qui s'étale sur une longeur d'environ 200 km dans la région d'étude entre la Baie Audhild et le fond du Hare Fiord. Cette ceinture est caractérisée par une série de constructions récifales massives et s'est developpée lors d'une régression majeure dans le Bassin de Sverdrup. Les constructions à la marge de la plate-forme sont principalement composées par des boundstones à algue phylloide possédant une abondante cimentation marine précoce. Des constructions récifales à fenestellidés sont aussi présentes mais on les retrouve que dans des milieux plus profonds comme sur la pente ou encore dans le bassin. À l'arrière de cette ceinture récifale, on retrouve des dépôts de la plate-forme externe et médiane lesquels font aussi partie de la Formation de Nansen. Les dépôts de la plate-forme externe comprennent surtout des grainstones bien lités à ooides et à foraminifères formant des haut-fonds sablonneux en eau peu profonde situés immédiatement à l'arrière de la ceinture récifale. Sur la plate-forme médiane, on trouve des dépôts mixtes de packstone-grainstone à bryozoaire et crinoide, à foraminifère, et à péloide parsemés de haut-fonds sablonneux ou de petites constructions récifales normalement dominées par un seul taxon (i.e. chaetetidés, béresillidés, dasycladacés). Au large de la ceinture récifale, on trouve les dépôts contemporains de milieu de pente à bassin de la Formation de Hare Fiord. Les dépôts de la pente proximale sont dominés par des calcisiltites tandis que les dépôts de pente plus distale comprennent des calcisiltites, des siltstones et des shales interlités avec des turbidites et des débrites calcaires.

Les constructions récifales forment un corps sédimentaire massif à nature progradante vers le bassin et atteingnent des épaisseurs jusqu'à 1 km dans la région d'étude. La ceinture récifale du Nansen était un complexe dont la bordure était toujours submergée à une assez grande profondeur mais tout en demeurant dans la zone photique.

La profondeur de croissance optimale pour les principaux constructeurs, soient les algues phylloides en forme de grands feuillets fragiles, était probablement controllée par l'hydrodynamisme du milieu lequelle pouvait arrêter leur croissance verticale vers la surface. La continuité de cette ceinture récifale est inhabituelle pour les constructions récifales datant de la fin du Carbonifère; une période au cours de laquelle les constructions récifales ont principalement formées de petits monticules en milieu de plate-forme interne ou encore en milieu plus profond sur la pente.

Les dépôts cycliques de plate-forme externe ont été modulées par des fluctutations relatives du niveau marin dans le Bassin de Sverdrup. En général, la plate-forme externe a maintenue des conditions marines ouvertes toujours à l'intérieur de la zone photique au cours de ces fluctuations relatives du niveau marin. Les plate-formes interne et médiane, cependant, ont été périodiquement exposées lors des bas niveaux marins permettant ainsi l'influx de sédiments siliciclastiques sur la plate-forme externe submergée.

Les sédiments déposés en milieu de pente ont aussi enregistrés les effets des fluctuations relatives du niveau marin avec en plus la déposition de sédiments à caractère épisodique comme des turbidites ou des débrites. La nature récessive de ces dépôts, cependant, rend plus difficile l'identification d'une cyclicité. La pente proximale était relativement abrupte et laissait passer les sédiments transportés par gravité et éventuellement accumulés vers le bas de la pente pour former un corps sédimentaire de bas de pente ("base-of-slope apron").

Les contructions récifales du Nansen, qu'elles se situent en milieu de plate-forme, marge de plate-forme, ou pente-bassin, représentent d'important pièges stratigraphiques à hydrocarbure dans le Bassin de Sverdrup. Lorsque ces constructions se retrouvent sous la surface, elles deviennent des cibles intéressantes pour l'exploration pétrolière. La porosité identifiée dans ces constructions, cependant, y est très faible et représente un facteur negatif à leur potentiel comme piège à hydrocarbure. Par contre, ces constructions représentent d'excellentes cibles où elles ont été dolomitisées car leur porosité-perméabilité y est grandement accrue.

TABLE OF CONTENTS

LIST OF TABLES

LIST OF FIGURES

LIST OF PLATES

CHAPTER 1: INTRODUCTION

1.1 Purpose and Objectives

The transition from continental platform to deep basin can be readily observed in the modern oceans. The various sediment types and the depositional relief inherent to this off-shore system are also apparent in recent deposits (Stanley and Moore, 1983). The shelf-slope break in a carbonate depositional system, as recognized by James and Mountjoy (1983), is the crucial element of the shelf anatomy, where facies record its evolution with time. At this narrow, and relatively elusive location, the most diverse community of organisms grows and the most rapid accretion takes place. In addition, it is likely to be the site of the most intense diagenetic processes and the most rewarding accumulations of hydrocarbon and mineral deposits (James and Mountjoy, 1983; Coniglio and Dix, 1992). This transition, and the numerous depositional environments present within it, have also been inferred in ancient rock successions. However, only a few localities display a complete ancient shelf-to-basin transition that can be identified by simple field observations, conducted in conjunction with detailed sedimentologic and stratigraphic analyses. In most field studies the shelf-slope break is interpreted rather than observed and information is synthesized based upon information from surrounding facies rather than from the shelf-break deposits themselves.

The Upper Carboniferous succession of the Sverdrup Basin is recognized as one of the best exposed in the world. Verification of this was provided by the rare opportunity to study an ancient shelf edge extending for approximately 200 km across northwestern Ellesmere and northern Axel Heiberg islands (Sherry et al., 1993). The shelf and shelf edge carbonates of the Nansen Formation and the mixed carbonate-siliciclastic slope-to-basin deposits of the Hare Fiord Formation are partly contained within this succession and have previously been identified by Arctic researchers (Thorsteinsson, 1974; Davies, 1977;

Beauchamp, 1987; Davies and Nassichuk, 1990). Few detailed studies, however, have been conducted in the northern areas of the basin. This study provides a unique opportunity to investigate a complete and continuous stratigraphic succession of which little is currently known and where exposure is exceptional, even for this region.

Northwestern Ellesmere Island (Figure 1) was the focus of this study not only because it is largely unexplored, but also because it displays some unusual and spectacular geologic features. The type sections of both the Nansen (Plate 1a) and the Hare Fiord formations are located within the study area. In addition, lateral facies changes between correlatable shelf and basin deposits are easily visible over short distances (Figure 2; Plate 1b). Finally, there is an elongate, massive carbonate deposit delineating the paleoshelf edge throughout much of the region.

The Nansen paleoshelf edge provides yet another unique window of opportunity to study the variations in reef complexes (e.g. reefs versus mounds) which have been recognized throughout the geological record (James and Bourque, 1992). The development of an extensive, shelf-edge tract of carbonate buildups is very unusual during the Late Carboniferous, a time period otherwise dominated by relatively fragile reef builders forming mainly small inner shelf biogenic mounds and deep water mud mounds. The elongate, well-indurated Nansen carbonate buildups thus appear to display attributes of both reef and mound development.

The present study focuses on the Upper Carboniferous Nansen and Hare Fiord formations on northwestern Ellesmere Island. The specific objectives of the study are:

1. To provide a more detailed stratigraphic framework for the study area.
2. To identify distinct lithofacies, and determine their spatial distribution.
3. To describe the various facies assemblages, and interpret their depositional environments and their early diagenetic features.
4. To describe the cyclic pattern of sedimentation, and determine its controlling mechanism.

Figure 1. Map of the Canadian Arctic Archipelago showing the general outline of the Upper Paleozoic to Tertiary Sverdrup Basin, and the location of the study area.

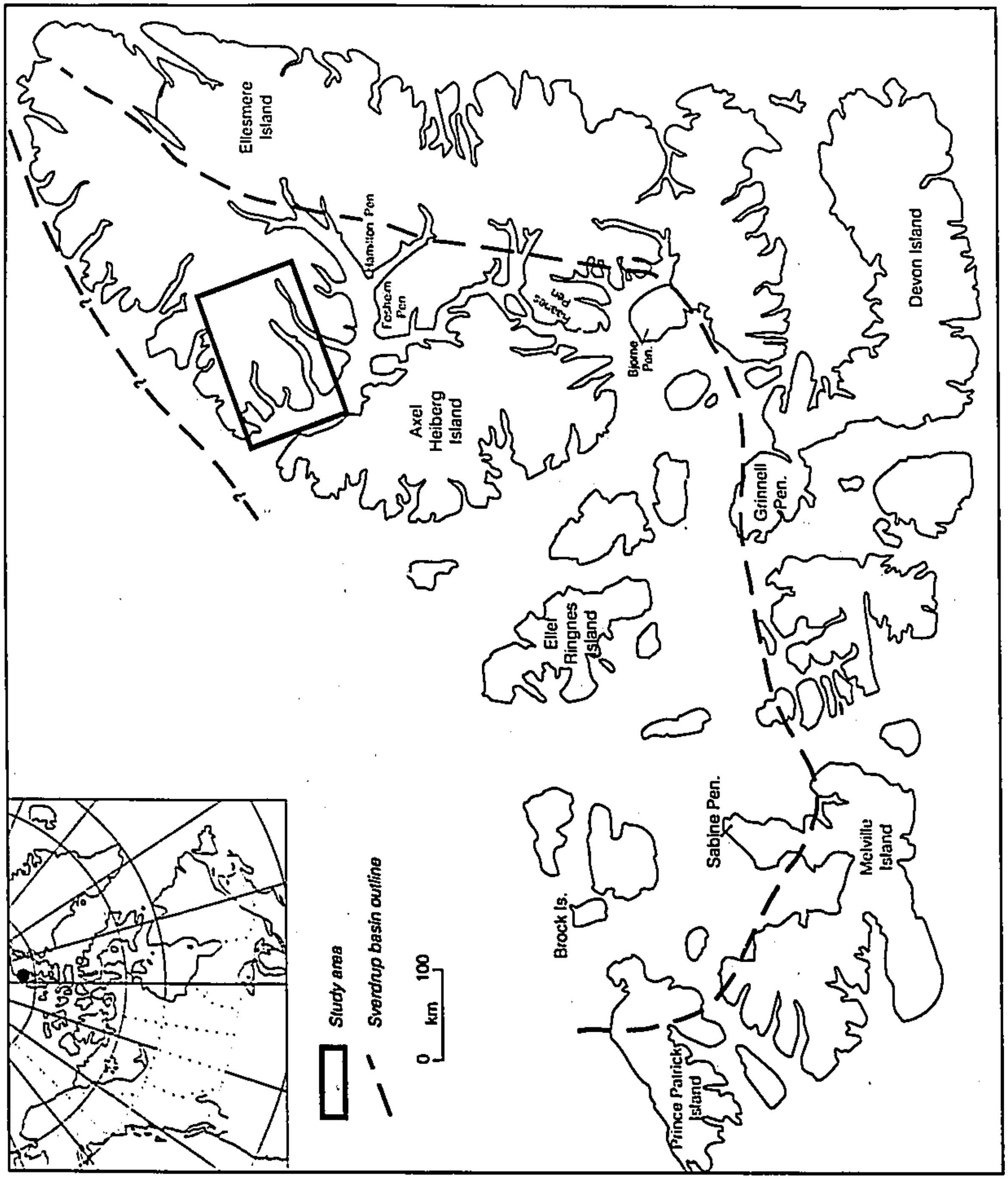
Ellesmere Island
Hamilton Pen
Fosheim Pen
Raanes Pen
Bjorne Pen.
Axel Heiberg Island
Devon Island
Grinnell Pen.
Ellef Ringnes Island
Sabine Pen.
Melville Island
Brock Is.
Prince Patrick Island
Study area
Sverdrup basin outline
0 km 100

Figure 2. Map of study area, northwestern Ellesmere Island (modified from Thorsteinsson, 1974; Maps 1305A and 1309A), showing measured sections, lines of cross-sections A-A' (Figures 5, 12 and 14) and B-B' (Figures 6, 13 and 15) and approximated position of maximum Nansen carbonate progradation (from field observations compiled in 1992). Sections 10 and 11 were measured and described by B. Beauchamp.

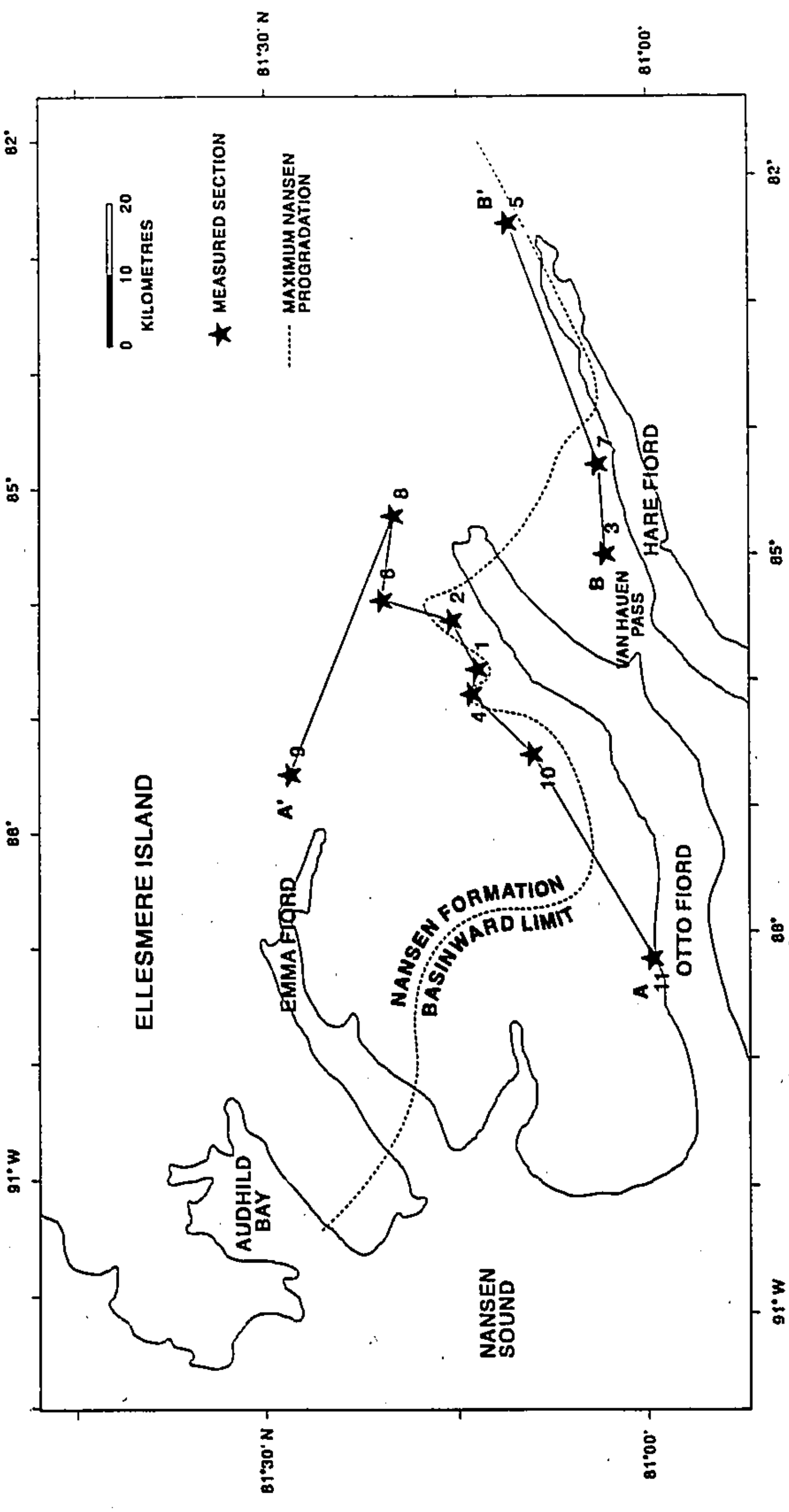

ELLESMERE ISLAND
EMMA FIORD
AUDHILD BAY
NANSEN SOUND
NANSEN FORMATION
BASINWARD LIMIT
OTTO FIORD
VAN HAUEN PASS
HARE FIORD
0 10 20
KILOMETRES
MEASURED SECTION
MAXIMUM NANSEN PROGRADATION
A
A'
B
B'
1
2
3
4
5
6
7
8
9
10
11
82°
85°
88°
91°W
81°30' N
81°00'

5. To reconstruct the paleogeography of the study area during Late Carboniferous time.

6. To provide a preliminary appraisal of the hydrocarbon potential of the studied formations.

This study complements that of previous workers (Thorsteinsson, 1974; Davies, 1977; Beauchamp, 1987; Davies and Nassichuk, 1990) and enhances the description and understanding of Upper Carboniferous Nansen shelf and shelf edge, and Hare Fiord slope deposits. The subsequent findings are of importance to the geological interpretation of both the Sverdrup Basin specifically and the circum-Arctic region in general.

1.2 Geologic Setting

1.2.1 Sverdrup Basin

The Sverdrup Basin is a 1000 km long and 400 km wide north-easterly trending intracratonic paleorift basin (Figure 1) located in the northernmost islands of the Canadian Arctic Archipelago (Fortier et al., 1963; Thorsteinsson, 1974; Ziegler, 1988). It originated during the Early Carboniferous through lithospheric extension and faulting (Figure 3) which resulted in the subsequent collapse of the underlying Precambrian to Devonian rocks of the Franklinian Mobile Belt (Thorsteinsson, 1974; Trettin, 1989; Beauchamp et al., 1989a).

Throughout its history, the Sverdrup Basin maintained an intracontinental position, with continental land masses occurring to both the north and south (Embry, 1992). Within the broad circum-Arctic paleogeography, it formed a narrow sigmoidal seaway that was part of an extensive rift system linking northern Alaska with north Greenland, Svalbard and the Barents Sea (Figure 4). The narrow straits connecting Sverdrup Basin waters with the global ocean system restricted circulation during major sea-level lowstands (Beauchamp et al., 1987).

Figure 3. Carboniferous and Permian stratigraphy in the Sverdrup Basin (from Beauchamp, 1994).

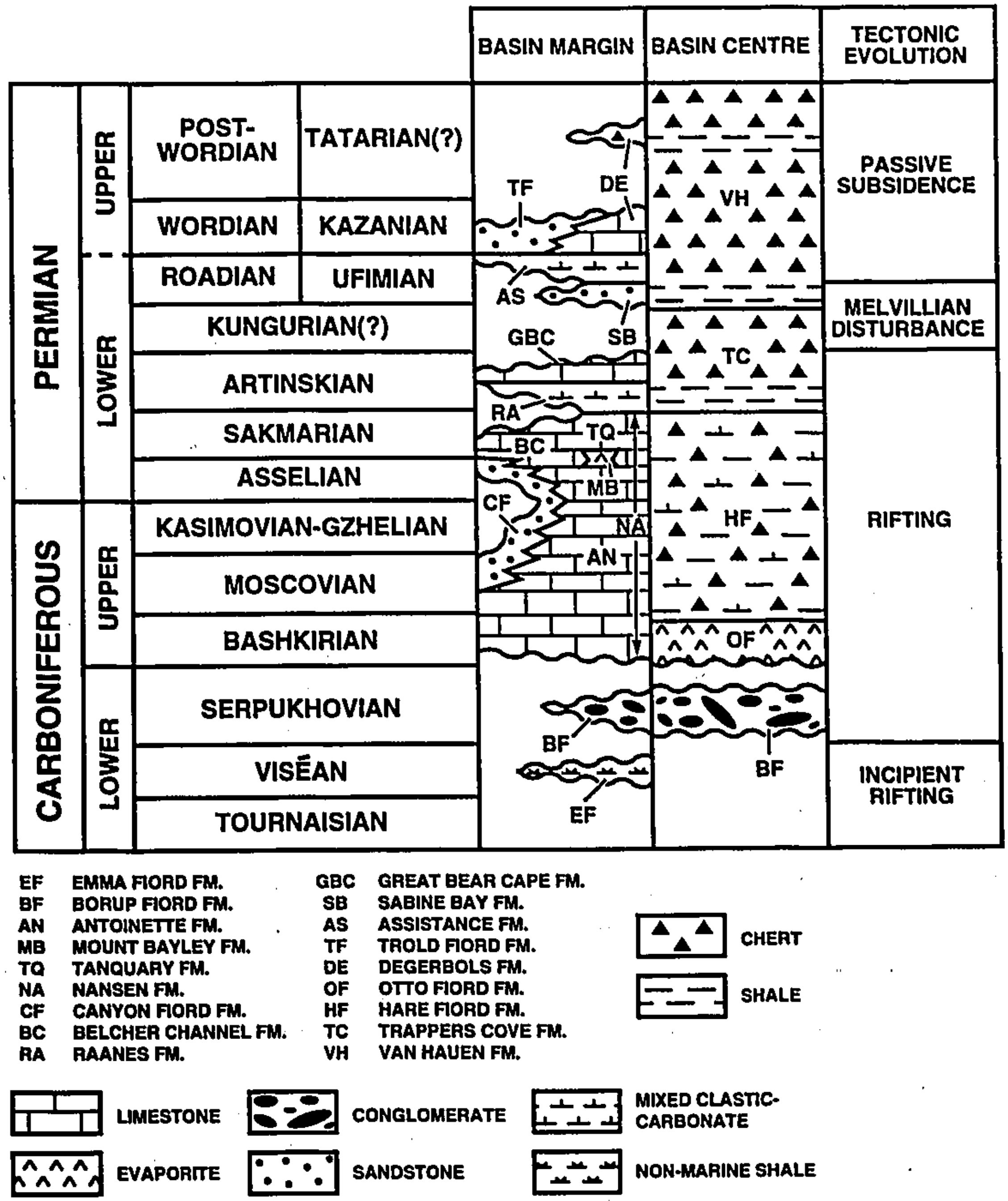
BASIN MARGIN
BASIN CENTRE
TECTONIC EVOLUTION
PERMIAN
UPPER
LOWER
CARBONIFEROUS
POST-WORDIAN
TATARIAN(?)
WORDIAN
KAZANIAN
ROADIAN
UFIMIAN
KUNGURIAN(?)
ARTINSKIAN
SAKMARIAN
ASSELIAN
KASIMOVIAN-GZHELIAN
MOSCOVIAN
BASHKIRIAN
SERPUKHOVIAN
VISÉAN
TOURNAISIAN
TF
DE
VH
AS
GBC
SB
TC
RA
TQ
BC
MB
CF
NA
AN
HF
OF
BF
EF
PASSIVE SUBSIDENCE
MELVILLIAN DISTURBANCE
RIFTING
INCIPIENT RIFTING
EF EMMA FIORD FM.
BF BORUP FIORD FM.
AN ANTOINETTE FM.
MB MOUNT BAYLEY FM.
TQ TANQUARY FM.
NA NANSEN FM.
CF CANYON FIORD FM.
BC BELCHER CHANNEL FM.
RA RAANES FM.
GBC GREAT BEAR CAPE FM.
SB SABINE BAY FM.
AS ASSISTANCE FM.
TF TROLD FIORD FM.
DE DEGERBOLS FM.
OF OTTO FIORD FM.
HF HARE FIORD FM.
TC TRAPPERS COVE FM.
VH VAN HAUEN FM.
CHERT
SHALE
LIMESTONE
CONGLOMERATE
MIXED CLASTIC-CARBONATE
EVAPORITE
SANDSTONE
NON-MARINE SHALE

Figure 4. Late Paleozoic circum-Arctic paleogeography showing relative positions of the Sverdrup Basin, northern Alaska (rotated), Svalbard and the Barents Sea (from Embry, 1992).

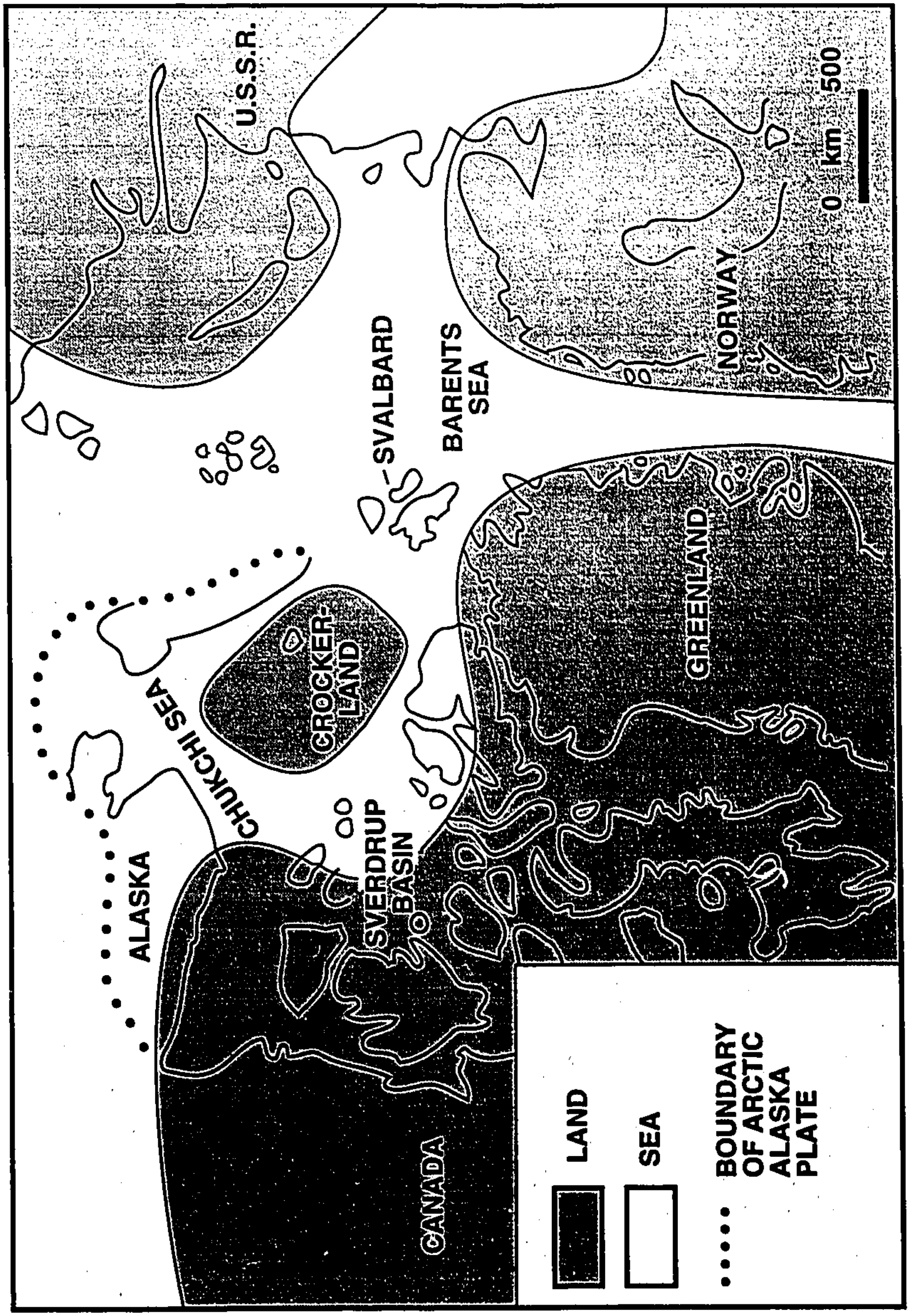
U.S.S.R.
SVALBARD
BARENTS SEA
NORWAY
0 km 500
GREENLAND
CROCKER-LAND
CHUKCHI SEA
ALASKA
SVERDRUP BASIN
CANADA
LAND
SEA
BOUNDARY OF ARCTIC ALASKA PLATE

Throughout the period of initial rifting and subsequent basement subsidence a thick succession of sediments and minor volcanics was deposited within the basin (Figure 3). Following a brief tectonic episode, known as the Melvillian Disturbance, a regime of passive subsidence prevailed across the Sverdrup Basin. Deposition terminated in the Tertiary with the culmination of the Eurekan Orogeny. This orogenic phase produced mountain ranges in the eastern Arctic through folding and faulting (the structural geometry of these faults precludes horizontal displacements of more than a few kilometres; Davies, 1977) of the Carboniferous to Tertiary strata contained within the Sverdrup Basin (Thorsteinsson, 1974; Trettin, 1989; Beauchamp et al., 1989a, b; Beauchamp, 1994). This tectonic activity resulted in the excellent exposure of Sverdrup Basin strata now observed on Ellesmere and Axel Heiberg Islands.

Sedimentological and paleontological observations have shown that the late Paleozoic climate of the Sverdrup Basin underwent a dramatic cooling trend. The climate evolved from tropical sub-humid in the Early Carboniferous, to tropical arid/semi-arid in the Late Carboniferous and Early Permian, to temperate sub-humid in the middle Permian, to sub-polar/polar in the latest Permian (Beauchamp et al., 1989a; Beauchamp, 1994). This climatic shift is in accord, to a limited degree, with that expected from plate tectonic reconstructions. It has been demonstrated that the Canadian High Arctic migrated from approximately 25°N in the Late Carboniferous, to 35-40°N or more in the Late Permian (Scotese et al., 1979; Smith et al., 1981). Although the paleolatitudinal shift would produce a cooling trend, it is insufficient in itself to result in the dramatic climatic deterioration experienced not only in the Sverdrup Basin but elsewhere throughout the circum-Arctic region (Ustritsky, 1973; Stemmerik and Worsley, 1989). The causes of this trend are still unknown but could be related to a long lasting change in the global pattern of oceanic and/or atmospheric circulation in the Northern Hemisphere (Beauchamp, 1994).

The Upper Carboniferous succession, consisting of portions of the Nansen and Hare Fiord formations, was deposited during tropical arid to semi-arid conditions, as evidenced by characteristic warm-water biotic constituents (e.g. calcareous algae, abundant and diverse foraminifera, and ooids). In addition, local marine evaporites and well developed red beds and caliche paleosols in laterally correlatable Canyon Fiord Formation deposits support the occurrence of such a climatic regime (Thériault, 1991; Thériault and Desrochers, 1993).

1.2.2 Upper Carboniferous Stratigraphy

The Upper Paleozoic sediments of the Sverdrup Basin are characterized by eight long term (5-50 Ma) transgressive-regressive sequences (Figure 3; Beauchamp and Henderson, 1994; Beauchamp, in press; Beauchamp et al., in press). Each sequence is bounded by significant unconformities at the basin margin that pass basinward into their respective correlatable conformities. The Upper Carboniferous sequence (Beauchamp, in press) comprises sedimentary deposits exceeding 1 km in thickness and is well exposed on northwestern Ellesmere Island.

Both the lower transgressive and upper regressive portions of the Upper Carboniferous sequence were deposited during active rifting early in Sverdrup Basin history (Figure 3). Evidence of recurring tectonic cycles indicates that rifting was not continuous but occurred in pulses, affecting sediment deposition and enhancing sedimentary cycle expression within each individual sequence (Beauchamp, 1993). The transgressive portion (Bashkirian) of the sequence is represented by the deposits of the Otto Fiord Formation and strata at the base of the Canyon Fiord, Antoinette, Nansen and Hare Fiord formations. The regressive portion (Moscovian-Kasimovian), of interest to this study, is represented by parts of the Canyon Fiord, Nansen and Hare Fiord formations. The Canyon Fiord Formation is present at the basin margin and is dominated by continental to nearshore clastic sediments (Thériault, 1991); the Nansen Formation represents the carbonate shelf and shelf edge deposits (Thorsteinsson, 1974; Sherry et al., 1993); the Hare Fiord Formation represents mixed carbonate-clastic slope to basin deposits (Davies, 1977; Sherry et al., 1993); and the Otto Fiord Formation is composed of interbedded anhydrite, limestone and sandstone, and is confined to the axis of the Sverdrup Basin (Davies and Nassichuk, 1975; Nassichuk and Davies, 1980).

1.3 Study Area

The study area is located on northwestern Ellesmere Island and extends from southeast of the head of Hare Fiord to northwest of Audhild Bay (Figure 2). Particular attention was paid to the region surrounding Otto Fiord and Hare Fiord.

The Nansen Formation is well exposed throughout the study area and in this region either conformably overlies the Upper Carboniferous Hare Fiord Formation or unconformably overlies the Lower Carboniferous Borup Fiord Formation. The type section is located near the head of Hare Fiord (section 5 of this study is adjacent to the type section; Plate 1a) and was first described by Thorsteinsson (1974).

The Hare Fiord Formation is well exposed between Hare Fiord and Otto Fiord, and along the western portion of the north shore of Otto Fiord. It conformably overlies the Otto Fiord Formation throughout the study area. The type section is located at Van Hauen Pass and was first described by Thorsteinsson (1974).

The study area is structurally complex (Harrison et al., in press). North- and northeasterly-trending folds, thrusts and strike-slip faults dominate the region. The rigid carbonates of the Nansen Formation form many cliffs and are largely undeformed. The mixed deposits of the Hare Fiord Formation often serve as a decoupling level within the thrust belts and are more often deformed.

1.4 Methods

Field work on northwestern Ellesmere Island was conducted during the summer of 1992. The field study was divided into two parts: 1) regional reconnaissance locating the extensive shelf edge reef tract (Figure 2); and 2) detailed outcrop measurements along an approximately north-south transect across the Nansen shelf and reefal shelf edge carbonates through the Hare Fiord slope-to-basin mudrocks.

A total of seven stratigraphic sections were measured, described, and closely sampled (Appendices 1 and 2). Nine sections were actually measured but two were later determined to contain sediments deposited outside the time frame of this particular study (sections 4 and 8). This represents more than 4500 m of measured strata from shelf, shelf edge and slope-to-basin environments. Approximately 500 samples were collected for petrographic (Appendices 2 and 3) and biostratigraphic analyses (Appendices 4 and 5). Polished hand samples (30) and standard petrographic thin sections (20 large and 400 standard) stained with Alizarin Red-S and potassium ferricyanide (Dickson, 1966) were produced for petrographic observations (Appendix 3). Small foraminifers were identified by Dr. Sylvie Pinard and fusulinaceans were identified by Dr. Rui Lin (Appendix 4), both at the Institute of Sedimentary and Petroleum Geology in Calgary (Geological Survey of Canada).

Regional reconnaissance was conducted by helicopter throughout the study area. Visual identification of shelf, shelf edge and slope/basin deposits was made based on their distinct field expressions. Locations of each were then recorded on a regional map (Figure 2).

CHAPTER 2: STRATIGRAPHY

2.1 Previous Work

Although preliminary regional studies of the Upper Paleozoic strata within the Sverdrup Basin were initiated early (Schei, 1903; Troelsen, 1950; Troelsen, 1952; Thorsteinsson and Tozer, 1957; Harker and Thorsteinsson, 1960; Fortier et al., 1963; Dawes and Christie; 1982), the first formal investigation of the stratigraphy of the Nansen and Hare Fiord formations was begun by Thorsteinsson (1974). As part of a regional mapping project conducted by the Geological Survey of Canada between 1956 and 1963, fourteen geological maps (1:250,000) were compiled along with a comprehensive report on the Carboniferous and Permian stratigraphy of Axel Heiberg and western Ellesmere Islands. The conceptual stratigraphic framework of the Upper Paleozoic designed by Thorsteinsson (1974) was based on the recognition of five stratigraphic sequences. The boundaries of these sequences were represented by basin-wide erosional unconformities. Each sequence was characterized by a specific set of formations and included: 1) a Lower Carboniferous nonmarine sequence; 2) an Upper Carboniferous to Lower Permian marine sequence; 3) a Lower Permian nonmarine sequence; 4) a Lower Permian marine sequence; and 5) an Upper Permian marine sequence.

The Upper Carboniferous to Lower Permian marine sequence was recognized by Thorsteinsson (1974) to be the thickest sequence in the Sverdrup Basin. It displays a complex lithological spectrum subdivided into five facies belts. Extending from northwest to southeast, these belts include: A) the Northwest Carbonate Belt; B) the Basinal Evaporitic and Clastic Belt; C) the Southeastern Carbonate Belt; D) the Marginal Clastic and Carbonate Belt; and E) the Marginal Clastic Belt.

The original stratigraphic framework proposed by Thorsteinsson (1974) was modified slightly by Nassichuk (1975a,b) and by Nassichuk and Wilde (1977) who worked mainly on southern Ellesmere Island. They suggested that rocks previously mapped as Nansen Formation in their area of interest could be subdivided into three distinct and mappable formations (i.e. Canyon Fiord, Belcher Channel and an unnamed formation).

Beauchamp et al. (1989a,b) substantially revised the Upper Paleozoic framework of the Sverdrup Basin and informally designated seven long term transgressive-regressive sequences bounded by major basin margin unconformities that pass basinward into their equivalent conformities. Each sequence comprised a complex association of facies ranging from basin margin fluvial and nearshore sandstones, to shelf carbonates and clastics, to slope and basin carbonates, shales, cherts and evaporites. The sequences were genetically related to four phases of tectonic evolution experienced by the Sverdrup Basin during its development: 1) thermal uplift; 2) rifting; 3) tectonism (Melvillian Disturbance); and 4) passive subsidence. The formations of interest to the present study (i.e. Upper Carboniferous portions of the Nansen and Hare Fiord formations) were shown to be contained within the Serpukhovian to Asselian sequence (Sequence 2), encompassing more than 50Ma of deposition. The sequence contains up to 1800 m of clastics, carbonates and evaporites (Borup Fiord, Otto Fiord, Hare Fiord, Nansen and Canyon Fiord formations), and minor volcanics (Audhild Formation). In smaller tectonically controlled subbasins within the main Sverdrup Basin the stratigraphy is more complex as the Nansen Formation is further subdivided based on lithologic variations (e.g. Antoinette, Mount Bayley and Tanquary formations).

Continued field investigations further constrained the detailed stratigraphy and sedimentology of the sequence boundaries within the basin. A recent revision to the stratigraphic framework (Beauchamp, 1994) characterized the Upper Paleozoic succession of the Sverdrup Basin as having eight long-term transgressive-regressive sequences (Figure 3) rather than seven, as formerly proposed. In this revision the formations of interest to the present study (i.e. Upper Carboniferous portions of the Nansen and Hare Fiord formations) occur within the Bashkirian to Kasimovian sequence (the third sequence) which encompasses a 20Ma time interval and contains up to 1500 m of sediments. It is represented by the marginal sandstones and conglomerates of the Canyon Fiord Formation, platform carbonates of the Nansen Formation, slope-to-basin argillaceous limestones, siltstones, shales and cherts of the Hare Fiord Formation, and evaporites of the Otto Fiord Formation.

The Bashkirian to Kasimovian sequence accumulated while active rifting occurred in the Sverdrup Basin (Figure 3). All low-order sequences deposited during this regime resulted from recurrent multi-phase tectonic cycles, represented by six distinct phases: 1) buckling; 2) flooding; 3) rifting; 4) drowning; 5) rebound; and 6) sagging (Beauchamp, 1993). The sagging phase of each sequence represents a variably long period of regional passive subsidence and usually accounts for the majority of sediments deposited within each sequence. During this phase an overall regressive succession was deposited in which carbonate and clastic shelf facies prograded toward the basin center. This study focuses mainly on the regressive Nansen and Hare Fiord sediments deposited during the sagging phase of the Bashkirian to Kasimovian sequence (Figures 5 and 6).

2.2 Lithostratigraphy

2.2.1 Nansen Formation

The Nansen Formation comprises a thick succession of carbonate with subordinate amounts of quartzose clastic sediments. After informally describing the formation (Thorsteinsson and Tozer, 1970), Thorsteinsson (1974) designated the type section along Girty Creek near the head of Hare Fiord on northwestern Ellesmere Island (adjacent to section 5 in Appendix 2; Figure 2; Plate 1a). At that locality, the Nansen Formation is more than 2300 m thick. It is underlain by conglomerates and sandstones of the Borup Fiord Formation and overlain by the Artinskian Esayoo volcanics. The age of the type Nansen ranges from Bashkirian to Sakmarian, and possibly Artinskian.

Figure 5. Lithostratigraphic cross-section A-A' across the western portion of the study area. Sections 10 and 11 were measured and described by B. Beauchamp.

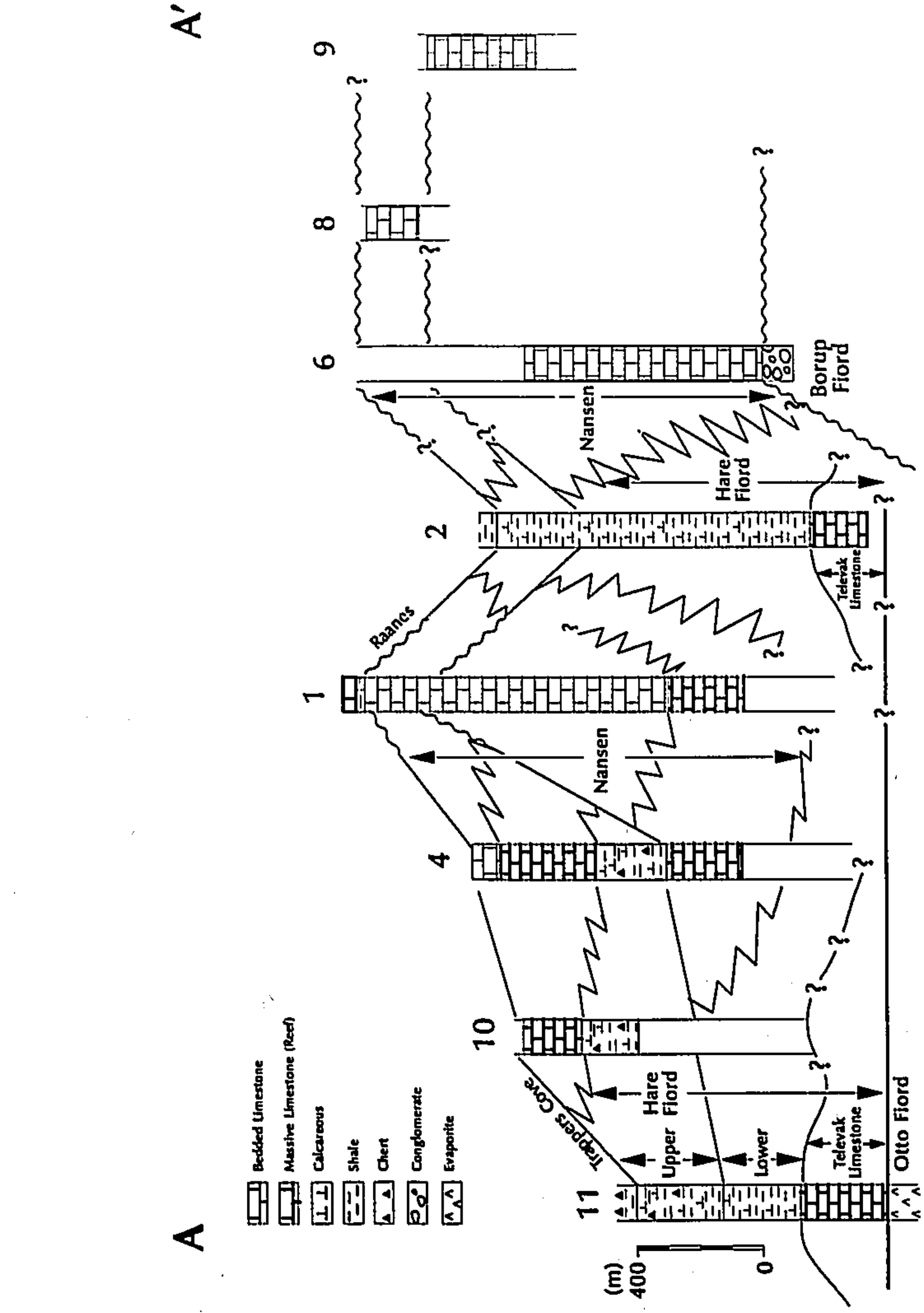
A
A′
Bedded Limestone
Massive Limestone (Reef)
Calcareous
Shale
Chert
Conglomerate
Evaporite
(m)
400
0
11
10
4
1
2
6
8
9
Trappers Cove
Upper
Lower
Hare Fiord
Televak Limestone
Otto Fiord
Nansen
Raanes
Borup Fiord

Figure 6. Lithostratigraphic cross-section B-B' across the eastern portion of the study area.

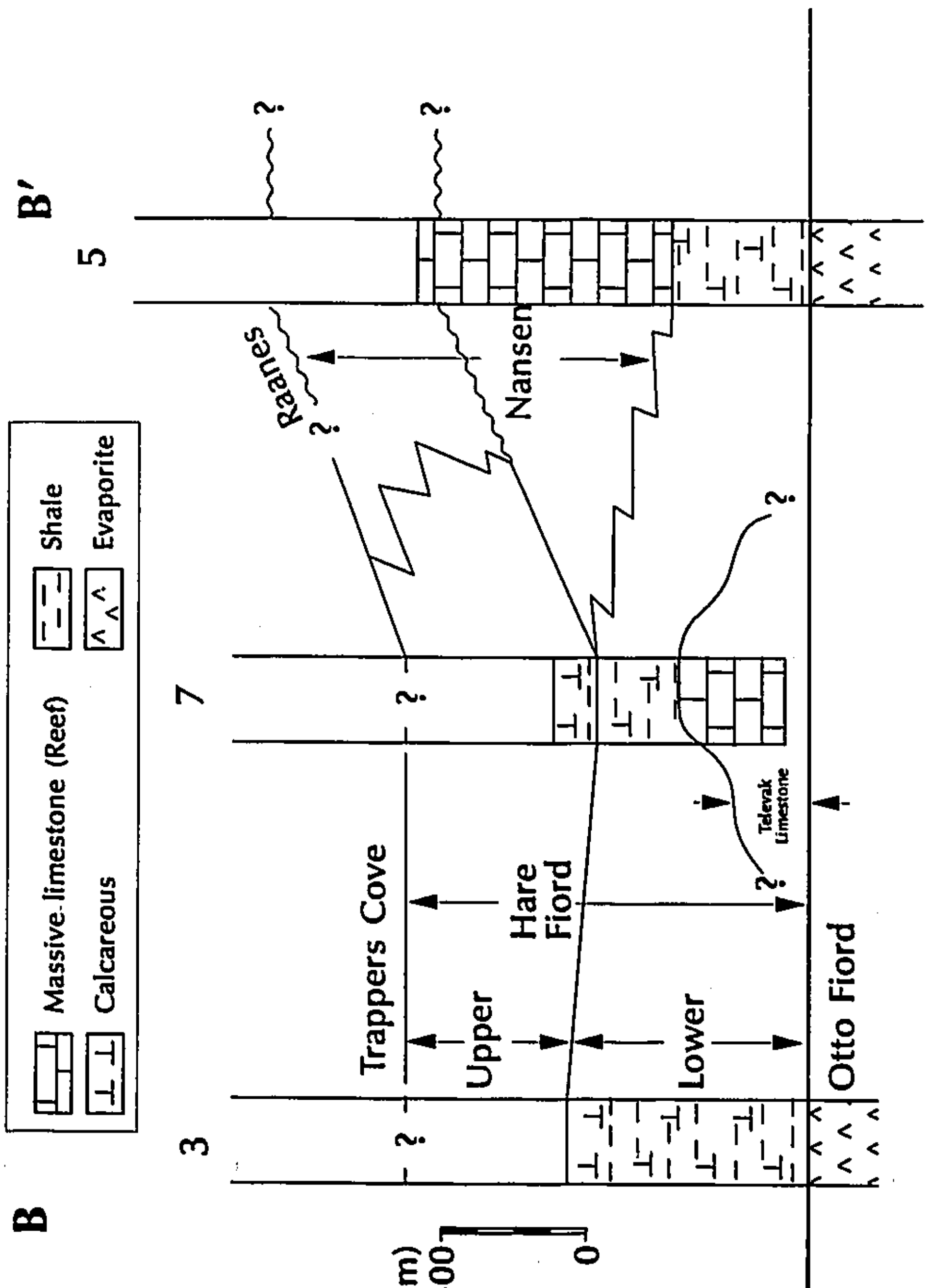

B
B′
3
7
5
(m)
400
0
Massive-limestone (Reef)
Calcareous
Shale
Evaporite
Trappers Cove
Upper
Lower
Hare Fiord
Otto Fiord
Raanes
Nansen
Tolevak Limestone
?

Thorsteinsson (1974) determined that the Nansen Formation outcrops in two broad belts within the Sverdrup Basin: 1) the Northwestern Carbonate Belt, a 100 km wide exposure belt extending along northwestern Axel Heiberg and Ellesmere Islands; and 2) the Southeastern Carbonate Belt, a narrower (25 km) exposure belt on western Ellesmere Island. The thickness of the formation varies greatly across the Sverdrup Basin, largely due to truncation by Eurekan structures. Complete exposures range in thickness from approximately 700 m at the northwest extremities of Ellesmere Island to greater than 2300 m at the type section. The type section is believed to represent the maximum thickness value for the Nansen Formation.

The formation is characterized by a wide variety of carbonate-dominated lithologies. It ranges from finely crystalline, slightly fossiliferous limestone to biogenic limestones with a granular texture. The field expression also varies between two distinct profiles: 1) bedded, with alternating recessive and resistant units (shelf deposits); and 2) massive and resistant (shelf edge deposits). In each case the Nansen carbonate weathers to a light grey or yellowish-grey while the fresh surface is light to medium grey.

High-frequency depositional cycles within the shelf deposits are defined by the recurrence of facies and are expressed in the field as alternating resistant and recessive units (Figure 7) of varying thickness (3 to 33 m). The resistant units of each individual cycle are composed of thickly bedded packstone or grainstone to rarely boundstone while the recessive units are thinner bedded wackestone to packstone. The entire cycle is formed of subtidal facies but displays a shallowing upward trend. The vertical facies variation is accompanied by a net decrease in the proportions of clay or fine-silt clastic admixtures and an increase in grain size. The cycle composition varies throughout the formation within the study area.

The massive carbonate buildups are dominated by boundstones with associated grainstones (Figure 8). Primary reef builders comprise either phylloid algae (associated with *Palaeoaplysina* in Permian deposits), or beresellid algae, or dasycladacean algae, or

Figure 7. Representative shallowing-upward shelf cycle (section 9, 28.5-44.5 m). Note general vertical trends in composition and texture. (Line thicknesses denote relative size and abundance.)

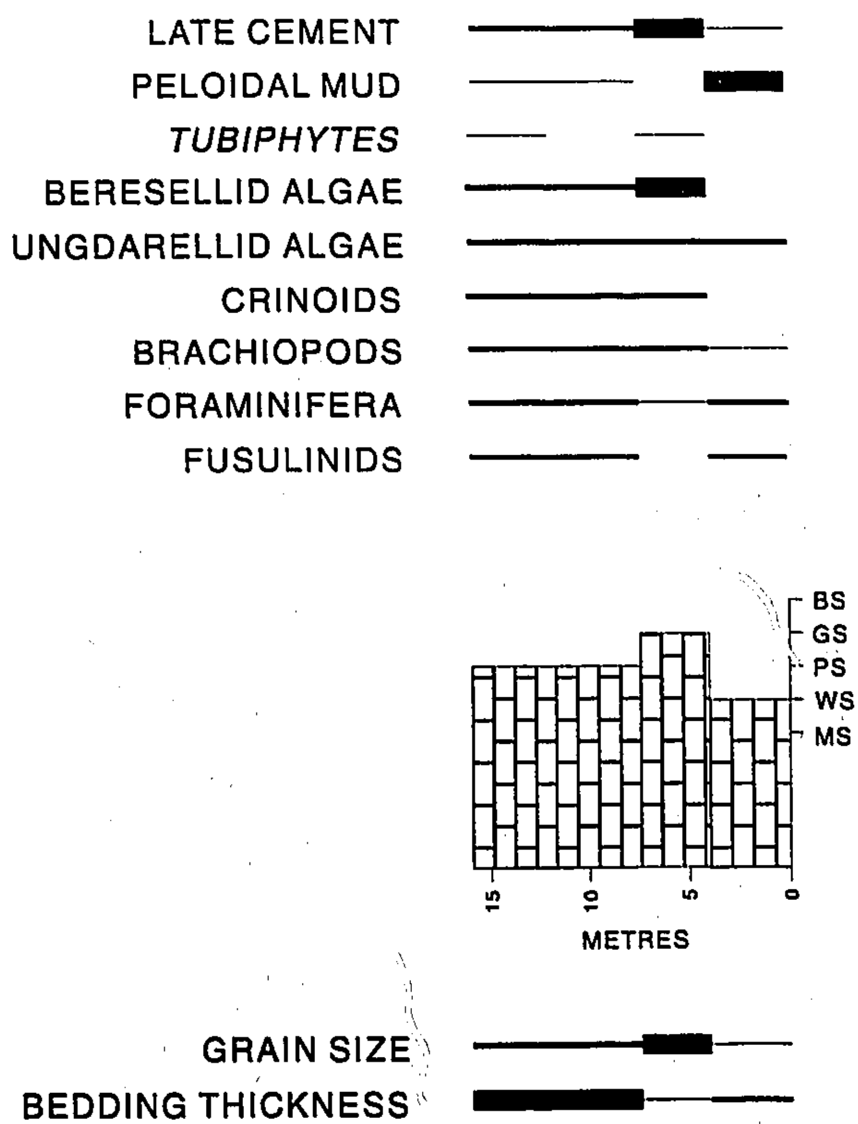
LATE CEMENT
PELOIDAL MUD
TUBIPHYTES
BERESELLID ALGAE
UNGDARELLID ALGAE
CRINOIDS
BRACHIOPODS
FORAMINIFERA
FUSULINIDS
BS
GS
PS
WS
MS
15
10
5
0
METRES
GRAIN SIZE
BEDDING THICKNESS

Figure 8. Representative non-cyclic shelf edge succession (section 1, 417.5-444.5 m). Massive mounds consist of a patchwork of variable compositions and textures rather than a noticeable vertical trend. (Line thicknesses denote relative size and abundance.)

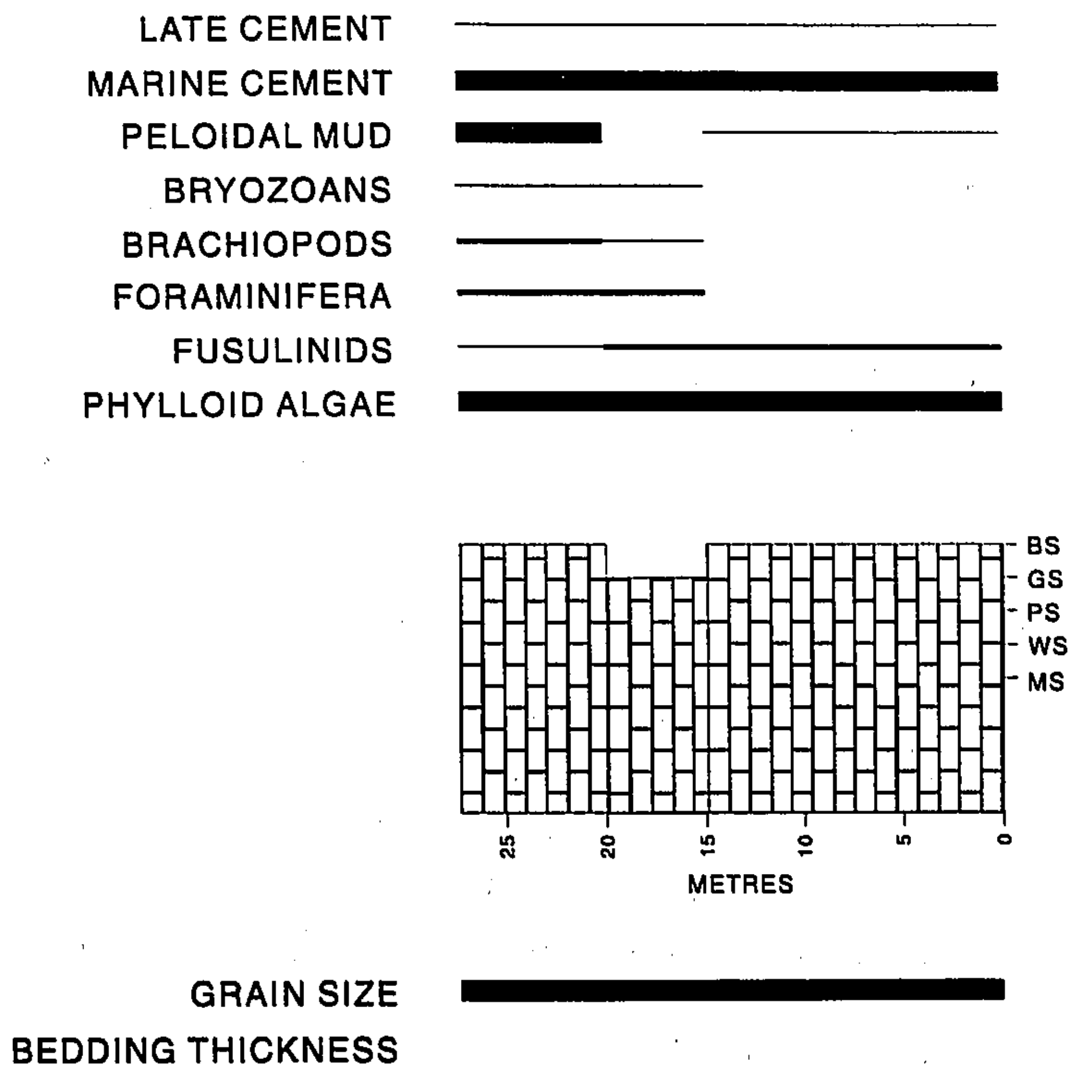
LATE CEMENT
MARINE CEMENT
PELOIDAL MUD
BRYOZOANS
BRACHIOPODS
FORAMINIFERA
FUSULINIDS
PHYLLOID ALGAE
BS
GS
PS
WS
MS
25
20
15
10
5
0
METRES
GRAIN SIZE
BEDDING THICKNESS

chaetetids, or bryozoans, all mutually exclusive. The phylloid algal reefs dominate at the shelf edge where numerous individual buildups coalesce to form large (up to 1000 m thick), massive deposits. Bryozoans, mainly fenestellids and branching forms, also occurred near the shelf edge but actually developed on the upper slope below the phylloid algal buildups. As the bryozoan mounds grew upwards through the water column they were replaced by phylloid algae which dominated at the shallower depth. Beresellids, dasycladaceans and chaetetids occur in shelf deposits and often form the capping unit of shallowing upward shelf cycles. Abundant and diverse biota occur in association with these framebuilders. Extensive early marine cements occur in most buildups, especially those of the shelf edge and upper slope environments.

The Nansen Formation is correlative with the Otto Fiord and Hare Fiord formations, which occupy axial regions of the Sverdrup Basin (Thorsteinsson, 1974; Davies, 1977). In southern areas the Nansen passes into the Marginal Clastic and Carbonate Belt which comprises either a combination of two formations, the Canyon Fiord and overlying Belcher Channel, or a combination of four formations which are, in ascending order, the Canyon Fiord, Antoinette, Mount Bayley and Tanquary (Figure 3). The transition from the Nansen to the Canyon Fiord and Mount Bayley formations involves a lithologic change. The Antoinette, Tanquary and Belcher Channel formations are lithologically similar to the Nansen and are separated from it by arbitrary boundaries (Thorsteinsson, 1974).

In the present study, Nansen Formation sediments deposited during Moscovian to Kasimovian time are of interest (Figures 5, 6 and 9). Four sections were measured (Appendix 2), including both shelf and shelf edge deposits: a) shelf: section 6 (244 m) and section 9 (390.5 m); and b) shelf and shelf edge: section 1 (843 m; Plate 1c); and c) shelf edge: section 5 (1141 m - complete; Plate 1a).

Figure 9. Idealized shelf-to-basin cross section indicating lithology of the Moscovian-Kasimovian portions of the Nansen and Hare Fiord formations (locations of measured sections transposed onto N-S transect). The current study was conducted on the regressive portion of the low order depositional sequence. The carbonate mound is contained within the lower transgressive portion of the sequence. The clastic shoreline facies is assumed and was never observed in the field.

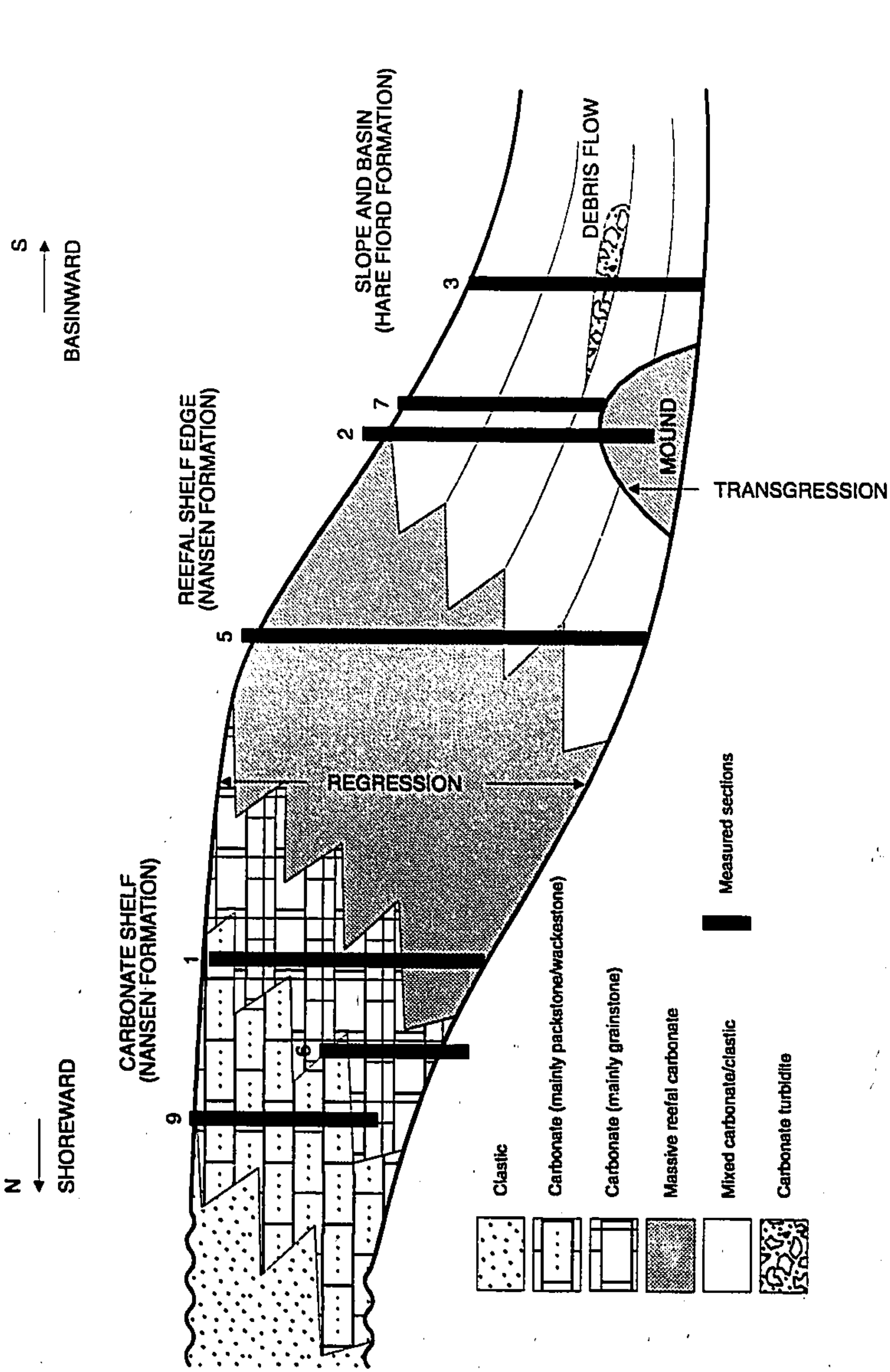
N
SHOREWARD
S
BASINWARD
CARBONATE SHELF
(NANSEN FORMATION)
REEFAL SHELF EDGE
(NANSEN FORMATION)
SLOPE AND BASIN
(HARE FIORD FORMATION)
DEBRIS FLOW
MOUND
TRANSGRESSION
REGRESSION
9
6
1
5
2
7
3
Clastic
Carbonate (mainly packstone/wackestone)
Carbonate (mainly grainstone)
Massive reefal carbonate
Mixed carbonate/clastic
Carbonate turbidite
Measured sections

2.2.2 Hare Fiord Formation

The Hare Fiord Formation is composed of interbedded quartzose siltstone, shale, and argillaceous and dolomitic limestone, with lesser amounts of chert and quartzose sandstone. It was first informally described by Thorsteinsson and Tozer (1970). The type section was designated by Thorsteinsson (1974) along the north side of Hare Fiord, northeast of Van Hauen Pass (Figure 2). At this locality, the Hare Fiord Formation is approximately 760 m thick. It is underlain by Otto Fiord mixed carbonates and evaporites, and disconformably overlain by the Van Hauen Formation. The Hare Fiord Formation is considered to range in age from early Moscovian to Sakmarian.

The Hare Fiord Formation outcrops in the environs of Hare Fiord and Nansen Sound on northwestern Ellesmere Island and on eastern Axel Heiberg Island. It was considered by Thorsteinsson (1974) to form part of the Basinal Clastic and Evaporitic Belt of the Sverdrup Basin. Its thickness varies from 300 to 1250 m across the basin.

The formation is characterized by both carbonate and mixed carbonate-clastic deposits (Figure 9). The proportions of the lithologic types vary throughout the basin. Siltstone, shale and minor sandstone are variably calcareous, argillaceous and siliceous. The limestone occurs in three distinct forms, either as bedded, finely crystalline, unfossiliferous deposits, or as bedded, coarse, bioclastic deposits, or alternatively as massive buildups. The chert can occur as bedded deposits or as nodules and irregular masses distributed in the limestone. Throughout the basin the Hare Fiord Formation appears as a rhythmic, medium grey to dark grey and rarely brown, relatively recessive unit.

The formation is characterized by high-order depositional cycles of various thicknesses (5.5 to 57 m). The cycles appear as alternating recessive and relatively resistant units (Figure 10; Plate 2c). The recessive units are dominated by shales and argillaceous limestones while the resistant units comprise thin to thickly bedded limestone and siltstone with abundant chert. Interbedded within the resistant portions are thin to

Figure 10. Representative shallowing-upward slope cycle (section 2, 357.5-417.5 m). This upper slope deposit is dominated by a wackestone facies with a relatively recessive base and episodic packstone and grainstone deposits throughout. This package could represent amalgamated multiple cycles not apparent in the field. (Line thicknesses denote relative size and abundance.)

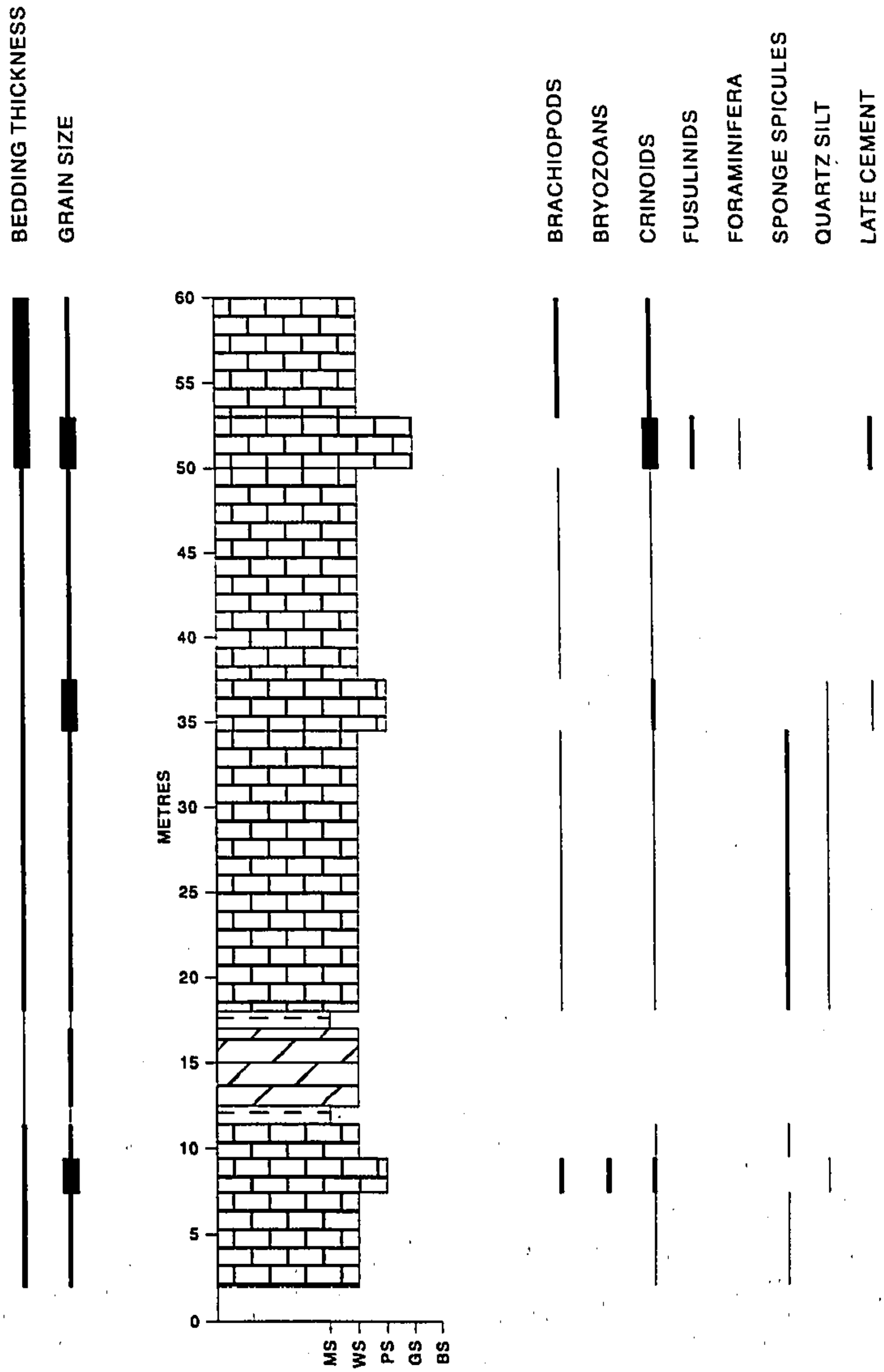
BEDDING THICKNESS
GRAIN SIZE
BRACHIOPODS
BRYOZOANS
CRINOIDS
FUSULINIDS
FORAMINIFERA
SPONGE SPICULES
QUARTZ SILT
LATE CEMENT
METRES
0
5
10
15
20
25
30
35
40
45
50
55
60
MS
WS
PS
GS
BS

medium bedded, coarser grained, graded bioclastic carbonate units. At intervals, massive carbonate debrites can also be seen. Cyclic deposits have a deep water character and display a shallowing upward trend.

Massive carbonate buildups (informally designated as the Televak Limestone; Bonham-Carter, 1966; Plate 2d) occur in the basal portion of the Hare Fiord Formation. They appear sporadically throughout the basin and range in thickness from several metres to as much as 460 m (Bonham-Carter, 1966; Thorsteinsson, 1974; Davies et al., 1988; Besemann, 1993; Brunton et al., 1993). These mounds are dominated by bryozoans and are pervasively cemented by early marine fibrous calcite. They appear lighter coloured than the surrounding sediments which onlap the mound flanks.

The Hare Fiord Formation is a lateral facies equivalent of the Nansen Formation. The facies boundary was arbitrarily established at the change from dark coloured, mixed carbonate-clastic rocks, to light coloured, dominantly carbonate rocks (Thorsteinsson, 1974).

In the present study Hare Fiord Formation strata deposited during the Moscovian to Kasimovian interval is of primary interest (Figures 5, 6 and 9). Sections measured include sediments from slope to basin environments (Appendix 2): section 2 (764 m; Plate 2b), section 3 (693 m; Plate 2a), section 5 (394 m; Plate 1a) and section 7 (354 m; Plate 2d).

2.3 Biostratigraphy

Measured sections of the Nansen and Hare Fiord formations were correlated in this study using generic and specific determinations of two fossil groups (Figure 11 and Appendix 4): small foraminifers (Sylvie Pinard, pers. comm. 1993-94) and fusulinaceans (Rui Lin, pers. comm. 1993-94). Each of the fossil groups was used to group the strata into zones based on biotic assemblages, as well as first appearances, last appearances and

Figure 11. Biostratigraphic correlation chart based on small foraminifera (Pinard, 1990) and fusulinaceans (Harker and Thorsteinsson, 1960; Nassichuk and Wilde, 1977; Nassichuk and Bamber, 1978; Lin et al., 1991; Groves et al., 1994) of the Sverdrup Basin. This study focuses on Moscovian and Kasimovian strata.

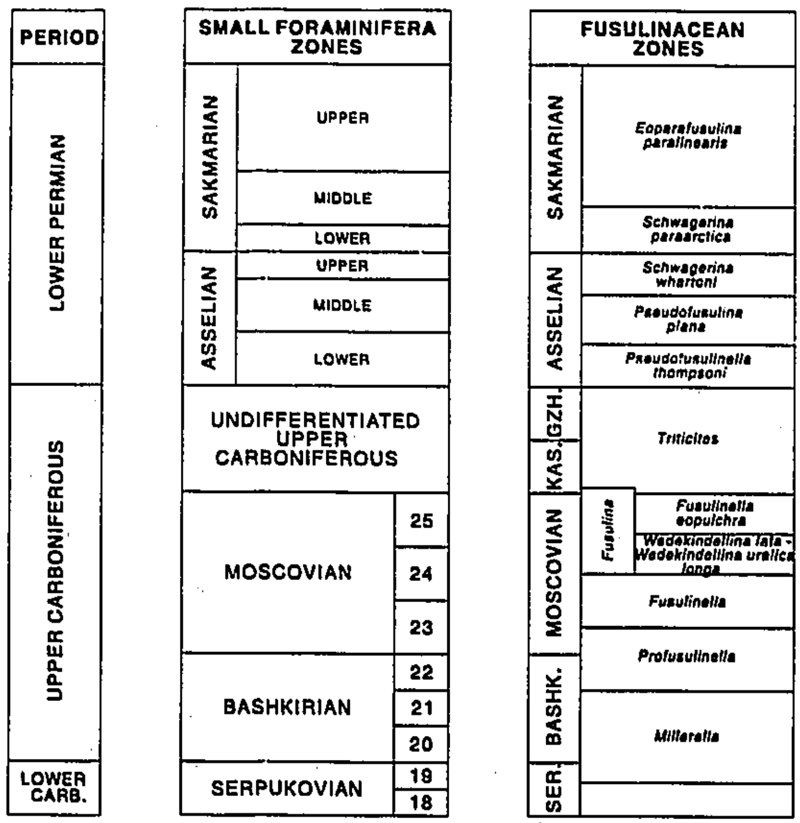
PERIOD
LOWER PERMIAN
UPPER CARBONIFEROUS
LOWER CARB.
SMALL FORAMINIFERA ZONES
SAKMARIAN
UPPER
MIDDLE
LOWER
ASSELIAN
UPPER
MIDDLE
LOWER
UNDIFFERENTIATED UPPER CARBONIFEROUS
MOSCOVIAN
25
24
23
BASHKIRIAN
22
21
20
SERPUKOVIAN
19
18
FUSULINACEAN ZONES
SAKMARIAN
Eoparafusulina paralinearis
Schwagerina paraarctica
ASSELIAN
Schwagerina whartoni
Pseudofusulina plana
Pseudofusulinella thompsoni
GZH.
KAS.
Triticites
MOSCOVIAN
Fusulina
Fusulinella eopulchra
Wedekindellina lata - Wedekindellina uralica longa
Fusulinella
Profusulinella
BASHK.
Millerella
SER.

single occurrences of specific index fossils (Harker and Thorsteinsson; 1960; Nassichuk and Wilde, 1977; Nassichuk and Bamber, 1978; Pinard, 1990; Lin et al., 1991; Groves et al., 1994). Distribution of these zones in measured sections is independent of local facies variations (Figures 12 and 13).

This study focuses on two Late Carboniferous chronostratigraphic stages, Moscovian and Kasimovian. Also recognized within the studied formations were strata of possible Bashkirian and Gzhelian (Carboniferous), and of Asselian and Sakmarian (Permian) age.

Main small foraminifer genera used for age determination included: a) Moscovian - *Asselodiscus*, *Bradyina*, *Climacammina*, *Globivalvulina*, *Glomospiroides*, *Hemidiscus*, *Mediocris*, thick Palaeotextulariidae, *Syzrania*, and *Turrispiroides*; and b) Kasimovian - *Hemigordius*, *Nodosinelloides*, and *Protonodosaria*. Main fusulinacean genera used for age determination included: a) Moscovian - *Beedeina*, *Fusulinella*, *Millerella*, *Neostafella*, *Ozawainella*, *Pseudostaffella*, and *Wedekindellina*; and b) Kasimovian - *Pseudofusulinella*.

2.4 Sequence Stratigraphy

Within the study area the lowermost portions of the Nansen and Hare Fiord formations and the entire Otto Fiord Formation form a low order transgressive-regressive (T-R) sequence of Bashkirian to Kasimovian age (Figures 14 and 15). The overlying Nansen and Hare Fiord formations belong to an overlying lower Permian T-R sequence.

2.4.1 Late Carboniferous Sequence

Lower Sequence Boundary

The basal sequence boundary is marked by an erosional unconformity between the Borup Fiord Formation below and either the Nansen Formation (shoreward) or the Otto

Figure 12. Biostratigraphic cross-section A-A' across the western portion of the study area illustrating the extent of foraminifera and fusulinacean biostratigraphic information available for correlation. Sections 10 and 11 were measured and described by B. Beauchamp. (A - Asselian; G - Gzhelian; K - Kasimovian; M - Moscovian; ? - questionable)

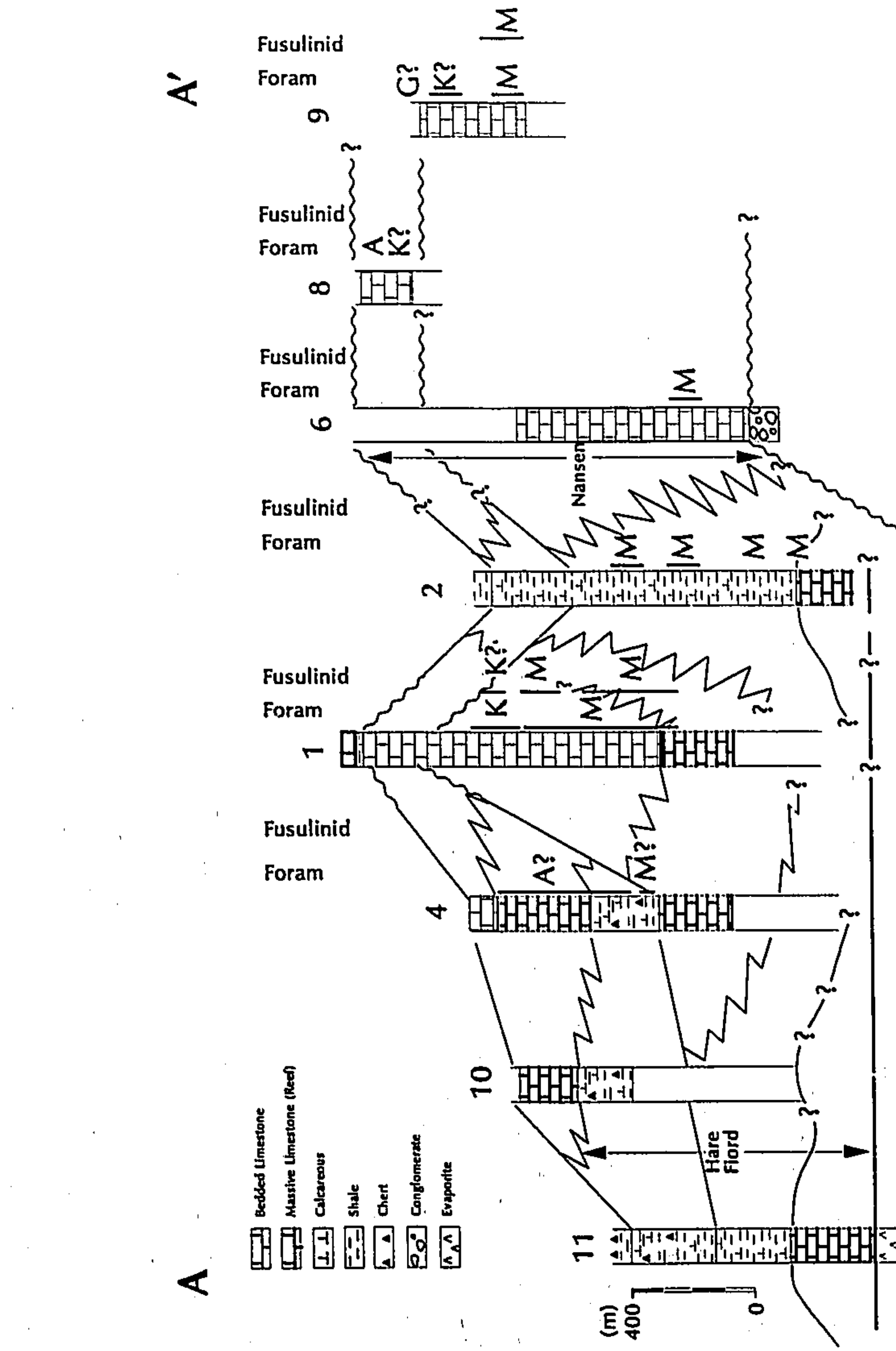
A
A′
Bedded Limestone
Massive Limestone (Reef)
Calcareous
Shale
Chert
Conglomerate
Evaporite
(m)
400
0
11
10
4
1
2
6
8
9
Fusulinid
Foram
Hare Fiord
Nansen

Figure 13. Biostratigraphic cross-section B-B' across the eastern portion of the study area illustrating the extent of foraminifera and fusulinacean biostratigraphic information available for correlation. Sections 10 and 11 were measured and described by B. Beauchamp. (S - Sakmarian; A - Asselian; G - Gzhelian; K - Kasimovian; M - Moscovian; ? - questionable)

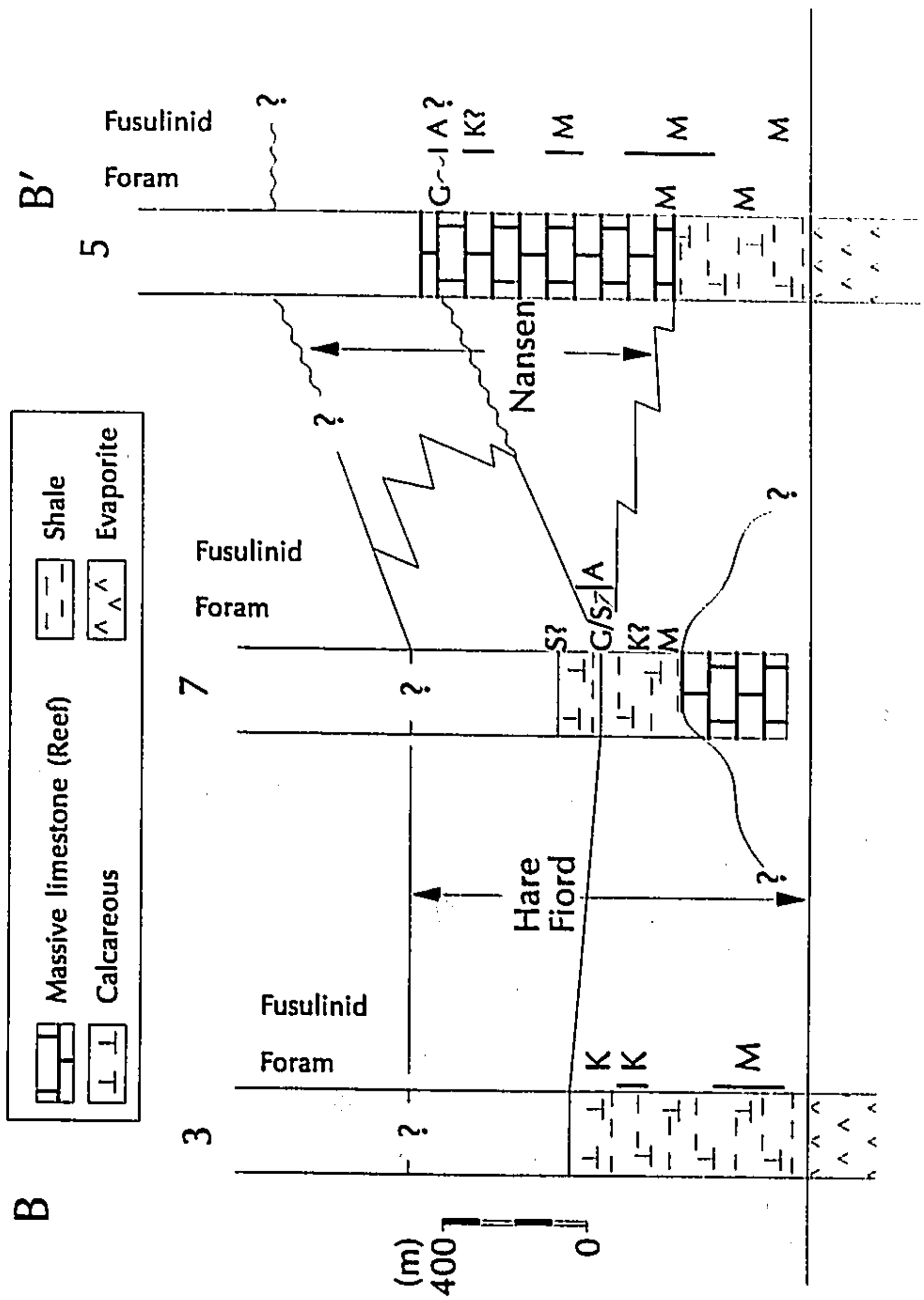
B
B′
3
7
5
Fusulinid
Foram
Massive limestone (Reef)
Calcareous
Shale
Evaporite
Hare Fiord
Nansen
(m)
400
0

Figure 14. Sequence stratigraphic cross-section A-A' across the western portion of the study area. Sections 10 and 11 were measured and described by B. Beauchamp. (SB - sequence boundary; MFS - maximum flooding surface; T - transgressive package; R - regressive package)

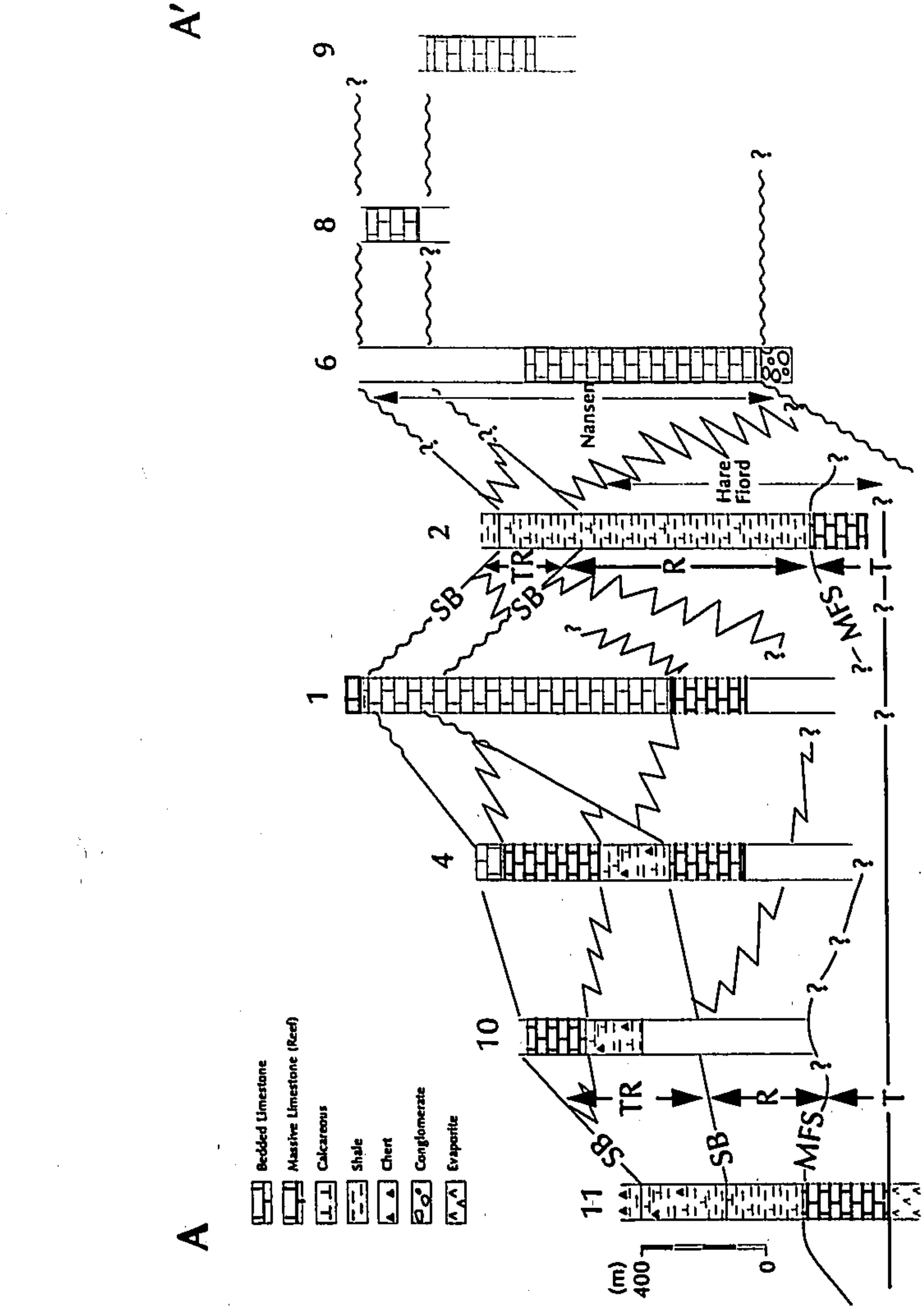
A
A′
Bedded Limestone
Massive Limestone (Reef)
Calcareous
Shale
Chert
Conglomerate
Evaporite
(m)
400
0
11
10
4
1
2
6
8
9
SB
TR
R
T
MFS
Nansen
Hare
Fiord

Figure 15. Sequence stratigraphic cross-section B-B' across the eastern portion of the study area. (SB - sequence boundary; MFS - maximum flooding surface; T - transgressive package; R - regressive package)

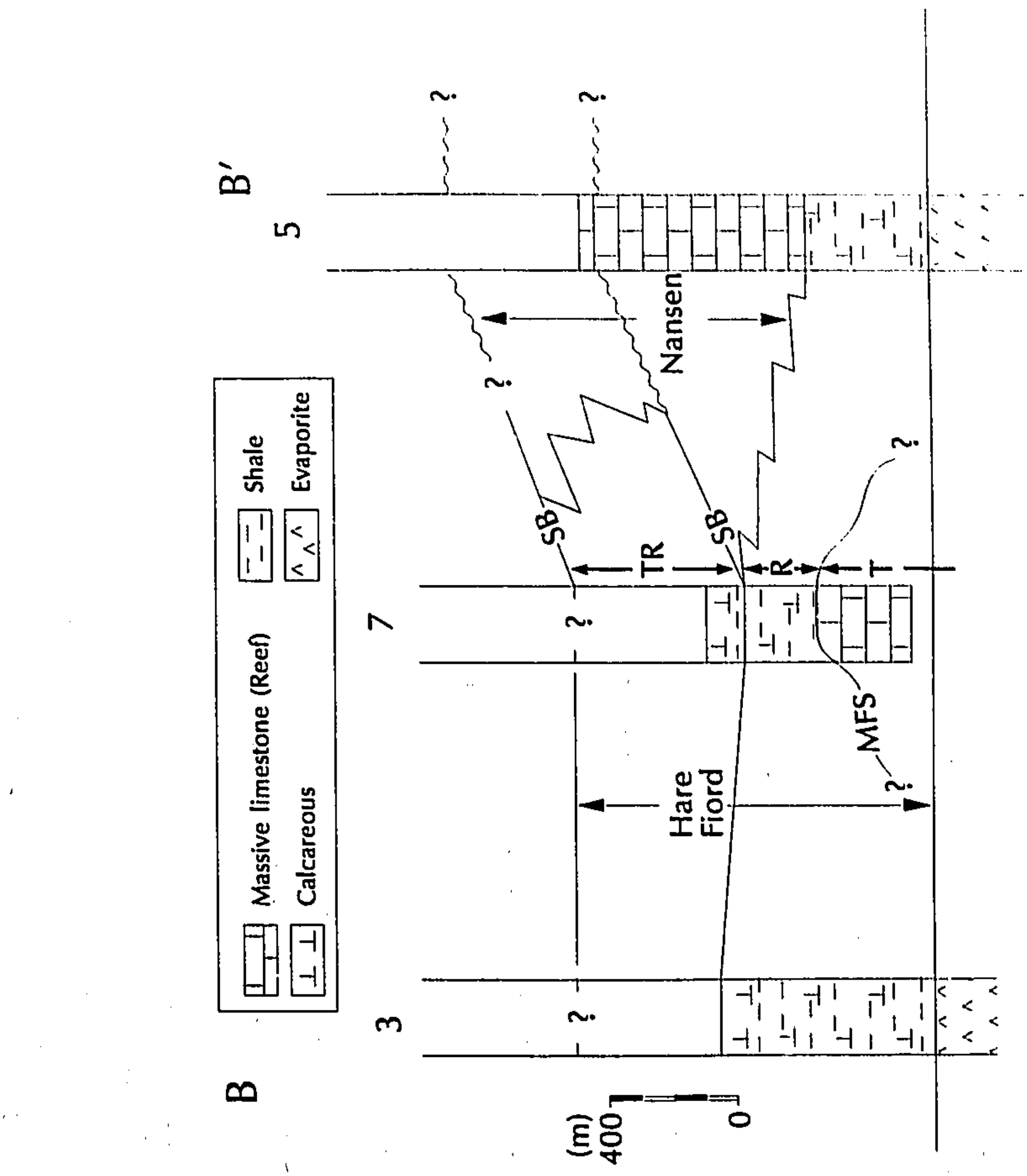

B
B′
3
7
5
(m)
400
0
Massive limestone (Reef)
Calcareous
Shale
Evaporite
Hare Fiord
Nansen
SB
SB
TR
R
T
MFS
?

Fiord Formation (basinward) above. The sequence boundary coincides with the lithostratigraphic contact between the noted formations and describes a transition from continental clastic deposition to fully marine carbonates and evaporites.

Upper Sequence Boundary

The upper sequence boundary is a localized subaerial unconformity that lies within the Nansen Formation (most notably at Section 1; Plate 1c). The succession beneath the erosion surface is a shallowing upward, coarsening upward package culminating in a very coarse grained crinoidal limestone. The erosional surface itself is marked by soil-derived red and green clays. Above this the sediments are again fully marine in origin.

The upper sequence boundary becomes a conformable surface where exposure did not occur. Terra rosa surfaces developed only on localized paleohighs on the Nansen shelf.

In the more distal areas the boundary can be traced in the correlative basin facies of the Hare Fiord Formation. The succession below the sequence boundary is a thickening and shallowing upward, relatively shale-free, fine grained carbonate. The deposits above the sequence boundary are thinner bedded and increasingly shaly.

Maximum Flooding Surface

In proximal areas the maximum flooding surface lies within the Nansen Formation. It is marked by the deepest water shelf facies above which the shelf facies backstep. In the more distal areas the maximum flooding surface is marked by the lithostratigraphic boundary between the Hare Fiord Formation above and either the Otto Fiord Formation or the Televak limestones of the Hare Fiord Formation below.

Transgressive Systems Tract

The stratigraphic succession between the lower sequence boundary and the maximum flooding surface is the Transgressive Systems Tract. It is represented by the lowermost Nansen and Otto Fiord formations.

Regressive Systems Tract

The stratigraphic succession between the maximum flooding surface and the upper sequence boundary is the Regressive Systems Tract. This systems tract is represented by shallowing upward, progradational shelf and shelf edge carbonates of the Nansen Formation and laterally equivalent slope and basin deposits of fine grained carbonates, silts and shales of the Hare Fiord Formation.

2.4.2 Early Permian Sequence

Lower Sequence Boundary

The basal sequence boundary is the upper sequence boundary of the underlying Late Carboniferous Sequence. It is represented by a localized subaerial unconformity within the Nansen Formation and its correlative basin conformity within the Hare Fiord Formation.

Upper Sequence Boundary

The upper sequence boundary is a subaerial unconformity within the uppermost Nansen Formation. It is marked by thin layers of terra rosa paleosol clay (Kells et al., in press). It may also coincide with the lithostratigraphic contact between the Great Bear Cape and underlying Nansen formations. The unconformity becomes a correlative conformity towards the basin centre. The upper sequence boundary then occurs within the uppermost Hare Fiord Formation (Kells et al., in press).

Maximum Flooding Surface

In proximal areas the maximum flooding surface lies within the Nansen Formation and locally is visible as the contact with the Mount Bayley Formation evaporites. In distal areas the surface lies within the Hare Fiord Formation.

Transgressive Systems Tract

The stratigraphic succession between the lower sequence boundary and the maximum flooding surface is the Transgressive Systems Tract. It is represented by a portion of the upper Nansen (and Antoinette) and Hare Fiord formations.

Regressive Systems Tract

The stratigraphic succession between the maximum flooding surface and the upper sequence boundary is the Regressive Systems Tract. This systems tract is represented by the uppermost Nansen (and Tanquary) and Hare Fiord formations and the entire Mount Bayley Formation.

CHAPTER 3: SEDIMENTOLOGY

The Upper Carboniferous Nansen Formation comprises distinct shelf and shelf edge facies assemblages while the coeval Hare Fiord Formation contains sediments representing a slope-to-basin facies assemblage. These three facies assemblages (for a summary see Table 1) are easily identified in the field by their unique field expressions (Plates 1 and 2) produced by distinct lithologies, high frequency cycles and stratal geometries. In addition, facies are defined on the basis of microfacies characteristics (Flügel, 1982) such as grain composition and texture (Figure 16), in combination with megascopic features such as bedding, sedimentary structures, colour and bioturbation.

Fourteen carbonate and mixed carbonate-siliciclastic facies are recognized in the Moscovian-Kasimovian parts of the Nansen and Hare Fiord formations on northwestern Ellesmere Island. The determination and description of these facies is not an end in itself but is rather a means to an end. The facies are intended to depict petrology in terms that reflect patterns and environments of deposition. The goal is to recreate and to picture the organic and physical earth during the Late Carboniferous in the Sverdrup Basin (see Chapter 4).

3.1 Shelf Assemblage

The shelf assemblage is exposed north of Otto Fiord (Figures 2 and 3), at sections 1, 6, and 9 (Appendix 2). It is composed of seven distinct lithofacies (for a summary see Table 2): 1) Crinoid-Bryozoan Facies; 2) Foraminiferal Facies; 3) Peloidal Facies; 4) Oolitic Facies; 5) Chaetetid Facies; 6) Beresellid Facies; and 7) Dasycladacean Facies. The shelf assemblage is dominated by light-coloured, well-bedded, cyclic carbonates with sporadic occurrences of small, massive biogenic mounds.

Table 1. Facies Assemblages.

Assemblage	Facies	Cycle/Geometry	Interpretation
Shelf	Crinoid-Bryozoan Foraminiferal Peloidal Oolitic Chaetetid Beresellid Dasycladacean	resistant cyclic - shallowing upward packages (3 to 33 m thick)	open marine conditions moderate to high energy within photic zone
Shelf Edge	Phylloid Algal Bryozoan	resistant massive - coalesced mounds	open marine conditions moderate energy below active wave base
Slope/Basin	Calcisiltite Siltstone Shale Calcarenite Debrite	recessive cyclic - shallowing upward packages (5.5 to 57 m thick)	open marine conditions low energy deep water episodic event sedimentation

Figure 16. Microfacies attributes of carbonate facies. Variations in abundance of allochem grains and in texture are provided for shelf, shelf edge and slope/basin deposits.

- rare
— present
■ abundant

		FACIES													
		SHELF							SHELF EDGE		SLOPE/BASIN				
		Crinoid-Bryozoan	Foraminiferal	Peloidal	Oolitic	Chaetetid	Beresellid	Dasycladacean	Phylloid Algal	Bryozoan	Calcisiltite	Siltstone	Shale	Calcarenite	Debrite
MAIN BIOTIC AND ABIOTIC ELEMENTS	brachiopod	—	—	-	-	—	-		—	—	—	-		—	—
	echinoderm	■	—	-	—	—			—	■	—	-		■	—
	fenestellid bryozoan	■	—	-	-	-				■	—			■	—
	ramose bryozoan	■		-		-	-			—				■	—
	fusulinid	—	■	—	—	—	—	-	—					■	—
	small foram	—	■	—	—	—	—	—	—	-	-			—	—
	encrusting foram	-	■	—			—	—	—	—					
	Tubiphytes		—	-		-	—	—	—	—					
	fasciellid algae		-	-	-		-	-							
	phylloid algae		—	-	—				■						-
	dasycladacean algae		—		-			■	-						
	beresellid algae		-	-	-	—	■		-						
	ungdarellid algae		-	-	-	—	—		—						
	chaetetid					■									
	ostracode			—	-			-	-						
	gastropod	-		-	-	-			-	-				-	-
	solitary coral	-												-	-
	colonial coral	-	-											-	-
	sponge spicule										—	-		—	
	calcisphere	-		-							—	-		—	
	ooid				■										
	coated grain				■										
	peloid	—	-	■	-		-	—	—	-				—	—
	micritized grain		-	■	—										
	intraclast	-		-	-									—	—
	silt	—			-					-	—	■		—	-
	marine cement	-	—	—	—		-	■	■	■					—
DEPOSITIONAL TEXTURES	boundstone					■	—		■	■					
	grainstone	—	—		■		—	■	■	—				■	
	packstone	■	■	■										■	■
	wackestone		-	-							■	—			
	mudstone										—	■	■		

Table 2. Facies of the Shelf Assemblage.

Facies Designation	Crinoid-Bryozoan Facies	Foraminiferal Facies	Peloidal Facies	Oolitic Facies	Chaetetid Facies	Beresellid Facies	Dasycladacean Facies
Bedding and Sedimentary Structures	well bedded	well bedded bioturbated	well bedded	cross bedded	small, massive biostrome	small, massive biostrome	massive biostrome
Rock Type	packstone to grainstone	packstone-grainstone to wackestone	packstone to wackestone	grainstone	boundstone	boundstone to grainstone	grainstone
Major Grain Types	crinoids, fenestellid and ramose bryozoans	forams, fusulinids	peloids, micritized grains	ooids, coated grains	chaetetids	beresellid algae	dasycladacean algae
Minor Grain Types	fusulinids, forams, brachiopods, peloids, silt	bryozoans, brachiopods, *Tubiphytes*, phylloid and dasycladacean algae	fusulinids, forams, ostracodes	phylloid algae, fusulinids, forams, crinoids, micritized grains	brachiopods, crinoids, fusulinids, forams, beresellid and ungdarellid algae	fusulinids, forams, *Tubiphytes*, ungdarellid algae	forams, *Tubiphytes*, peloids
Main Diagenetic Features	late sparry calcite cement	early isopachous fibrous cement late sparry calcite cement	early isopachous fibrous cement late sparry calcite cement	early isopachous fibrous cement micrite dissolution voids neomorphosed grains	dolomite silica late sparry calcite cement	early isopachous fibrous cement late sparry calcite cement	early isopachous fibrous cement dissolution voids
Depositional Environment	mid- to outer shelf open marine shallow to moderate depths	mid- to outer shelf open marine moderate to high energy	mid-shelf and shelf edge low energy	outer shelf high energy shoal shallow water	patch reefs on shelf shallow water	patch reefs on mid-shelf at fair weather wave base	small shoal complexes on shelf relatively high energy

Shelf cycles range in thickness from 3 to 33 m and comprise a recessive-resistant couplet whose lithologic content varies gradationally upward (Figure 7). The lithologic spectrum of each cycle varies both vertically and laterally throughout the study area. Vertically each cycle displays a general shallowing upward and coarsening upward trend characterized by the transition from relatively mud-rich carbonates at the base (wackestone to packstone) to well-winnowed carbonate (grainstone to boundstone) at the top. This trend is also commonly accompanied by an increase in the diversity and abundance of biotic and abiotic carbonate elements, an increase in bedding thickness, and a transition towards a more resistant outcrop profile. Laterally cycles generally become more grainstone-rich towards the shelf edge.

Shelf cycles are laterally continuous and well-bedded. They are easily visible at the outcrop scale. Biogenic mounds are scattered throughout the shelf deposits and are dominated by small, biostromal units occurring near the upper boundaries of shelf cycles.

3.1.1 Crinoid-Bryozoan Facies

Description

The Crinoid-Bryozoan Facies (Plate 3a, b) is a well-bedded packstone to grainstone unit dominated by echinoderms and fenestrate bryozoans with abundant ramose bryozoans. Brachiopods, small foraminifers and fusulinids are also present along with rare gastropods, solitary rugosans and syringoporids. Shells are commonly fragmented but display little evidence of sorting or abrasion. Internal structure has commonly been removed by bioturbation. Peloids and quartz silt are locally abundant. Sparry calcite cement occludes porosity.

The Crinoid-Bryozoan Facies is relatively abundant on the shelf at a distance from the shelf edge (especially section 9) and is less common near the shelf edge (e.g. section 6). It occurs dominantly in the lower to mid-portions of shelf cycles (as packstone) and is commonly found in close vertical association with the mid-shelf Peloidal Facies (see below).

Interpretation

The Crinoid-Bryozoan Facies was deposited in an open marine, mid- to outer-shelf setting in shallow to moderate water depths, below fair weather wave base. Similar facies dominated by bryozoans and containing abundant crinoids have been recognized by Beauchamp (1987) and Morin (1992) in the Sverdrup Basin. Marcantel (1975) also recognized a similar facies in Late Carboniferous to Early Permian deposits of northeastern Nevada and interpreted them to represent quiet water deposition of shallow to moderate shelf depths on soft but firm, nonmobile substrates. Similar biotic assemblages occur in both modern and ancient cool water shelf carbonates but in warm water settings, such as those of the Late Carboniferous Sverdrup Basin, these biota dominate in deeper and cooler water shelf environments (Nelson, 1978).

Crinoid-dominated grainstones containing abundant quartz silt occur at the top of some high frequency cycles (e.g. section 1). Shell fragments in these grainstones are relatively well sorted and commonly abraded indicating a higher energy level, above fair-weather wave base, than is normally represented by the Crinoid-Bryozoan Facies. The grainstones are locally stained and occur as discontinuous red terra rosa-like horizons that represent short-lived paleoexposure surfaces. These represent a transgressive facies.

3.1.2 Foraminiferal Facies

Description

The Foraminiferal Facies (Plate 3c-e) is characterized in outcrop by a variably well-bedded, bioturbated packstone-grainstone to rare wackestone dominated by a diverse foraminiferal assemblage, containing abundant paleotextulariids, tetrataxids, globivalvulinids, and fusulinids, with locally abundant bradyinids and encrusting forms (apterinellids and tuberitinids). Associated biota include crinoids, fenestrate bryozoans, brachiopods, syringoporids, ammonoids and ungdarellid, beresellid, dasycladacean and phylloid algae. Micritized grains of unknown origin also occur. Early submarine fibrous calcite cement is locally present especially where phylloid algae occurs. Vadose silts locally fill intergranular porosity along with rare sparry calcite cement.

The Foraminiferal Facies dominates the shelf environment within the study area. It is most common at a distance from the shelf edge (e.g. section 9) but also occurs proximal to the shelf edge (e.g. sections 1 and 6). In the latter location the grainstone subfacies dominates and occurs in association with Oolitic and Phylloid Facies grainstones. The facies occurs most commonly in the mid- to upper portions of individual shelf cycles.

Interpretation

The Foraminiferal Facies represents sediments deposited within open marine conditions across the Nansen shelf below fair weather wave base but within the photic zone (e.g. sections 6 and 9). In Upper Pennsylvanian and Lower Permian sediments of Nevada Marcantel (1975) recognized a similar facies and interpreted it to represent deposits of normal salinity, open marine shelf conditions affected by local currents but with insufficient water energy to remove fine grained material. The abundance of fusulinids also indicates an offshore open-water environment (Thompson, 1964). Where encrusting forams are abundant, this is interpreted as relatively restricted marine conditions (Beauchamp, 1987; Morin et al., 1994; Pl. 3d).

Foraminiferal grainstones associated with other high energy deposits (Oolitic and Phylloid Algal facies; e.g. section 5), indicate a higher energy depositional environment on the outer shelf.

3.1.3 Peloidal Facies

Description

The Peloidal Facies (Plate 3f) comprises well-bedded packstone to rare wackestone containing abundant silt to fine sand-sized peloids and an ubiquitous fossil assemblage. Peloids are dominantly elongate, subangular to subrounded, and average 0.1 mm in size. Although some are fecal pellets (Flügel, 1982) many are more irregular in shape suggesting an origin as either fragments of micritized allochems, or algae or small intraclasts (Tucker and Wright, 1990).

A variety of small foraminifera are common, including: globivalvulinids, endothyrids, pseudoendothyrids, bradyinids and encrusting forms. Ostracodes and fusulinids, with rare crinoids, brachiopods, beresellid and ungdarellid algae, and fenestrate and ramose bryozoans are also present. Sparry calcite cement occludes intergranular porosity. Cloudy submarine fibrous calcite cement is locally present.

The Peloidal Facies is not well represented in the study area but occurs most commonly at a distance from the shelf edge (e.g. section 9) associated with the Crinoid-Bryozoan Facies, forming the basal and middle portions of shelf cycles. It also occurs locally associated with phylloid algal boundstones at the shelf edge (e.g. sections 1 and 5).

Interpretation

The Peloidal Facies has two distinct occurrences within the study area: 1) mid-shelf; and 2) shelf edge. Peloids are common in the mid-shelf subtidal environment where they occur preferentially in low energy zones. They are indicative of relatively deep, quiet water below wave base but within the photic zone or shallower shelf areas where topographic variations upon the ocean floor restrict current flow. In modern environments they similarly occur in subtidal and shallow intertidal areas, preferentially in low energy zones (Flügel, 1982). Peloids are also major contributors to intra-reef sedimentation where they are found in association with the Phylloid Facies. Peloids on the shelf edge can be produced by boring organisms (Flügel, 1982) and by chemical processes (Macintyre, 1985).

3.1.4 Oolitic Facies

Description

The Oolitic Facies (Plate 4a, b, d) is characterized in outcrop by poorly developed, large scale (>1 m), low-angle (<20°) cross-beds. It is composed mainly of oolitic grainstone and includes coated grains and abraded, rounded bioclasts. Ooids are moderately well sorted but range locally from 0.05-0.5 mm in diameter. The larger ooids commonly display a concentric cortex fabric while the smaller ooids display a radial cortex fabric. Other ooids are commonly micritized (especially the smaller grains) or recrystallized, or rarely dissolved. A thin isopachous cloudy cement rim surrounds numerous grains. Nuclei consist of either bioclasts, peloids, or rarely, quartz silt grains. Associated bioclasts include phylloid algae, fusulinids, foraminifers, crinoids and rare brachiopods.

The Oolitic Facies is rarely observed within the study area. It is present adjacent to the shelf edge and occurs high in the shelf cycles associated with Phylloid Algal and Foraminiferal facies (e.g. sections 1 and 5).

Interpretation

The Oolitic Facies represents moderately well sorted oolitic sand accumulating in a relatively high energy shoal environment. Active oolitic sand shoals occur on Holocene carbonate platforms as beach-barrier island, nearshore, and shelf-margin sands (Tucker and Wright, 1990). Most of these shoals form only a few metres below sea level. The Oolitic Facies of this study dominantly represents shelf-margin sands as dictated by its position within the study area and associated facies. The occurrence of high energy sedimentary structures and well-winnowed depositional textures confirms this interpretation. A single occurrence of a barrier island sand or a shoal extending in from the shelf edge is also possible as a small oolitic outcrop occurs in the mid-shelf environment (e.g. section 6). Ooids likely had aragonitic (tangential fabric - aragonitic origin) and high-

Mg (radial fabric - calcitic origin) precursors as indicated by their preserved textures (Beauchamp, 1994).

3.1.5 Chaetetid Facies

Description

In outcrop the Chaetetid Facies (Plate 4c) occurs as a thin biostromal unit (averaging 1-2 m thick) comprising massive boundstone dominated by chaetetids, either toppled or in growth position (single colonies reach diameters up to 15 cm). Growth cavities are filled with bioclastic packstone containing fusulinids, brachiopods, crinoids, various small forams, and beresellid and ungdarellid algae. Fenestrate and ramose bryozoans, gastropods and *Tubiphytes* are also present. The chaetetid skeletons are often dolomitized whereas the matrix is commonly replaced by silica. Remaining porosity is occluded by calcite spar.

The Chaetetid Facies occurs rarely in the study area on the shelf (e.g. sections 5 and 6). Where present it occurs within the upper portions of shelf cycles in association with the Foraminiferal Facies.

Interpretation

Chaetetids likely formed small patch reefs on the shelf. They tend to favor local topographic highs on a slightly irregular sea floor (Lustig, 1971; Spaw, 1977). Colonies usually required a locally firm substrate for initial settlement and growth, and thrived in warm, shallow, sunlit waters of normal salinity (West and Clark, 1983; Stemmerik, 1988; Kershaw and West, 1991). The presence of algae also indicates a relatively shallow water setting. As suspension feeders the chaetetids required an environment free from sediment influx (Suchy and West, 1988).

3.1.6 Beresellid Facies

Description

This facies is a beresellid-dominated boundstone to grainstone (Plate 4e) which forms thin (<3 m thick) biostromes. A diverse fossil assemblage is associated, including fusulinids, pseudoendothyrids, paleotextulariids, globivalvulinids, encrusting forams, ungdarellid algae, *Tubiphytes*, and rare tetrataxids, bradyinids, brachiopods, ramose bryozoans and peloids. Some interskeletal pores display a thin isopachous fibrous calcite cement rim. Remaining pore space is filled with equant spar.

Beresellid algae represent relatively abundant shelf mound framebuilders in the study area especially at a distance from the shelf edge (e.g. sections 6 and 9). They occur in the mid- to upper portions of shelf cycles, in association with the Foraminiferal Facies.

Interpretation

Biostromes of the Beresellid Facies, dominated by the small tubular green calcareous algae, represent laterally extensive buildups that developed on the mid-shelf with little significant relief. They have been recognized as a very important 'reef' builder during Carboniferous time that formed small, on-shelf mounds (Mamet, 1991). Similar biostromes were recognized in the Permian of the Sverdrup Basin by Morin (1992) who interpreted them as having developed in a relatively shallow shelf setting at, or near, fair-weather wave base in warm, clear water.

3.1.7 Dasycladacean Facies

Description

The Dasycladacean Facies (Plate 4f) is a massive grainstone dominated by dasycladacean algae in thin biostromes (up to several metres in thickness). The original skeletons of the algae are not preserved, rather pores are filled with micrite and the skeleton itself is infilled and surrounded by early marine fibrous calcite cement. The grains can be heavily abraded. Some of the algae are encrusted by *Tubiphytes* and forams. Other associated biota include globivalvulinids, paleotextulariids, peloids, and rare fusulinids and ostracodes.

The Dasycladacean Facies is rarely observed in the study area (e.g. section 1). Where present it occurs near the shelf edge in the middle of a shelf cycle, in association with Foraminiferal and Phylloid Algal Facies.

Interpretation

The Dasycladacean Facies formed small shoal complexes in shallow, warm, open marine conditions. They developed in a relatively high energy zone within the shelf environment where vigorous water circulation allowed grain abrasion and the extensive development of early marine cements. Both sandy and muddy substrates were suitable for colonization. Comparisons with modern algal counterparts have verified this habitat as one in which dasycladacean algae thrived (Ginsburg et al., 1971; Elliot, 1991).

3.2 Shelf Edge Assemblage

The shelf edge assemblage crops out as a discontinuous elongate feature (several kilometres wide and approximately 200 km long through the study area) extending in a northwesterly direction from east of the head of Hare Fiord to the environs of Audhild Bay (sections 1 and 5; Appendix 2). The shelf edge assemblage comprises two distinct lithofacies (for a summary see Table 3): 1) Phylloid Algal Facies; and 2) Bryozoan Facies. It is dominated by massive, light-coloured carbonate buildups flanked by bedded sediment.

Cycles are not visible within the shelf edge assemblage. Individual biogenic carbonate buildups coalesce to form massive mound-like features. Patches of variable carbonate texture occur randomly throughout the reefs (Figure 8). The large, massive appearance of the shelf edge assemblage makes it easily visible at outcrop scale. It forms a discontinuous marker separating the shelf deposits from those of the slope-to-basin.

Table 3. Facies of the Shelf Edge Assemblage.

Facies Designation	Phylloid Algal Facies	Bryozoan Facies
Bedding and Sedimentary Structures	massive bioherms coalesce to form units > 1 km in thickness	massive bioherms up to 60 m high, 100's m wide (in study area)
Rock Type	boundstone (cementstone to bafflestone) grainstone/flakestone	boundstone grainstone
Major Grain Types	phylloid algae	fenestellid bryozoans, crinoids
Minor Grain Types	fusulinids, small forams, brachiopods, crinoids, encrusting forams, *Tubiphytes*, ungdarellid algae, peloids	ramose bryozoans, brachiopods, encrusting forams, *Tubiphytes*
Main Diagenetic Features	early isopachous fibrous cement micrite dissolution voids dolomite	early isopachous fibrous cement late sparry calcite cement dolomite
Depositional Environment	shelf edge high energy grows to wave base	shelf edge/upper slope high energy grows below wave base and possibly below photic zone

3.2.1 Phylloid Algal Facies

Description

The Phylloid Algal Facies (Plate 5a-e) is characterized by massive bioherms which coalesce to form outcrops greater than 1000 m in stratigraphic thickness (e.g. sections 1 and 5). It is dominated by phylloid algal boundstones and grainstones. The boundstone texture displays a relatively open framework of phylloid plates. The growth cavities are alternately filled with multiple layers of marine fibrous calcite cements (similar to cementstone of James and Bourque, 1992) or geopetal peloidal muds (bafflestone). Grainstones contain broken and abraded phylloid plates (flakestone; Davies and Nassichuk, 1988) with an abundant and diverse fossil assemblage (see below). In most cases the formerly aragonitic phylloid plates are poorly preserved and are visible only as a micritic rim surrounding a submarine cement-filled cavity.

Mamet et al. (1987) assigned phylloid algae to platy codiaceans (green algae) and recognized three distinct genera which have been observed within the Sverdrup Basin: *Eugonophyllum*, *Neoanchicodium* and *Ivanovia*. The phylloid thalli are often encrusted by *Tubiphytes* and by tuberitinid and apterrinellid foraminifera. Additional associated biotic elements include: fusulinids, brachiopods, echinoderms, pseudoendothyrids, paleotextulariids, tetrataxids, ungdarellids and peloids, and rare beresellids, dasyclads, ostracodes, gastropods, globivalvulinids and bradyinids.

Boundstones of the Phylloid Algal Facies dominate the shelf edge setting (e.g. sections 1 and 5). Grainstones flank the massive reef core and are found intermingling with the Oolitic and Foraminiferal Facies adjacent to the shelf edge. Boundstones dominate the massive shelf edge itself (Figure 9). In this setting phylloid algae can occur independently or in association with the Bryozoan Facies at greater depths (see below). The Phylloid Algal Facies occurs rarely in the upper portions of shelf cycles (e.g. section 9) but at the shelf edge the massive buildups display no apparent cyclicity.

Interpretation

The Phylloid Algal Facies is an integral facies within the shelf edge buildups and more rarely within shelf mounds. The phylloid algae thalli played an important role in bioherm construction as the loci for early marine cementation (cementstone) and less commonly as bafflers and trappers of sediment (bafflestone; Wilson, 1975). Phylloid algal grainstone/flakestone occurs in a flanking and back reef position.

The presence of abundant early marine fibrous calcite cements in the phylloid cementstone subfacies, in addition to the abraded skeletal grains and scarcity of mud indicate an open marine, relatively high energy environment able to winnow fine grained material. The field position of this subfacies, forming an elongate feature separating the shelf from the deep water deposits, also indicates its shelf edge location. Phylloid algae likely grew near fair-weather wave base at the shelf edge but did not reach to sea level as the fragile growth forms were incapable of withstanding such an extreme energy environment. The bafflestone texture is much less common in the study area and contains more mud and less early marine fibrous calcite cement than the cementstone subfacies, indicating growth within a lower water energy level. Bafflestones occur in the upper portion of shelf cycles associated with shelf facies indicating growth upon the shelf rather than at the shelf edge. Beauchamp et al. (1988) described the ideal setting for growth of shelf phylloid algal buildup within the photic zone, in well oxygenated, detritus-free waters.

3.2.2 Bryozoan Facies

Description

The Bryozoan Facies (Plates 2d, 5f) occurs as massive bioherms attaining measured thicknesses of up to 60 m and widths of several hundreds of metres, comprising boundstones (core subfacies) to grainstones (flank subfacies) dominated by fenestrate bryozoans with abundant crinoid debris. Ramose bryozoans and brachiopods are also significant components while gastropods and tetrataxids occur rarely. Apterrinellids and *Tubiphytes* commonly encrust the skeletal surfaces of the fenestrate bryozoans. The bryozoans form an open framework in which growth cavities are largely infilled by cloudy isopachous fibrous calcite cements. Remaining space is filled with equant spar or geopetal pelleted lime mud which is commonly recrystallized to dolomite microspar.

The Bryozoan Facies occurs in two settings, along the shelf edge (e.g. section 1) and associated with slope-to-basin facies (e.g. sections 2 and 7). Along the shelf edge bryozoans coexisted with Phylloid Algal Facies. The latter occurrence is known as Televak limestone (Bonham-Carter, 1966; Besemann, 1993; Brunton et al., 1993), massive bryozoan-dominated mounds formed during a Carboniferous marine transgression and onlapped by bedded sediments of the Hare Fiord Formation.

Interpretation

Bryozoan mounds are interpreted to have developed in deeper water conditions than the associated phylloid algal buildups, below fair-weather wave base to below the photic zone. The absence of algae from the deeper mounds confirms this interpretation. They have been described as having a 'Waulsortian'-like character (Davies et al., 1988). The extensive early marine cements indicate that even at these lower water depths current energy was sufficient to allow the constant infusion of sea water into framework cavities and winnowing of fine-grained sediment.

Occasionally (e.g. section 1) the bryozoan mounds grew upward into a position optimal for phylloid algal growth. The bryozoans were then replaced by these later forms which proceeded to create the shelf edge phylloid buildups (see above).

3.3 Slope-To-Basin Assemblage

The slope-to-basin assemblage is exposed between Hare Fiord and Otto Fiord, and along the western portion of the north shore of Otto Fiord (Figure 2), at sections 2, 3, 5 and 7 (Appendix 2). The slope-to-basinal assemblage is composed of five distinct lithofacies (for a summary see Table 4): 1) Calcisiltite Facies; 2) Siltstone Facies; 3) Shale Facies; 4) Calcarenite Facies; and 5) Debrite Facies. The Bryozoan Facies can also be observed locally in association with the slope-to-basinal assemblage (see above). The assemblage appears as dark, bedded strata onlapping onto lighter, massive biogenic mounds (Plate 2).

Slope cycles range in thickness from 5.5 to 57 m and comprise recessive-resistant packages whose lithologic content varies gradationally upward (Figure 10). Each cycle displays a coarsening upward and shallowing upward trend from relatively shale-rich deposits at the base (mudstone) grading upward into mixed carbonates (wackestone to packstone). This trend is also paralleled by an increase in bedding thickness, and a transition towards a more resistant outcrop profile. As distance increases away from the shelf edge the shale component within each cycle increases proportionally.

Slope cycles are laterally continuous and relatively well bedded but due to the recessive nature of the deposit can often be difficult to recognize. The episodic nature of the coarse deposits also obscures the cyclicity. Bioherms occur near the base of the deposit and display no internal cyclicity. These buildups form part of the lower transgressive package.

3.3.1 Calcisiltite Facies

Description

The Calcisiltite Facies (Plate 6a-e) comprises thin to thickly bedded (10 cm - 1 m), dark, argillaceous, cherty and dolomitic mudstone to wackestone with shaly interbeds. Individual beds are planar, parallel and continuous over long distances. The facies can be either well laminated or disrupted by abundant bioturbation. Horizontal feeding burrows (fodinichnia) and grazing traces (pascichnia; Ekdale et al., 1984) representing both *Zoophycos* and *Nereites* ichnofacies are visible along bedding surfaces. Organic-rich

Table 4. Facies of the Slope-To-Basin Assemblage.

Facies Designation	Calcisiltite Facies	Siltstone Facies	Shale Facies	Calcarenite Facies	Debrite Facies
Bedding and Sedimentary Structures	thin to thickly bedded laminated bioturbated	thin to thickly bedded laminated bioturbated	recessive fissile	thin to thickly bedded graded basal scour	massive thick (up to 12 m) laterally discontinuous
Rock Type	mudstone to wackestone	siltstone with mudstone to wackestone matrix	shale (mudstone)	packstone to grainstone	conglomerate (packstone)
Major Grain Types	carbonate silt	quartz silt	shale	crinoids, bryozoans, fusulinids	clasts
Minor Grain Types	brachiopods, crinoids, fenestellid bryozoans, sponge spicules, calcispheres, quartz silt	brachiopods, crinoids, sponge spicules, calcispheres		brachiopods, forams, sponge spicules, calcispheres, peloids, intraclasts, quartz silt	brachiopods, crinoids, bryozoans, fusulinids, forams, peloids, intraclasts
Main Diagenetic Features	dolomite silica	silica		silica late sparry calcite cement	early isopachous fibrous cement
Depositional Environment	slope hemipelagic	slope hemipelagic	slope hemipelagic anaerobic conditions	slope turbidites	lower slope debris flows

laminae are locally significant. Autochthonous skeletal components include thin-walled brachiopods, crinoid debris, fenestrate bryozoans and locally abundant siliceous sponge spicules and calcispheres. Quartz silt is locally common. The limestone matrix is commonly replaced by micro-crystalline dolomite and/or silica.

The Calcisiltite Facies dominates locally the slope-to-basin deposits within the study area. It is most abundant in the slope setting close to the shelf edge (e.g. sections 2, 5 and 7) within the mid- to upper portions of slope cycles but is also found well (e.g. section 3) into the basin. It is often underlain by the shale facies and interlayered with both the Calcarenite and Debrite facies.

Interpretation

The hemipelagic sediments of the Calcisiltite Facies were deposited on a deep water slope. The sparse bryonoderm skeletal assemblage (Beauchamp, 1994) and the occurrence of the relatively deep water *Zoophycos* to bathyal *Nereites* trace fossil assemblage indicate deposition in a deep water environment, likely below the photic zone (Seilacher, 1967; Pemberton et al., 1992). The presence of laminae confirm hemipelagic deposition in a low energy environment. Remobilization of biogenic opal after solution-replacement of sponge spicules by calcite may be a major source of silica in these rocks (Davies, 1977).

3.3.2 Siltstone Facies

Description

The Siltstone Facies (Plate 6c-f) is thin to thickly bedded (<1 m) and weathers to buff in outcrop. Individual beds are relatively planar and laterally continuous. The facies is often parallel laminated and comprises lime mudstone to wackestone matrix with abundant angular to subrounded quartz silt (>30% of rock by volume). Rare skeletal components include crinoid and brachiopod fragments. Some bioclasts are partly silicified and the mudstone matrix is variably replaced by chert. Abundant *Zoophycos* and various horizontal trace fossils (Plate 7a, b) occur along bedding plane surfaces and in argillaceous partings.

The Siltstone Facies is rare within the study area. It occurs most commonly at a distance from the Nansen Formation-Hare Fiord Formation transition (e.g. sections 3, 5 and 7). It is associated with the Calcisiltite Facies in mid- to upper portions of slope cycles.

Interpretation

The Siltstone Facies represents mixed hemipelagic sediments deposited in a slope environment. Quartz silt was either derived from the land mass to the north (Embry, 1992) through probable river input and largely bypassed the shelf during sea level lowstands, to be deposited on the slope, or by lateral drift from elsewhere in basin (long shore currents). The scarcity of skeletal components as well as the occurrence of the *Zoophycos* to *Nereites* (Seilacher, 1967; Pemberton et al., 1992) trace fossil assemblages indicate deposition below both wave base and the photic zone. The occurrence of well preserved laminae confirms a low energy depositional environment.

3.3.3 Shale Facies

Description

The Shale Facies (Plate 7c) is poorly exposed and rarely represented in outcrop. It is dark brown to green to black, fissile and highly recessive with a minor carbonate and variable silt component. Bioturbation is rarely visible in outcrop.

Thin shale interbeds are common throughout the slope-to-basin environment. Thick shale deposits are rare but do occur at a distance from the Nansen Formation-Hare Fiord Formation transition (e.g. sections 3 and 7). The shale occurs in the basal portions of slope cycles and is overlain by calcisiltite. Many covered intervals between slope outcrops likely represent additional shale deposits.

Interpretation

The Shale Facies represents hemipelagic deposition on a low energy, deep water slope-to-basin. The apparent scarcity of benthic trace fossils and body fossils indicates anoxic conditions in the deep basin.

3.3.4 Calcarenite Facies

Description

The Calcarenite Facies (Plates 7d, 8a-d) appears as dark grey, thin to thickly bedded (10 cm to 1m), bioclastic packstone to grainstone. Deposits are either laterally continuous over relatively long distances (thinner beds) or pinch-out over several metres to tens of metres (thicker beds). The basal contact is sharp and often scoured while the upper contacts are transitional. Individual beds display well-developed fining upward trends and locally poorly developed cross bedding. The dominant skeletal components include crinoids, fusulinids, and ramose and fenestrate bryozoans. Also present are small forams, brachiopods, siliceous sponge spicules, peloids, intraclasts, calcispheres and quartz silt. Rare are solitary rugosans, syringoporids and gastropods. Silicified matrix and bioclasts are locally abundant. Sparry calcite cement occludes remaining porosity.

Laterally discontinuous calcarenite deposits are relatively rare and occur near to the Nansen Formation-Hare Fiord Formation transition (e.g. section 2). Laterally continuous deposits are more abundant and occur dominantly at a distance from the transition (e.g. section 3). In both instances, calcarenites are interbedded with calcisiltite at various levels within slope cycles.

Interpretation

The Calcarenite Facies represents carbonate turbidites (Coniglio and Dix, 1992), submarine slope gravity-displaced deposits. Sediment source appears to have included both shelf edge and upper slope deposits. Laterally discontinuous units represent upper slope, channelized deposits while laterally extensive units dominate in the lower slope-to-basin where sediments emerge from the submarine channels to spread out over the basin floor. The turbidites are well-bedded, internally size-graded units deposited from turbidity currents (Middleton and Hampton, 1976). This interpretation is further verified by the occurrence of scoured basal contacts.

3.3.5 Debrite Facies

Description

The Debrite Facies (Plates 7e, f, 8e) is represented by very thick (up to 12 m), massive, clast-supported, yellow-grey-weathering deposits. They are local and laterally discontinuous. The Debrite Facies is composed of small (decimetre-scale) to large angular clasts up to several metres in diameter which are chaotically distributed with no apparent size grading. Both the basal and upper contacts are sharp and basal scouring is locally evident. Skeletal components within the clasts include fusulinids, small forams, crinoids, ramose and fenestrate bryozoans, brachiopods, peloids and intraclasts. Rare occurrences of phylloid algae, solitary rugosans, syringoporids, gastropods and quartz silt were observed. Cloudy isopachous fibrous calcite cement occasionally rims bioclasts within large clasts.

Debrites form a rare but conspicuous facies. They occur at a distance from the Nansen Formation-Hare Fiord Formation transition along specific horizons, disrupting interbedded Calcisiltite and Calcarenite facies (e.g. section 3). They occur at various levels within slope cycles but the largest debrite caps a cycle.

Interpretation

The Debrite Facies represents debris sheets, a distinct style of submarine slope gravity-displaced deposit (Middleton and Hampton, 1976). Debris sheets are massive, often discontinuous, breccia-like units deposited by mass flow. The large angular clasts contained within the deposits are largely derived from local sources along the shelf-edge as evidenced by the biota and presence of early submarine cements.

CHAPTER 4: DEPOSITIONAL MODEL

4.1 Depositional Environment and Paleogeography

During the Upper Carboniferous the Sverdrup Basin was experiencing warm, subtropical to tropical temperatures and arid to semiarid climatic conditions (Beauchamp et al., 1989a; Beauchamp, 1994). Recurring rifting phases had led to the creation of a northeasterly trending fault-formed basin, producing a narrow sigmoidal seaway that was part of an extensive rift system (several thousands of kilometres long) linking northern Alaska with North Greenland, Svalbard and the Barents Sea (Figure 4; Embry, 1992; Beauchamp, 1994).

The Sverdrup Basin consisted of a deep central trough surrounded by a shallow platform. The shallow water marine platform was dominated by carbonate production and sedimentation while the central basin received both carbonate and minor clastic debris. Major clastic sources lay to the east and south of the Sverdrup Basin. A secondary region supplying terrigenous material was a northern landmass, Crockerland, which was later rifted away following creation of the Arctic Ocean (Figure 4; Embry, 1992).

The Upper Paleozoic history of the Sverdrup Basin sediments is characterized by numerous long term depositional sequences (Figure 3; Thorsteinsson, 1974; Beauchamp et al., 1989a; Beauchamp, 1994). One such sequence was produced by a major marine transgression initiated during the Bashkirian and followed by a regression beginning during the middle Moscovian and terminating at the close of the Kasimovian stage. This regressive period promoted the progradation and aggradation of marine sediments and resulted in a thick and complete platform-to-basin marine succession outcropping within the Sverdrup Basin on northwestern Ellesmere Island.

In the present study 14 facies are recognized in this succession. These facies are grouped into genetically related facies assemblages which are themselves defined and interpreted on the basis of their constituent facies, packaging patterns, overall geometry and relative positions (see Table 1). They represent shelf, shelf edge and slope/basin depositional settings (Figures 17 and 18).

4.1.1 Shelf

In the study area the platform carbonate facies form a significant portion of the Nansen Formation. Inner shelf facies, however, are not commonly present as they were largely deposited beyond the present erosional edge of the Upper Carboniferous strata along the Sverdrup Basin margin. Mid- and outer shelf deposits are abundant and are dominated by a diverse biotic assemblage arranged in a wide array of lithofacies (see Chapter 3) stacked vertically into high frequency cycles. The shelf biota are classified as part of the "Chloroforam" assemblage (i.e. mainly calcareous algae, large forams, etc.), indicating warm water, tropical-like shelf carbonates (Beauchamp, 1994).

The Nansen shelf gradually sloped down away from a paleoshoreline to the mid-shelf. Although the depth increased towards the mid-shelf the depositional textures (packstones dominate, some winnowing of mud occurred) as well as the presence of algae and vertical burrows indicate that the energy level remained moderate and the sea floor remained within the photic zone. The irregular surface provided loci for the development of various carbonate mounds of differing lithologies (James and Bourque, 1992). These include chaetetid-, beresellid-, dasyclad-, and phylloid alga-dominated mounds which created local lee side, low energy zones due to their topographic relief where wackestones and peloidal muds developed to a limited degree. Although the mounds formed topographic highs upon the seafloor they did not restrict water circulation to the extent of causing the development of evaporitic facies or significant deposits containing restricted biotic assemblages. If lagoons were present within the area they occurred northward of the erosional edge and have since been eroded.

Figure 17. Paleogeography of the study area. Location of the Upper Carboniferous Nansen shelf edge within the study area is illustrated with Nansen shelf lying to the north and Hare Fiord slope-to-basin lying to the south.

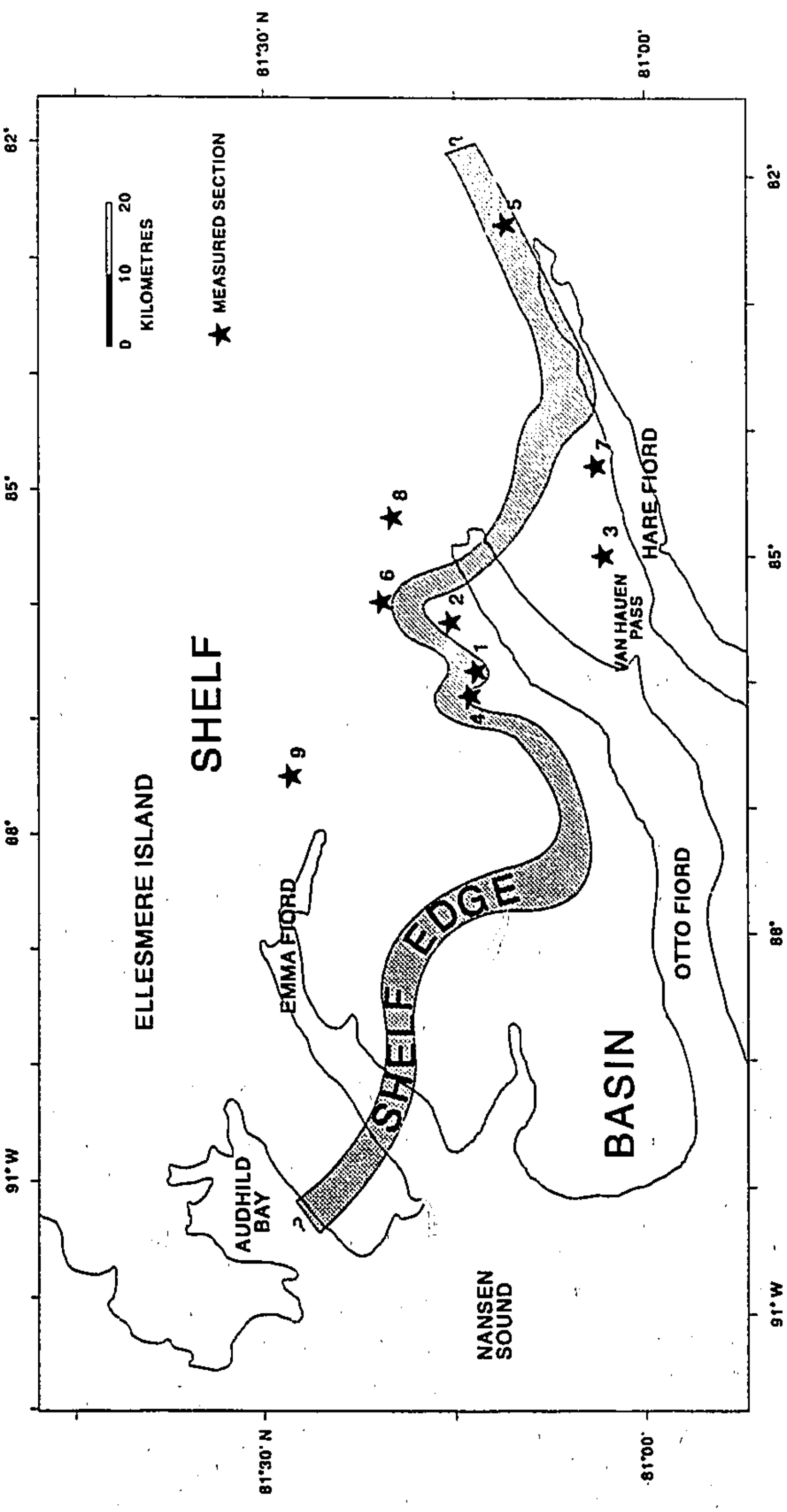
ELLESMERE ISLAND
SHELF
BASIN
SHELF EDGE
EMMA FIORD
AUDHILD BAY
NANSEN SOUND
OTTO FIORD
VAN HAUEN PASS
HARE FIORD
0 10 20
KILOMETRES
MEASURED SECTION
82°
85°
88°
91° W
81°30' N
81°00'

Figure 18. Schematic block diagram showing depositional model of the shelf-to-basin transition. Note that shelf edge reefs formed a discontinuous fringe surrounding the basin. Where the reefs were present the upper slope had an increased gradient and the lower slope contained debris flow deposits. (No scale is intended.)

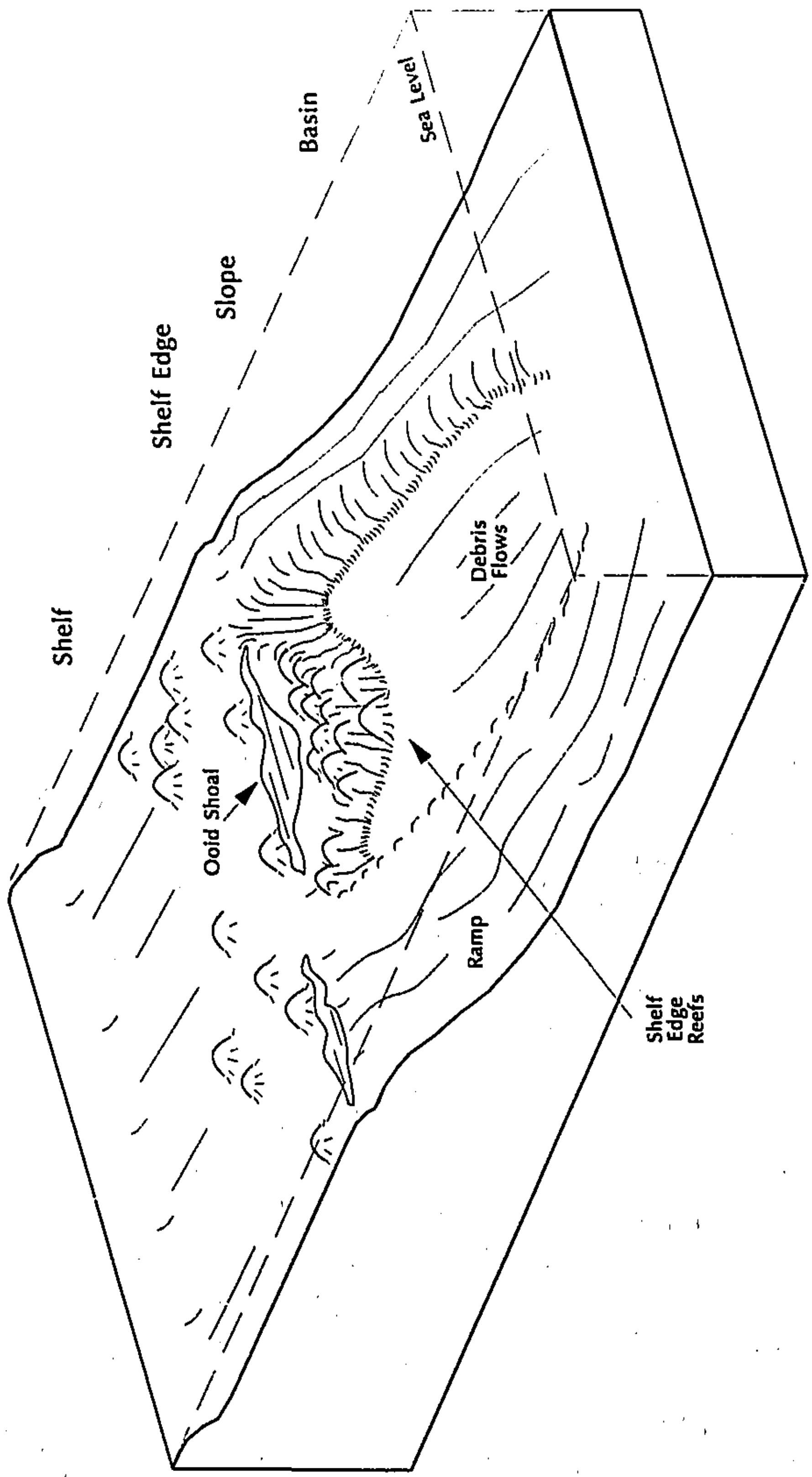
Basin
Sea Level
Slope
Shelf Edge
Shelf
Debris Flows
Ooid Shoal
Ramp
Shelf Edge Reefs

The outer shelf was dominated by a shoaling succession. Large scale cross-bedding and the development of ooids and coated grains indicate a high energy environment. Abundant bioclasts derived mainly from the phylloid alga-dominated shelf edge reefs demonstrate both the high water energy and windward position of the coastline. Although these deposits represent the shallowest on the studied portion of the marine shelf they apparently did not develop fully to sea level across the region and did not restrict water circulation. There is evidence of several short-term episodes of shelf exposure in distinct but rare, red and green, siliciclastic-rich horizons (only in the upper part of the second order regressive systems tract).

The Nansen shelf represents a wave-dominated hydraulic regime rather than a tide-dominated system. The abundant bioclastic debris, especially on the outer shelf, and the relatively abundant siliciclastic silt episodically removed from coastal areas then transported seaward to be deposited on the slope suggest storm surge ebb currents. Beauchamp (1987) also recognized this condition on southwestern Ellesmere Island where coastal and nearshore deposits were observed. He also indicated that the semi-enclosed setting of the Sverdrup basin probably created a microtidal range, probably not exceeding 1 or 2 m daily.

4.1.2 Shelf Edge

The Nansen Formation also contains the massive shelf edge deposits in which coalesced phylloid alga-dominated reefs are interpreted to represent the slope break (Figure 19). The fragile leaf-like reef builders were able to form extensive, resistant structures due to the stabilizing effects of pervasive early marine cementation. Growth of each reef resulted from the growth of erect to semi-erect phylloid algae. The thalli acted as baffling and trapping agents, collecting lime mud and bioclastic carbonate particles. Accessory fenestellid and ramose bryozoans likely had a similar role. Epibionts,

Figure 19. General depositional model of the Nansen-Hare Fiord shelf-to-basin transition where the reefal shelf edge was well developed.

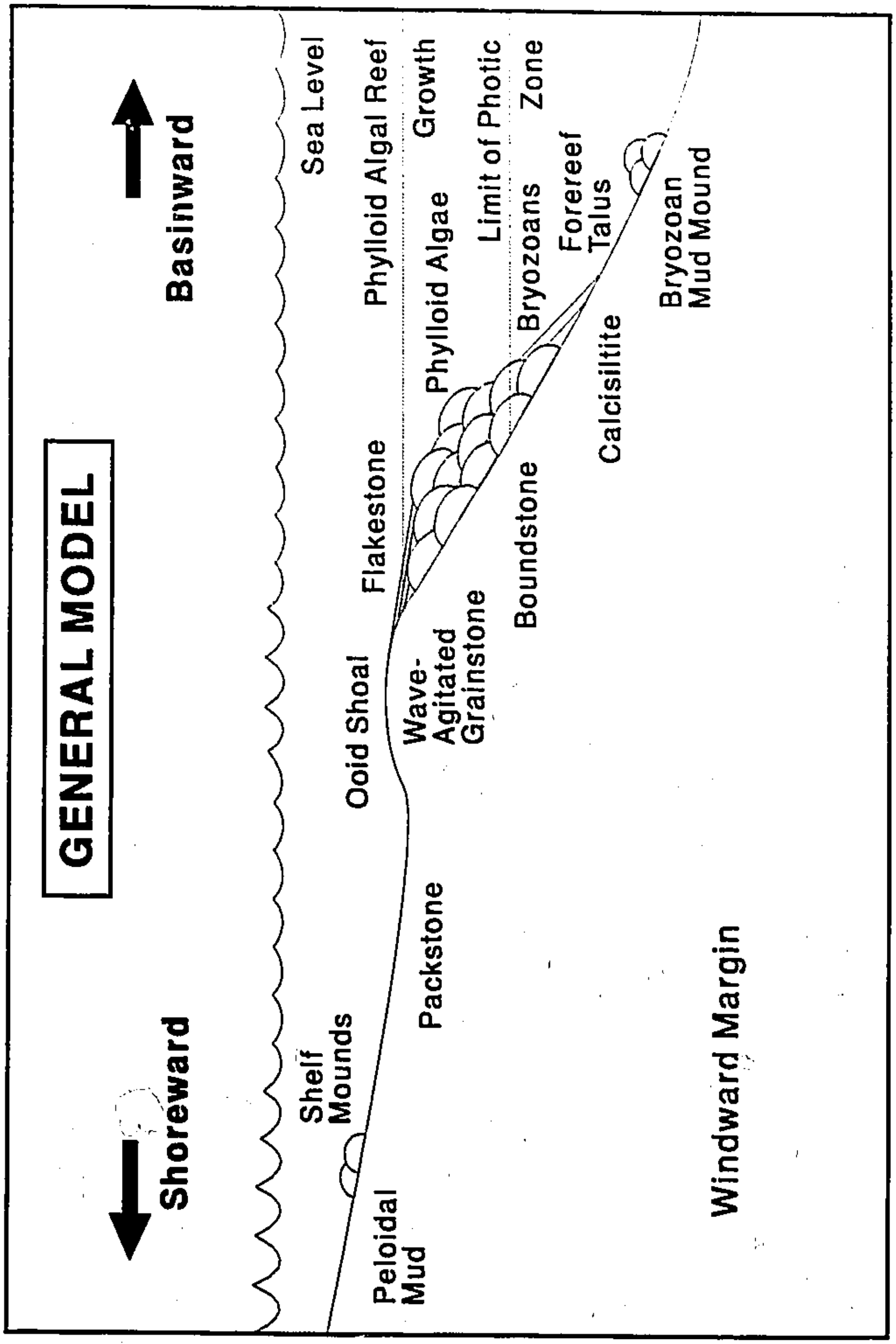
GENERAL MODEL
Shoreward
Basinward
Sea Level
Phylloid Algal Reef Growth
Limit of Photic Zone
Peloidal Mud
Shelf Mounds
Packstone
Ooid Shoal
Wave-Agitated Grainstone
Flakestone
Phylloid Algae
Boundstone
Bryozoans
Calcisiltite
Forereef Talus
Bryozoan Mud Mound
Windward Margin

dominantly foraminifers, ungdarellid algae and brachiopods, also contributed to reef growth as they attached themselves to the plates and leaves of the main reefal constituents.

The bases of these reefs are sometimes dominated by fenestellid bryozoans rather than phylloid algae. Apparently, bryozoans grew in deeper waters but as they grew upward through the water column they were replaced by shallower water organisms, the phylloid algae.

Although forming the shelf edge fringing reef, the phylloid algae did not grow to sea level. They are believed to have developed up to within the lower reaches of the wave zone, where wave energy was not sufficient to destroy these biogenic structures but the water circulation required for precipitation of extensive submarine cement was available. Although phylloid algae grew within the photic zone bryozoans colonized the sea floor at a greater depth indicating that Nansen buildups could have been initiated below the photic level. Within their growth window, the phylloid alga-dominated buildups prograded and aggraded to form the extensive features now visible in outcrop.

Pervasive cementation is a key feature of all the shelf edge buildups. Multiple generations of fibrous to radiaxial calcite cements have been described and interpreted as former early marine high-Mg calcite cements (Davies, 1977). The cement partially to wholly occludes intraparticle, interparticle and shelter voids. It also occurs within dykes which commonly cut through the reefs (Plate 5e). The lack of physical compactional features within the reefs further verifies the early nature of this process.

Deposits associated with the shelf edge reefs provide further evidence of their position and form. Grainstone and packstone beds flanking individual boundstone reef cores indicate that relief existed above the sea floor at the time of reef growth. In shallower water regions the associated deposits contain less mud than those buildups which developed in slightly deeper waters. Backreef debris was largely incorporated into the outer shelf shoal while forereef talus formed both foreslope beds, dipping locally as high as 40° (Davies, 1977), and large debris flows extended into the basin.

The shelf edge is not everywhere marked by a phylloid algal reef (Figure 18). The reef system is rather discontinuous, individual reef packages separated by areas of ramp development (Benoit Beauchamp, pers. comm. 1994). At these localities the shelf edge is simply a change in angle of slope with no extensive foreslope clinoforms or downslope debris flows.

Both the shelf and shelf edge carbonates are dominated by the "Chloroforam" faunal association (Beauchamp, 1994). This influenced the mineralogy of the carbonates as many of the organisms secreted aragonitic or high-Mg calcite skeletons. Aragonitic skeletons of phylloid algae, dasyclad algae, mollusks (pelecypods and gastropods), and stafellid and pseudoendothyrid forams, and some ooids, were invariably dissolved. High-Mg calcite skeletons included echinoderms, bryozoans, rugose corals, and most families of forams.

Cements were also dominated by these same minerals. Botryoids and fans of submarine aragonitic cement lined cavity walls in shelf edge reefs (Davies, 1977; Davies and Nassichuk, 1990). High-Mg calcite cements occurred as nonbotryoidal submarine cements in the reefs and other shelf carbonates. Also important in shelf carbonates were a variety of high-Mg fibrous calcite fabrics in both inter- and intraparticle pore space (Davies and Nassichuk, 1990).

4.1.3 Slope/Basin

The transition from shelf edge to slope environment is very abrupt in the Sverdrup Basin. The slope-to-basin sediments comprise the Hare Fiord Formation. These dark, rhythmic deposits extend away from the shelf edge facies becoming increasingly rich in shale and poor in *in situ* benthic biota. Depositional dips of shelf foreslope beds were locally up to 40°. In this high-relief setting, downslope gravitational displacement of sediment was common. Away from the shelf, the slope gradient increased more gently. Water depths of 300 to 1200 m have been estimated (Davies, 1977). At depth, anaerobic conditions are indicated by the dark colour of the shale and scarcity of body or trace fossils.

The Hare Fiord Formation comprises a complex variety of distinct sediment types arranged upon the slope. The upper slope was largely bypassed by shelf edge sediments as it exhibited the steepest gradient. Hemipelagic sediments dominated in this region, with fine carbonate material abundant in the upper reaches and shale increasing in abundance downslope. Channelized deposits were formed locally and display normally graded beds with scoured bases. Apparently, submarine canyons cutting through the upper slope provided conduits for turbidite flows to reach onto the lower slope (Mullins et al., 1984).

On the lower slope, laterally extensive, graded turbidite deposits were relatively abundant. As the slope gradient decreased the channels no longer cut into the slope thus allowing the turbidity currents to spread their deposits across the lower slope. At this point thick debris flows containing material derived from the massive shelf edge also came to rest as allochthonous, resistant, light-coloured limestone blocks.

Not only do the lithofacies indicate a deep water setting but the biota are representative of this environment as well. The "Bryonoderm" benthic association associated with these lithofacies is indicative of a lower temperature setting than that of the "Chloroforam" association (Beauchamp, 1994). A lower temperature can be achieved with increasing latitude or bathymetry. In the Hare Fiord Formation the "Bryonoderm" fossil assemblage, represented by an impoverished biota dominated by bryozoans, echinoderms and brachiopods (Rao, 1981; Rao, 1988), verifies decreasing temperature resulting from increasing water depth.

Bioturbation also demonstrates the deep water aspect of the Hare Fiord Formation deposits. Horizontal and subhorizontal tracks, trails and feeding traces (from *Zoophycos* to *Nereites*; Plate 7a, b; Seilacher, 1967; Pemberton et al., 1992) occur on bedding surfaces indicating quiet water slope-to-basin environments.

4.2 Cyclicity

High order depositional cycles are present in both the shelf deposits of the Nansen Formation and the slope-to-basin deposits of the Hare Fiord Formation (Figures 7 and 10; Appendix 2). Differences however are observed in the expression of cyclicity between these two depositional settings. Shelf cycles comprise shallower water facies with a purer carbonate composition, and are more fossil-rich, dominantly coarser grained, thinner on average, and lighter in colour. In comparison, slope cycles comprise deeper water facies with a much larger siliciclastic component, and are fossil-poor, dominantly finer grained, thicker on average, and dark in colour.

Despite these differences both shelf and slope/basin cycles share points in common. The facies succession consists of shallowing upward cycles (Wilson, 1975), delineated by flooding surfaces. This is confirmed by upward lithologic, sedimentologic, biogenic and diagenetic changes through each cycle. Mud content decreases upwards, accompanied by an increase in the diversity and abundance of biotic and abiotic carbonate elements, an increase in bedding thickness, and a transition to a more resistant outcrop profile. Also, with increased distance from the shelf edge and increased depth, either towards the mid-shelf or slope/basin, the amount of fine grained material increases.

Morin (1992) and Beauchamp (1993) determined that there were distinct time-stratigraphic cycle assemblages characterized by unique stacking patterns representing distinct episodes of tectonically controlled sedimentation within the Sverdrup Basin. Morin (1992) subdivided the Lower Permian sequence into three assemblages, pre-, syn-, and post-evaporite, which corresponded to phases of uplift, collapse and passive subsidence, respectively. During a passive subsidence regime, accumulation of high frequency cycles of relatively constant thickness and composition would occur within a single sedimentary environment that could be correlatable across the depositional gradient. During a regime of rifting and fault-controlled subsidence, cycles would accumulate with variable thickness and composition. These would be almost impossible to correlate on a regional scale. Within a single sedimentary sequence in the Sverdrup Basin, both tectonically-controlled and passive regimes are encountered. Beauchamp (1993) presented a more general scheme in which all low-order sequences deposited during active rifting in the Sverdrup Basin (Serphukovian to Artinskian) resulted from recurrent multi-phase tectonic cycles. These phases were: 1) buckling; 2) flooding; 3) rifting; 4) drowning; 5) rebound; and 6) sagging. The sagging phase, a period of regional passive subsidence, was ongoing during deposition of the Moscovian to Kasimovian Nansen and Hare Fiord deposits.

Although the Nansen and Hare Fiord cycles were deposited during an apparently quiescent tectonic period, their correlation is still complicated. Not only are shelf deposits being correlated with other shelf deposits but also with slope-to-basin sediments. As the cycles in both environments possibly have the same causal factor, in theory, they should be correlatable. In practice, the difficulty of correlating a single cycle on the shelf with its corresponding slope cycle make this exercise next to impossible without more precise dating than was possible in this study. This is especially apparent as the slope cycles often appear to be thicker than those on the shelf. This was unexpected as slope deposits are commonly thinner than time-equivalent shelf deposits. This irregularity is likely the product of amalgamation of numerous slope cycles into a single recognizable package.

Another concern is the apparent lack of cycles within the massive shelf edge reefs. If the depositional cycles resulted from eustatic and tectonic conditions experienced within the Sverdrup Basin, the reef-building organisms should have experienced these effects as readily as sediments elsewhere in the basin. Either the relative sea level fluctuations were insufficient to affect the reef construction, or variations in grain size and sediment composition within the reef core were so slight as to be unapparent at the scale of the investigation.

High-frequency depositional cycles are influenced by variations in: 1) eustasy; 2) subsidence; and 3) sediment input (Goldhammer et al., 1990). They are currently viewed as products of rate fluctuations which influence relative sea level, and no longer solely a product of absolute sea level. In addition, the type and geometry of the facies within the cycles are influenced by the hydraulic regime, climate, biological activity and diagenetic processes (Beauchamp, 1987).

The well-studied occurrences of Late Paleozoic high frequency cycles (Heckel, 1984) have been interpreted as having a glacio-eustatic origin, as evidence has been collected for glacial activity in the southern hemisphere. Acting in conjunction with this was the tectonic regime of the Sverdrup Basin, with periodic rifting during the Upper Carboniferous (Beauchamp, 1989b).

Nansen and Hare Fiord cycles of this study were apparently influenced largely by glacio-eustatic effects. Tectonics likely played a minor role through much of the period of interest as it appears that passive subsidence was ongoing. Sediment input affected basin deposits more readily than shelf deposits (gravity-induced deposition) which may be one of the reasons that correlation between the shelf and slope/basin environment is so difficult.

4.3 Specific Depositional Models

The Moscovian to Kasimovian Nansen and Hare Fiord formations were deposited during an overall marine regression but with numerous superimposed high order sea level fluctuations as discussed previously. High frequency highstands and lowstands created unique sedimentary deposits which can be recognized within the shelf-to-basin succession. Conceptual models have been created for highstands and lowstands based upon the empirical study of Nansen and Hare Fiord high-frequency cycles. These illustrate short term changes in sediment dynamics across the Nansen and Hare Fiord shelf-to-basin region (Figures 20 and 21).

4.3.1 Lowstand

A sealevel lowstand created relatively shallower water conditions which promoted the deposition of packstones to grainstones on the shelf (Figure 20). Exposure of nearshore shelf environments promoted the influx of minor amounts of siliciclastic sediment into the marine system which largely bypassed the shelf to be deposited on the slope. The shelf edge reef tract prograded and as the uppermost levels of the reef are moved into the higher energy zone, reef debris was created and deposited in the backreef sand wedge (such debris was also formed periodically due to storm activity). In addition to increased quartz silt sedimentation in the slope, the deposition of calcisiltite was also ongoing.

4.3.2 Highstand

A sealevel highstand created relatively deeper water conditions which promoted the deposition of wackestones and packstones across the shelf (Figure 21). In addition, the shelf edge phylloid alga-dominated reefs aggraded and also prograded to some degree. This produced oversteepening of the reef and created an unstable condition which allowed reefal blocks to form debris flows and move downslope. Cement-filled dykes within the reefs paralleling the shelf edge indicate fracture of the reef core due to slumping or compaction of the underlying sediment. Shale sedimentation dominated in the basin.

Figure 20. Idealized sea level lowstand depositional model. Note exposure of shelf and progradation of shelf edge phylloid algal reefs.

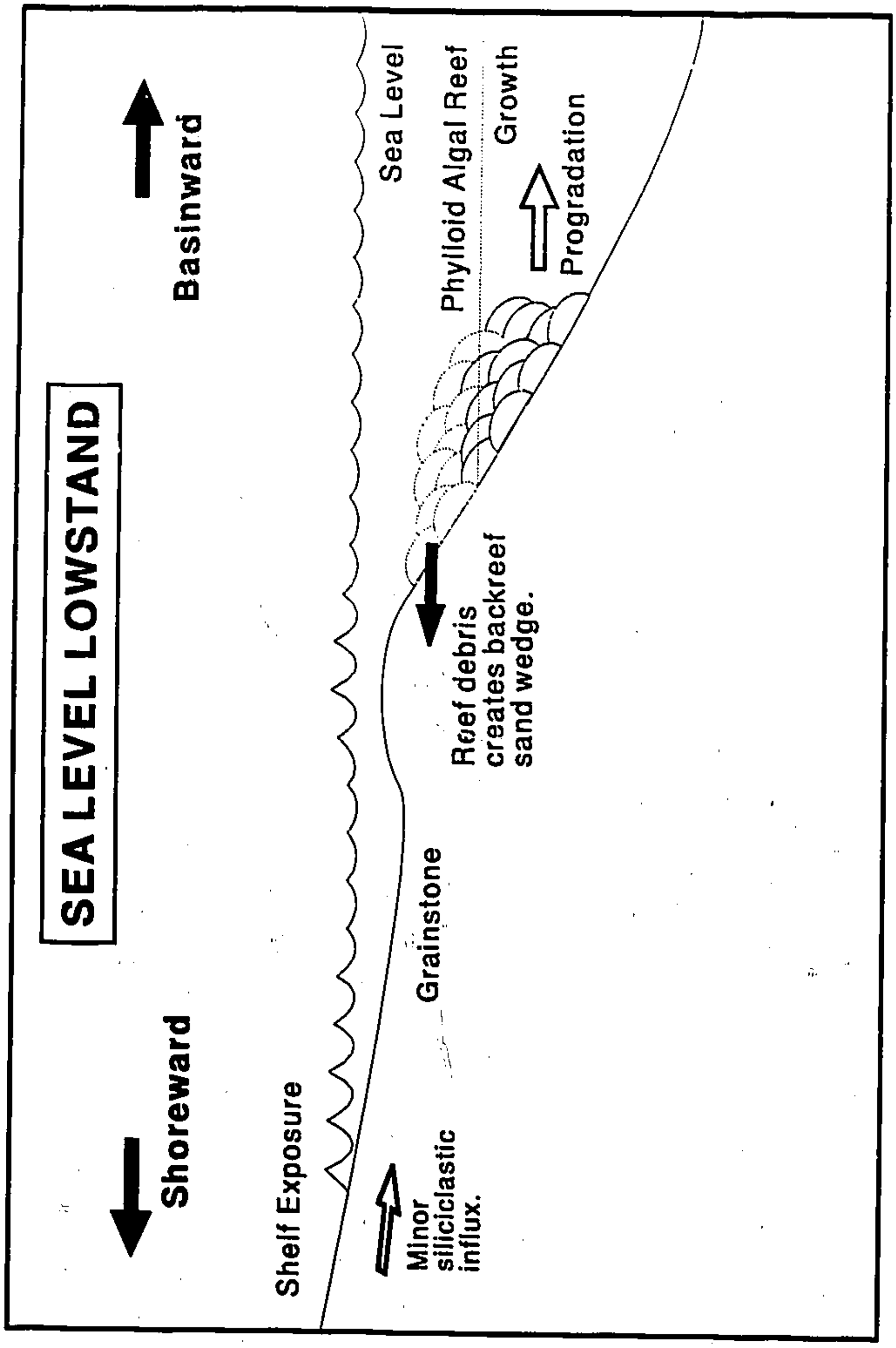
SEA LEVEL LOWSTAND
Basinward
Shoreward
Sea Level
Phylloid Algal Reef Growth
Progradation
Reef debris creates backreef sand wedge.
Grainstone
Shelf Exposure
Minor siliciclastic influx.

Figure 21. Idealized sea level highstand depositional model. Note aggradation of shelf edge reefs and development of debris flows.

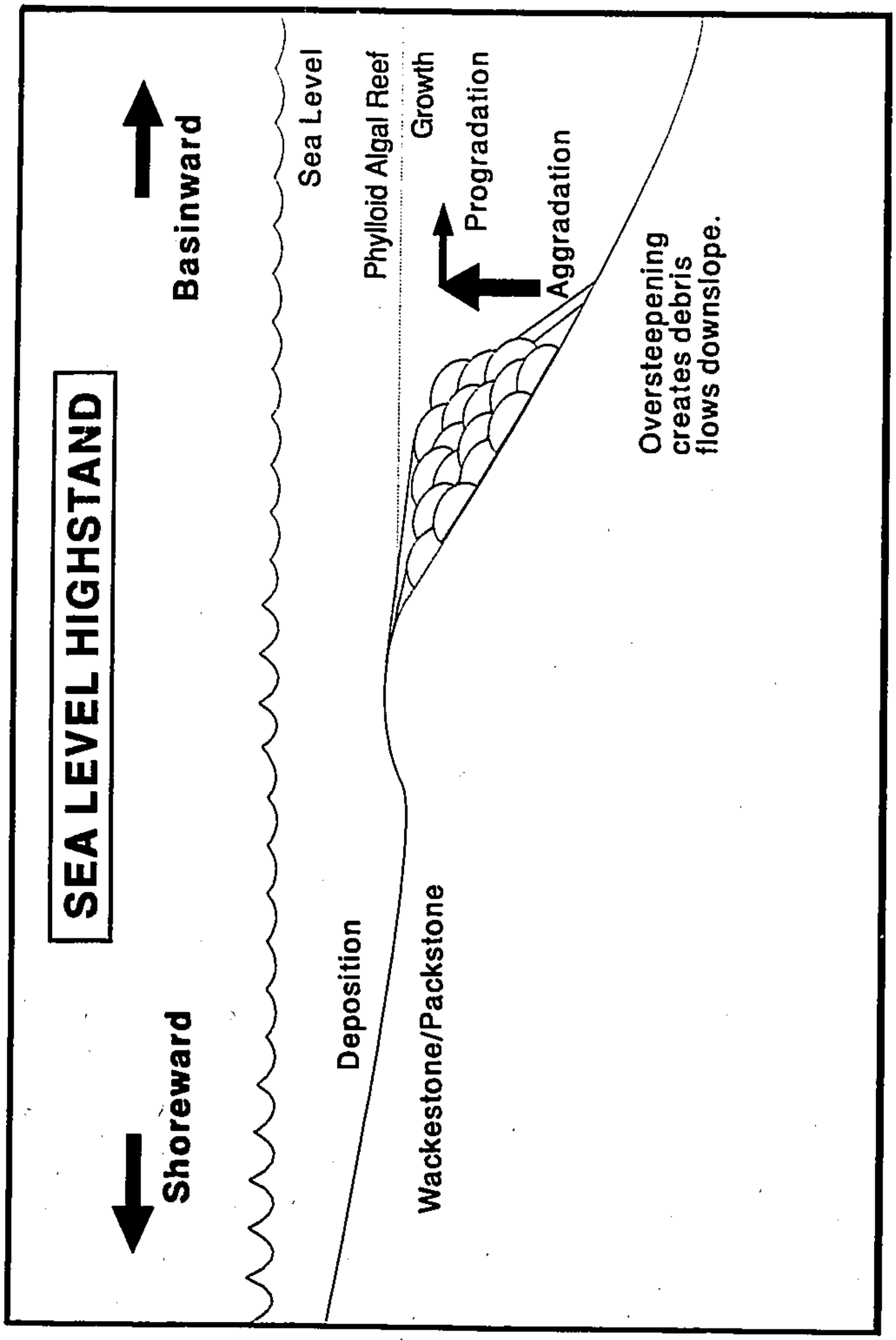
SEA LEVEL HIGHSTAND
Shoreward
Basinward
Sea Level
Deposition
Wackestone/Packstone
Phylloid Algal Reef
Growth
Progradation
Aggradation
Oversteepening
creates debris
flows downslope.

4.4 Analogues

4.4.1 Modern

Although there are numerous modern examples of rimmed platforms (e.g. adjacent to Florida, Belize and Queensland), they make poor analogues for the reefal shelf edge observed in the Upper Carboniferous Sverdrup Basin due to the biotic differences and the subsequent differing growth positions of these diverse organisms. In the modern oceans, metazoans construct the barrier reefs which develop on the outer shelf and grow to sea level. Conversely, the Nansen platform contains an outer shelf oolitic and bioclastic shoal while the carbonate algal buildups developed at the shelf edge in relatively deeper water. Because of these inherent and fundamental differences, ancient analogues are more appropriate in this study than modern ones.

4.4.2 Carboniferous

The Carboniferous characteristically has few large skeletal reefbuilders. Buildups are rich in phylloid algae and associated tubular foraminifera, bryozoans, stromatolites and *Tubiphytes* (James and Bourque, 1992). They generally occurred on slopes and inner parts of platforms.

Nansen buildups of the Sverdrup Basin are both age-equivalent to and morphologically similar to buildups in the Ural Mountains (Chuvashov, 1983), Spitsbergen and the Barents Sea (Bruce and Toomey, 1990; Beauchamp, 1992), northern Yukon (Davies, 1971), Idaho (Breuninger, 1976), and central and southwestern areas of the United States (Delaware Basin, Marathon Basin, Paradox Basin; Wilson, 1975). These studies have aided in the interpretation of the Nansen buildups and have also increased the interest of oil companies as some of these deposits are highly prospective. Important differences, however, result from the large extent of the Nansen shelf edge deposit and the extensive marine cementation present within the buildups.

4.4.3 Permian Reef Complex

The most obvious analogue for the Nansen shelf edge is the Permian Reef Complex (Capitan Reef) in West Texas and New Mexico. The Permian reef complex similarly consists of a submerged shelf edge reef system constructed dominantly of early marine cemented phylloid algae (Garber et al., 1989; Pray and Harris, 1989). The enormous amount of documentation on this deposit makes it an excellent comparative tool for the current study.

Although many similarities exist there are many differences apparent between the Sverdrup Basin and the Permian reef complex. The framework of the Capitan reef comprises not only phylloid algae but calcisponges as well (Garber et al., 1989). This biotic assemblage is typical of the "Chlorosponge" association, found in Tethyan regions (Flügel, 1982; Whalman, 1985; Beauchamp, 1994). Also different are the presence of a periodically exposed pisolitic shelf crest and extensive evaporites on the shelf, indicating a very restricted back reef environment in contrast to the Upper Carboniferous Sverdrup Basin. As well, there is a much larger siliciclastic component within the shelf-to-basinal succession of the Permian reef complex. This could have been due to a larger river influx or higher-standing clastic sources.

4.4.4 Reef Versus Mound

There is an ongoing debate as to what constitutes an ancient reef. James and Bourque (1992) described reefs as structures constructed by large, clonal elements capable of thriving in energetic environments, while mounds are structures built by smaller, delicate and/or solitary elements in tranquil settings. The buildups observed along the shelf edge of the Nansen Formation in the Sverdrup Basin do not fit easily into this classification scheme. Instead they combine elements of both reefs and mounds into their fabric.

Phylloid algae are small, fragile reef builders, often occurring in quiet water environments. However, along the Nansen shelf edge, extensive early marine cementation allowed these organisms to successfully colonize a relatively energetic environment and achieve substantial relief above the sea floor. The energy levels would have winnowed away much of the fine grained material, resulting in a largely "cementstone" reef core, especially in the shallower regions. Regardless of classification, these massive biogenic buildups are significant both in appearance and as aids in paleoenvironmental reconstruction.

For convenience, these buildups have been called reefs in this study, even though the constructors are anomalous for reefs as defined by James and Bourque (1992).

CHAPTER 5: ECONOMIC POTENTIAL

5.1 Introduction

Early geological studies of the Canadian Arctic Archipelago by the Geological Survey of Canada indicated that the area had good petroleum potential (Fortier et al., 1954; Douglas et al., 1963). The first well was drilled in 1962 and exploration flourished during the 1970's when the Arctic region of Canada piqued the interest of oil and gas companies. Since that time drilling activity has gradually declined (Embry et al., 1991) as economic constraints restricted frontier development.

During exploration numerous wells were drilled targeting Sverdrup Basin deposits (Powell, 1978; Beauchamp, 1987). Early interest focused on the Mesozoic formations but several wells (approximately 30) also penetrated portions of the upper Paleozoic succession in the search for potential reservoirs. No hydrocarbon discoveries have yet been made in Paleozoic sediments but good shows of oil and gas have been encountered indicating that the strata have the potential to contain significant reserves (Embry et al., 1991).

Little hope now remains for locating giant structural traps within the Sverdrup Basin. If exploration is to resume in Arctic Canada the focus will likely shift to the discovery of promising stratigraphic traps. The carbonate shelf and the numerous shelf, shelf edge and slope buildups are all suitable targets. This approach is more difficult and requires a multidisciplinary effort to successfully assess these features. A compilation of stratigraphic, sedimentologic, diagenetic and structural data is required to successfully guide subsurface explorationists. Upper Paleozoic basin analysis was begun by Beauchamp (1987), and continues to be a mandate of Arctic researchers. The current study presents only general remarks concerning the economic potential of the Nansen and Hare Fiord formations.

5.2 Diagenesis

Although a systematic diagenetic study was beyond the scope of the present study, petrographic observation of both thin sections and polished slabs allows a very preliminary indication of the various diagenetic processes within submarine and burial (and possibly minor meteoric) environments. These include: submarine and "burial" cementation, neomorphism, micritization, dissolution, dolomitization, silicification, bitumen inclusion and compaction (Figure 22).

Cements in the Nansen and Hare Fiord sediments, especially those of the shelf edge buildups, are the most obvious diagenetic products throughout the study area. Savard (1991) recognized evidence of three main diagenetic trends accounting for this process: 1) early marine cementation; 2) recrystallization of marine cements concurrent with late cementation during shallow burial, dominantly within the marine environment; and 3) continuing burial cementation at depth. Early marine cements were likely of aragonitic and high-Mg calcite mineralogy (Davies and Krouse, 1975; Davies, 1977; Davies and Nassichuk, 1990). Multiple generations of isopachous cements lined growth cavities within the reefs and rimmed reef-building organisms (Plate 5a-e). Fibrous calcite (including both radiaxial and nonradiaxial types) is the neomorphic product after original fibrous (bladed) to acicular magnesium calcite. The botryoidal calcite had an aragonite precursor (Davies, 1977). "Burial" cements include both blocky calcite (zoned ferroan and iron-depleted spar) and coarsely crystalline zoned dolomite. These occur in fractures and voids, dominantly in shelf and shelf edge environments but are also present in slope mounds.

Products of micritization and dissolution occur dominantly in the outer shelf and shelf edge deposits. Primary aragonitic fabrics are destroyed in each case. Micritization has also obscured primary textures. Dissolution occurred in two separate phases and allowed for replacement by early marine cements (early phase of dissolution - local

Figure 22. General diagenetic sequence for the Nansen and Hare Fiord formations in the study area. Early diagenetic processes may also have included short-lived meteoric diagenesis resulting from episodic subaerial exposures.

DIAGENETIC SEQUENCE

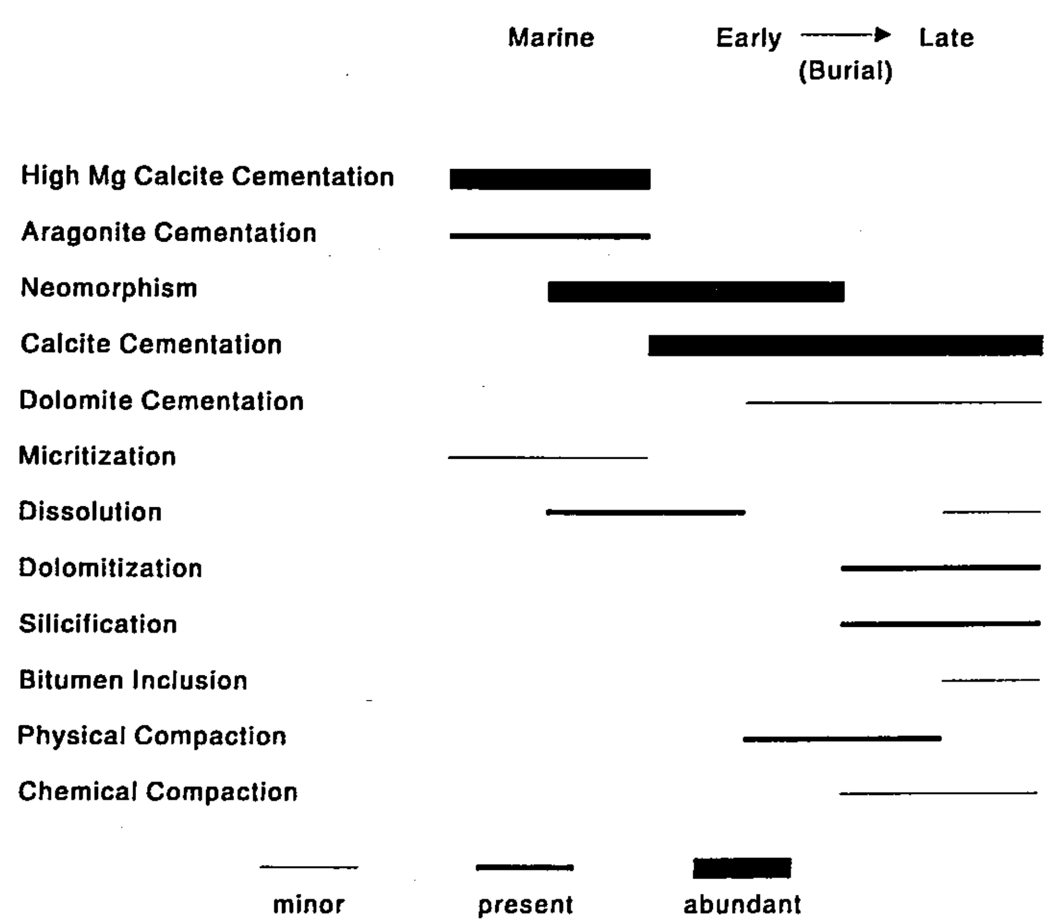

meteoric effects) or later burial cements (late phase of dissolution). Large scale dissolution due to prolonged subaerial exposure could also have resulted in extensive formation of secondary porosity as observed by Beauchamp (1992) on southwestern Ellesmere Island but was not well developed within the current study area.

The degree of dolomitization was variable throughout the study area. Locally, complete segments of both shelf and shelf edge sediments were pervasively dolomitized (Plate 8f). Beauchamp (1987) suggested that dolomitizing fluids may have had a hydrothermal origin and the proximity of synsedimentary normal faults could have influenced the dolomitization potential of the deposits. Fractures and residual interparticle and framework porosity could also provide passage for diagenetic fluids. Dolomitization is a late diagenetic process as its products are superimposed upon primary depositional components and submarine cements.

Silicification was most common in the slope-to-basinal deposits of the Hare Fiord Formation. Both silica replacement of primary fabrics and silica cements occur in some sediments. Remobilization of biogenic opal after solution-replacement of sponge spicules by calcite may have been a major source of silica in these rocks (Davies, 1977). Silicification appears also to have preferentially followed pre-existing burrows.

Bitumen inclusion was a very minor diagenetic component in the study area. Bitumen is the thermal alteration by-product of liquid hydrocarbons. The introduction of hydrocarbons into the pore system occurred contemporaneously with the thermal maturation of the organic matter of the source rocks and reef rocks under conditions of moderate burial (1500 - 4000 m; Davies, 1976). It was most prevalent in completely dolomitized rocks of shelf and shelf edge origin.

Deep burial compaction caused by overburden preferentially affected zones not containing early marine cements, namely the slope-to-basin deposits and some shelf areas. Stylolitization, grain-to-grain pressure solution and grain crushing were the most visible small scale effects of both physical and chemical compaction.

5.2.1 Porosity

The evolution of porosity follows that of diagenesis. Initial high porosities occurred in the Nansen reef buildup complexes. Growth cavities, and inter- and intra-particle porosities combined to reach greater than 75% porosity. Such high porosity and effective permeability provided space for active cementation and internal geopetal sedimentation. These processes led to the stabilization and preservation of these structures but also reduced primary porosity substantially. Much of the remaining porosity was occluded by later "burial" cements, including various ferroan and non-ferroan sparry calcite and saddle dolomite phases.

Secondary porosity-enhancing processes thus create the only porosity currently observed within the reefs. Secondary porosity was produced by two distinct processes, dolomitization and selective dissolution. Dolomitization was a local phenomenon in the Sverdrup Basin. Within the study area only a few reefs, or parts of reefs, were affected. The extent of dolomitization varied from partial to complete. Where dolomitization was complete it resulted in a coarsely crystalline porous fabric in which only ghosts of the primary features can be recognized (Plate 8f). Late dissolution of primary carbonates led to the creation of secondary pore space as some of the primary depositional and submarine diagenetic fabrics were dissolved to various extents. Dissolution was not fabric-selective, affecting lime mud matrix, fossils and submarine cements indiscriminately resulting in irregular mm- to cm-sized cavities (Beauchamp, 1992). This was not a very effective porosity producer in the study area.

Shelf deposits followed a similar porosity pathway although initial porosity was lower than that of the reef buildups, depending on initial percentage of lime mud. Shelf deposits also experienced a much lower degree of early marine cementation. Slope-to-basin deposits contained much lower initial porosity than shelf and shelf edge deposits and porosity reduction occurred as a result of dolomitization, silicification and compaction. Turbidite deposits and debris flows followed porosity reduction patterns similar to those on the shelf and shelf edge and possibly retained higher porosity and permeability than surrounding hemipelagic slope deposits. These might act as conduits to transport hydrocarbons from basin source rocks to shelf and shelf edge reservoirs (Coniglio and Dix, 1992).

5.3 Hydrocarbon Source Potential

The dark shales of the Hare Fiord Formation appear to contain abundant organic matter. Geochemical data suggested that the Sverdrup Basin has source potential to become a major hydrocarbon province (Baker et al., 1975). Beauchamp et al., (1987) recorded unusually high carbon isotope ratios which have been interpreted as preferential transport and preservation of organic matter in central parts of the basin. This could indicate that basinal Hare Fiord Formation, and other rocks of deep water origin within the Sverdrup Basin, could and did act as potential hydrocarbon source rocks.

Henderson (1988) and Utting et al. (1989), using the conodont colour alteration index, the thermal alteration index, and the reflectance of vitrinite and bitumen, determined that Upper Carboniferous sediments within the subsurface along the southern margin of the Sverdrup Basin lie within the oil window of organic matter maturation. Therefore, it is possible that potential reservoirs exist in that area.

5.4 Analogues

Numerous sedimentary analogues to the Upper Carboniferous Sverdrup Basin are also significant hydrocarbon producing zones, notably the Paradox Basin and the Barents Sea. Since the Nansen and Hare Fiord formations are so similar to deposits of these prospective regions, they should be attractive areas for hydrocarbon exploration.

5.4.1 Paradox Basin

The Paradox Basin of southeastern Utah and southwestern Colorado exhibits similar phylloid algal buildups developed in a shelf-margin setting as does the Nansen Formation of the Sverdrup Basin (Ginsburg et al., 1971; Choquette, 1983). Unlike the Sverdrup examples, these reefal facies maintain extensive primary and secondary porosity and thus form productive reservoirs. Apparently Paradox Basin strata did not experience such extensive early submarine cementation as was noted in the Sverdrup Basin and, therefore, did not experience the subsequent porosity loss associated with this process.

5.4.2 Barents Sea

The Carboniferous and Permian sequences in the Sverdrup Basin and on Svalbard and within the Barents Sea were influenced by the same tectonic and climatic conditions (Figure 5; Embry, 1992; Davies and Nassichuk, 1991). Because of the physical connection between these circum-Arctic regions the sediments are strongly analogous. This analogy is important as hydrocarbon exploration is ongoing in the Barents Sea but little is currently known about the sedimentological history of that basin.

The large Barents Sea reefs targeted for drilling are unlike those exposed on Svalbard but appear to be of similar size and composition to those in the Nansen Formation of the Sverdrup Basin. By studying the Nansen outcrops more can be learned about the Barents Sea deposits and future exploration and drilling can be made more efficient (Beauchamp, 1992). Additionally, exploration success in the Barents Sea could promote the re-evaluation of subsurface Sverdrup Basin deposits as potential hydrocarbon targets for Canadian Arctic exploration.

5.5 Recommendations

The Nansen buildups in the study area indicate the possibility of potential reservoirs in the subsurface Sverdrup Basin. Similar buildups have been identified in the subsurface of the southern regions of the Sverdrup Basin (Beauchamp and Lamirande, 1990). Exploration should concentrate on shelf edge-type buildups which have undergone extensive dolomitization as these are the most prospective lithologies in the study area.

The Nansen shelf edge reefs are even more valuable, however, as an analogue for continued exploration in areas that have already proven to be hydrocarbon-bearing (especially the Barents Sea). The excellent exposures found on northwestern Ellesmere Island are difficult to surpass anywhere in the world and explorationists should take advantage of this resource in their continued efforts.

CHAPTER 6: CONCLUSIONS

The Upper Carboniferous Nansen and Hare Fiord formations in the study area on northwestern Ellesmere Island represent three distinct depositional environments: 1) mid- to outer shelf (Nansen Formation); 2) shelf edge (Nansen Formation); and 3) slope-to-basin (Hare Fiord Formation). The shelf deposits comprise light coloured, fossiliferous, cyclic packstone-grainstone. The shelf edge facies is a light coloured, massive, phylloid algal-dominated reef complex. The slope-to-basin deposits are dark, fossil-poor, cyclic, mixed carbonate and siliciclastic sediments.

The strata can be grouped in 14 lithofacies representing: 1) shelf deposits composed of Crinoid-Bryozoan, Foraminiferal, Peloidal, Oolitic, Chaetetid, Beresellid and Dasycladacean Facies; 2) shelf edge deposits dominated by the Phylloid Algal and Bryozoan Facies; and 3) slope deposits represented by the occurrence of Calcisiltite, Siltstone, Shale, Calcarenite and Debrite Facies.

Depositional facies are commonly arranged in distinct high frequency cycles depending upon their environment of deposition. These cycles represent shallowing upward successions controlled by high frequency sea level fluctuations.

The elongate reef tract delineating the shelf edge is a unique feature. Similar well developed, extensive buildup complexes were highly unusual during Late Carboniferous time when most buildups were smaller scale features occurring on the shelf or slope environments. In addition it combines attributes of both reef (shelf edge position, elongate feature, moderate energy growth environment, and high relief) and mound (fragile reef builders, small size organisms, and growth window below active wave base) development.

The potential of the Nansen reef buildups as reservoir rocks has been largely destroyed by extensive cementation and infilling of primary pore systems by early diagenetic marine cements. However, there is still a potential for the discovery of hydrocarbons within the Nansen Formation in the subsurface of the southern Sverdrup

Basin. From field investigations it was seen that highly dolomitized regions within the shelf and shelf edge deposits could form effective reservoirs. The Hare Fiord Formation could be the source rock to provide the hydrocarbons for these updip stratigraphic traps.

6.1 Epilogue

Future Work

Previous diagenetic studies in the Sverdrup Basin have provided either a very broad, yet brief, overview of the entire basin (Savard, 1991), or have detailed a single, specific aspect (Davies and Nassichuk, 1990; Besemann, 1993). This leaves a large gap in the knowledge of the diagenetic processes that acted upon Sverdrup Basin sediments.

The current study has developed a stratigraphic and sedimentologic framework for the Moscovian to Kasimovian platform-to-basin sediments of northwestern Ellesmere Island based upon extensive field investigation and lithologic sampling. A systematic diagenetic analysis can now be conducted upon these same rocks to obtain a complete diagenetic history for an entire regressive sedimentologic sequence within the basin. This type of in-depth and well constrained analysis is required to obtain a better understanding of the diagenetic processes which have acted upon the Sverdrup Basin sediments during their history.

Further study of basinal shales and siltstones should also be pursued. Preliminary studies have been undertaken (Baker et al., 1975; Powell, 1978; Beauchamp, 1987; Henderson, 1988; Utting et al., 1989) to determine the hydrocarbon-producing potential of these deep water deposits. A more detailed study specifically on the Upper Paleozoic basinal deposits is required to fully realize the source potential, or lack thereof, within the Sverdrup Basin. If the sediments prove to be a rich hydrocarbon source it would indicate the need for further oil and gas exploration within the porous updip carbonate and siliciclastic deposits of the nearshore Sverdrup Basin formations.

There is also a need for more detailed mapping of the shelf edge facies and Nansen-Hare Fiord facies change which was only begun with this study. This type of analysis could reveal more information about the complexities of the shelf-to-basin transition. As is already becoming apparent, lateral changes from a reefal shelf edge to a ramp environment occur over relatively short distances (Benoit Beauchamp, pers. comm. 1994). The reefal areas formed actively prograding points over a fairly steep upper slope. In comparison, the ramp setting developed in embayments of the shelf-basin boundary over a moderate slope gradient.

REFERENCES

Baker, D.A., Illich, H.A., Martin, S.J. and Landin, R.R.
1975: Hydrocarbon source potential of sediments in the Sverdrup Basin; *in* Yorath, C.J., Parker, E.R. and Glass, D.J. (eds.); Canada's Continental Margins and Offshore Petroleum Exploration, Canadian Society of Petroleum Geologists, Memoir 4, p. 545-556.

Beauchamp, B.
1987: Stratigraphy and facies analysis of the Upper Carboniferous to Lower Permian Canyon Fiord, Belcher Channel and Nansen formations, southwestern Ellesmere Island; Unpublished Ph.D. thesis, University of Calgary, 370p.

1992: Carboniferous and Permian reefs of Sverdrup Basin, Canadian Arctic: an aid to Barents Sea exploration; *in* Vorren, T.O., Bergsager, E., Dahl-Stamnes, Ø.A., Holter, E. Johansen, B., Lie, E. and Lund, T.B. (eds.); Arctic Geology and Petroleum Potential, NPF Special Publication 2, p. 217-241.

1993: Tectonic cycles and the origin of Upper Paleozoic low-order sequences in the Sverdrup Basin, Canadian Arctic; Canadian Society of Petroleum Geologists, Annual Convention Program and Abstracts, p. 20.

1994: Permian climatic cooling in the Canadian Arctic; *in* Klein, G.D. (ed.); Pangea: Paleoclimate, Tectonics, and Sedimentation During Accretion, Zenith, and Breakup of a Supercontinent, Boulder, Colorado, Geological Society of America, Special Paper 288, p. 229-246.

in press: Permian history of Arctic North America; *in* Scholle, P.A., Peryt, T.M. and Ulmer-Scholle, D.S. (eds.); The Permian of Northern Pangea, vol. 1: Paleogeography, Paleoclimates, and Stratigraphy, New York, Springer-Verlag.

Beauchamp, B., Davies, G.R. and Nassichuk, W.W.
1988: Upper Carboniferous to Lower Permian Palaeoaplysina-phylloid algal buildups, Canadian Arctic Archipelago; *in* Geldsetzer, H.H.J, James, N.P. and Tebbutt, G.E. (eds.); Reefs, Canada and Adjacent Areas, Canadian Society of Petroleum Geologists, Memoir 13, p. 590-599.

Beauchamp, B., Harrison, J.C., and Henderson, C.M.
1989a: Upper Paleozoic stratigraphy and basin analysis of the Sverdrup Basin, Canadian Arctic Archipelago: Part 1, time frame and tectonic evolution; *in* Current Research, Part G, Geological Survey of Canada, Paper 89-1G, p. 105-113.

1989b: Upper Paleozoic stratigraphy and basin analysis of the Sverdrup Basin, Canadian Arctic Archipelago: Part 2, transgressive-regressive sequences; *in* Current Research, Part G, Geological Survey of Canada, Paper 89-1G, p. 115-124.

Beauchamp, B. and Henderson, C.M.

1994: The Lower Permian Raanes, Great Bear Cape and Trappers Cove formations, Sverdrup Basin, Canadian Arctic: stratigraphy and conodont zonation; Canadian Society of Petroleum Geologists Bulletin, vol. 42, p. 562-597.

Beauchamp, B. and Lamirande, J.

1990: The BP Graham C-52 well and upper Paleozoic subsurface stratigraphy in the Canadian Arctic; *in* Current Research, Part D, Geological Survey of Canada, Paper 90-1D, p. 115-122.

Beauchamp, B., Mayr, U. and Harrison, J.C.

in press: Carboniferous and Permian stratigraphic sequences on Hvitland Peninsula and adjacent areas, NW Ellesmere Island; *in* Current Research, Geological Survey of Canada.

Beauchamp, B., Oldershaw, A.E., and Krouse, H.R.

1987: Upper Carboniferous to Upper Permian ^{13}C-enriched primary carbonates in the Sverdrup Basin, Canadian Arctic: comparisons to coeval western North American ocean margins; Chemical Geology, vol. 65, p. 391-413.

Besemann, K.

1993: Petrography, carbon and oxygen isotopes of carbonate cements from Moscovian age reef mounds, Sverdrup Basin, Canadian Arctic Archipelago; Unpublished B.Sc. thesis, University of Ottawa, 49 p.

Bonham-Carter, G.F.

1966: The geology of the Pennsylvanian sequence of the Blue Mountains, northern Ellesmere Island; Unpublished Ph.D. thesis, University of Toronto, 172 p.

Breuninger, R.H.

1976: Palaeoaplysina (hydrozoan?) carbonate buildups from Upper Paleozoic of Idaho; American Association of Petroleum Geologists Bulletin, vol. 60, p. 584-607.

Bruce, J.R. and Toomey, D.F.

1990: Paleozoic bioherm occurrences on the Finnmark Shelf: analogues and regional significance; *in* International Conference on Arctic Geology and Petroleum Potential, Tromsø, Abstracts, p. 22.

Brunton, F.R., James, N.P and Besemann, K.
1993: Foreslope bryozoan-cementstone reef mounds of Moscovian age, Sverdrup Basin: possible ancient analogues for modern lithoherms in the straits of Florida; Canadian Society of Petroleum Geologists, Annual Convention Program and Abstracts, p. 41.

Choquette, P.W.
1983: Platy algal reef mounds, Paradox Basin; *in* Scholle, P.A., Bebout, D.G. and Moore, C.H. (eds.); Carbonate Depositional Environments, American Association of Petroleum Geologists, Memoir 33, p. 454-462.

Chuvashov, B.I.
1983: Permian reefs of the Urals; Facies, vol. 8, p. 191-212.

Coniglio, M. and Dix, G.R.
1992: Carbonate slopes; *in* Walker, R.G. and James, N.P. (eds.); Facies models: response to sea level change, Geological Association of Canada, p. 349-373.

Davies, G.R.
1971: A Permian hydrozoan mound, Yukon Territory; Canadian Journal of Earth Sciences, vol. 8, p. 973-988.

1976: "Bitumen" in post-burial diagenetic calcite; *in* Report of Activities, Part C, Geological Survey of Canada, Paper 76-1C, p. 107-114.

1977: Turbidites, debris sheets, and truncation structures in Upper Paleozoic deep-water carbonates of the Sverdrup Basin, Arctic Archipelago; *in* Deep-Water Carbonate Environments, Society of Economic Paleontologists and Mineralogists, Special Publication No. 25, p. 221-247.

Davies, G.R. and Krouse, H.R.
1975: Carbon and oxygen isotopic composition of Late Paleozoic calcite cements, Canadian Arctic Archipelago - preliminary results and interpretation; Report of Activities, Part B, Geological Survey of Canada, Paper 75-1, p. 215-220.

Davies, G.R. and Nassichuk, W.W.
1975: Subaqueous evaporites of the Carboniferous Otto Fiord Formation, Canadian Arctic Archipelago: A summary; Geology, vol. 3, p. 273-278.

1988: An Early Carboniferous (Viséan) lacustrine oil shale in Canadian Arctic Archipelago; American Association of Petroleum Geologists Bulletin, vol. 72, p. 8-20.

1990: Submarine cements and fabrics in Carboniferous to Lower Permian, reefal, shelf margin and slope carbonates, northwestern Ellesmere Island, Canadian Arctic Archipelago; Geological Survey of Canada, Bulletin 399, 77 p.

1991: Carboniferous and Permian history of the Sverdrup Basin, Arctic Islands; Chapter 13 *in* Trettin, H.P. (ed.); Geology of the Innuitian Orogen and Arctic Platform of Canada and Greenland, Geological Survey of Canada, Geology of Canada, no. 3, p. 345-367.

Davies, G.R., Nassichuk, W.W. and Beauchamp, B.,
1988: Upper Carboniferous "Waulsortian" reefs, Canadian Arctic Archipelago; *in* Geldsetzer, H.H.J., James, N.P. and Tebbutt, G.E. (eds.); Reefs, Canada and Adjacent Areas, Canadian Society of Petroleum Geologists, Memoir 13, p. 658-666.

Dawes, P.R. and Christie, R.L.
1982: History of exploration and geology in the Nares Strait region; *in* Dawes, P.R. and Kerr, J.W. (eds.); Nares Strait and the drift of Greenland: a conflict in plate tectonics, Meddelelser Om Grønland, Geoscience No. 8, p. 19-36.

Dickson, J.A.
1966: Carbonate identification and genesis as revealed by staining; Journal of Sedimentary Petrology, vol. 36, p. 491-505.

Douglas, R.J.W., Norris, D.K., Thorsteinsson, R. and Tozer, E.T.
1963: Geology and petroleum potentialities of northern Canada; World Petroleum Congress Proceedings, Frankfurt, Section 1, Paper 7, p. 519-571.

Ekdale, A.A, Bromley, R.G. and Pemberton, S.G. (eds.)
1984: Ichnology: the use of trace fossils in sedimentology and stratigraphy; Society of Economic Paleontologists and Mineralogists, Short Course Notes 15, 317 p.

Elliott, G.F.
1991: Dasycladacean algae of the Palaeozoic and Mesozoic; *in* Riding, R. (ed.); Calcareous Algae and Stromatolites, Springer-Verlag, Berlin, p. 125-130.

Embry, A.R.
1992: Crockerland - the northwest source area for the Sverdrup Basin, Canadian Arctic Islands; *in* Vorren, T.O., Bergsager, E., Dahl-Stamnes, Ø.A., Holter, E., Johansen, B., Lie, E. and Lund, T.B. (eds.); Arctic Geology and Petroleum Potential, NPF Special Publication 2, p. 205-216.

Embry, A.F., Powell, T.G. and Mayr, U.
1991 Petroleum resources, Arctic Islands; *in* Trettin, H.P. (ed.); Chapter 20 of Geology of the Innuitian Orogen and Arctic Platform of Canada and Greenland, Geological Survey of Canada, Geology of Canada, no. 3, p. 517-525.

Flügel, E.
1982: Microfacies Analysis of Limestones; Springer-Verlag, Berlin, 633 p.

Fortier, Y.O., Blackadar, R.G., Glenister, B.F., Greiner, H.R., McLaren, D.J., McMillan, N.J., Norris, A.W., Roots, E.F., Souther, J.G., Thorsteinsson, R. and Tozer, E.T.
1963: Geology of the north-central part of the Arctic Archipelago, Northwest Territories (Operation Franklin), Geological Survey of Canada Memoir 320, 671 p.

Fortier, Y.O., McNair, A.H. and Thorsteinsson, R.
1954: Geology and petroleum possibilities in Canadian Arctic Islands; American Association of Petroleum Geologists Bulletin, vol. 38, p. 2075-2109.

Garber, R.A., Grover, G.A. and Harris, P.M.
1989: Geology of the Capitan shelf margin - subsurface data from the northern Delaware Basin; *in* Harris, P.M. and Grover, G.A. (eds.); Subsurface and outcrop examination of the Capitan shelf margin, northern Delaware Basin, Society of Economic Paleontologists and Mineralogists, Core Workshop no. 13, p. 3-269.

Ginsburg, R.N., Rezak, R. and Wray, J.L.
1971: Geology of calcareous algae, notes for a short course; Rosenstiel School of Marine and Atmospheric Science, Comparative Sedimentology Laboratory, Miami, 61 p.

Goldhammer, R.K., Dunn, P.A. and Hardie, L.A.
1990: Depositional cycles, composite sea-level changes, cycle stacking patterns, and the hierarchy of stratigraphic forcing: examples from Alpine Triassic platform carbonates; Geological Society of America Bulletin, vol. 102, p. 535-562.

Groves, J.R., Nassichuk, W.W., Lin, R. and Pinard, S.
1994: Middle Carboniferous fusulinacean biostratigraphy, northern Ellesmere Island (Sverdrup Basin, Canadian Arctic Archipelago); Geological Survey of Canada, Bulletin 469, 55 p.

Harker, P. and Thorsteinsson, R.
1960: Permian rocks and faunas of Grinnell Peninsula, Arctic Archipelago; Geological Survey of Canada, Memoir 309, 89 p.

Harrison, J.C., Mayr, U. and Beauchamp, B.
in press: Preliminary observations on the structural geology of the Hvitland Peninsula, northwestern Ellesmere Island, Arctic Canada; *in* Current Research, Geological Survey of Canada.

Heckel, P.H.
1984: Factors in Midcontinent Pennsylvanian limestone deposition; *in* Hyne, N.J. (ed.); Limestone of the Mid-Continent, Tulsa Geological Society, Special Publication 2, p. 25-50.

Henderson, C.M.
1988: Conodont paleontology and biostratigraphy of the Upper Carboniferous to Lower Permian Canyon Fiord, Belcher Channel, Nansen, an unnamed, and Van Hauen formations, Canadian Arctic Archipelago; Unpublished Ph.D. thesis, University of Calgary, 287 p.

James, N.P. and Bourque, P.-A.
1992: Reefs and mounds; *in* Walker, R.G. and James, N.P. (eds.); Facies models: response to sea level change, Geological Association of Canada, p. 323-347.

James, N.P. and Mountjoy, E.W.
1983: Shelf-slope break in fossil carbonate platforms: an overview; *in* Stanley, D.J. and Moore, G.T. (eds.); The shelfbreak: critical interface on continental margins, Society of Economic Paleontologists and Mineralogists, Special Publication 33, p. 186-206.

Kells, M.P, Beauchamp, B. and Desrochers, A.
in press: Artinskian-Kungurian (Lower Permian) stratigraphy (Raanes, Great Bear Cape and Trappers Cove formations), Hvitland Peninsula and adjacent areas, NW Ellesmere Island, *in* Current Research, Geological Survey of Canada.

Kershaw, S. and West, R.R.
1991: Chaetetid growth form and its controlling factor; Lethaia, vol. 24, p. 333-346.

Lin, R., Ross, C.A. and Nassichuk, W.W.
1991: Upper Moscovian (Desmoinesian) fusulinaceans from the type section of the Nansen Formation, Ellesmere Island, Arctic Archipelago; Geological Survey of Canada, Bulletin 418, 121 p.

Lustig, L.D.
1971: Mid-Pennsylvanian chaetetids (Tabulata), from the Bird Springs Formation in southern Nevada; Unpublished M.Sc. thesis, University of California at Los Angeles, 147 p.

Macintyre, I.G.
1985: Submarine cements - the peloidal question; *in* Schneidermann, N. and Harris, P.M. (eds.); Carbonate Cements, Society of Economic Paleontologists and Mineralogists, Special Publication No. 36, p. 109-116.

Mamet, B.
1991: Carboniferous calcareous algae; *in* Riding, R. (ed.); Calcareous algae and stromatolites, Springer-Verlag, Berlin, p. 370-451.

Mamet, B., Roux, A. and Nassichuk, W.W.
1987: Algues Carbonifères et Permiennes de l'Arctique canadien; Geological Survey of Canada, Bulletin 342, 143 p.

Marcantel, J.
1975: Late Pennsylvanian and Early Permian sedimentation in northeast Nevada; American Association of Petroleum Geologists Bulletin, vol. 59, p. 2079-2098.

Middleton, G.V. and Hampton, M.A.
1976: Subaqueous sediment transport and deposition by sediment gravity flows; *in* Stanley, D.J. and Swift, D.J.P. (eds.); Marine sediment transport and environmental management, John Wiley and Sons, New York, p. 197-217.

Morin, J.
1992: Facies analysis of Lower Permian cyclic carbonates, west-central Ellesmere Island, Canadian Arctic; Unpublished M.Sc. thesis, University of Ottawa, 164p.

Morin, J., Desrochers, A. and Beauchamp, B.
1994: Facies analysis of Lower Permian platform carbonates, Sverdrup Basin, Canadian Arctic Archipelago; Facies, vol. 31, p. 105-130.

Mullins et al., 1985

Nassichuk, W.W.
1975a: Carboniferous ammonoids and stratigraphy in the Canadian Arctic Archipelago; Geological Survey of Canada, Bulletin 237, 240 p.

1975b: The stratigraphic significance of Permian ammonoids on Ellesmere Island; Geological Survey of Canada Paper 75-1B, p. 277-283.

Nassichuk, W.W. and Bamber, E.W.
1978: Middle Pennsylvanian biostratigraphy, eastern Cordillera and Arctic islands, Canada - A summary; *in* Stelck, C.R. and Chatterton, B.D.E. (eds.); Western and Arctic Canadian Biostratigraphy,. Geological Association of Canada, Special Paper 18, p. 395-413.

Nassichuk, W.W. and Davies, G.R.
1980: Stratigraphy and sedimentation of the Otto Fiord Formation, a major Mississippian-Pennsylvanian evaporite of subaqueous origin in the Canadian Arctic Archipelago; Geological Survey of Canada, Bulletin 286, 87 p.

Nassichuk, W.W. and Wilde, G.L.
1977: Permian fusulinaceans and stratigraphy at Blind Fiord, southwestern Ellesmere Island; Geological Survey of Canada, Bulletin 268, 59 p.

Nelson, C.S.
1978: Temperate shelf carbonate sediments in the Cenozoic of New Zealand; Sedimentology, vol. 25, p. 737-771.

Pemberton, S.G., MacEachern, J.A. and Frey, R.W.
1992: Trace fossil facies models: environmental and allostratigraphic significance; *in* Walker, R.G. and James, N.P. (eds.); Facies models: response to sea level change, Geological Association of Canada, p. 47-72.

Pinard, S.
1990: Taxonomie des petits foraminifères du Carbonifère-Permien inférieur du bassin de Sverdrup, Arctique canadien. Unpublished Ph.D. thesis, Université de Montréal, Montréal, Québec, 782 p.

Powell, T.G.
1978: An assessment of the hydrocarbon source rock potential of the Canadian Arctic Islands; Geological Survey of Canada, Paper 78-12, 82 p.

Pray, L.C. and Harris, P.M.
1989: The Capitan Reef Complex, West Texas and New Mexico; Permian Basin Section, Society of Economic Paleontologists and Mineralogists, Field Trip no. 1, seminar.

Rao, C.P.
1981: Criteria for recognition of cold-water carbonate sedimentation: Berriedale Limestone (Lower Permian), Tasmania, Australia; Journal of Sedimentary Petrology, vol. 51, p. 491-506.

1988: Paleoclimate of some Permo-Triassic carbonates of Malaysia; Sedimentary Geology, vol. 60, p. 163-172.

Savard, M.
1991: Calcite cements in carbonates of the Sverdrup Basin, Canadian Arctic Archipelago; Unpublished Ph.D. thesis, University of Ottawa, 209 p.

Schei, P.
1903: Summary of geological results (The Second Norwegian North Polar Expedition in the "Fram", 1898-1902); Geographical Journal, vol. 22, p. 56-65.

Scotese, C.R., Bambach, R.K., Barton, C., Van der Voo, R. and Ziegler, A.M.
1979: Paleozoic base maps; Journal of Geology, vol. 87, p. 217-277.

Seilacher, A.
1967: Bathymetry of trace fossils; Marine Geology, vol. 5, p. 413-428.

Sherry, C.T., Beauchamp, B. and Desrochers, A.
1993: Late Carboniferous shelf-to-basin transition, NW Ellesmere Island, Canadian Arctic; Canadian Society of Petroleum Geologists, Annual Convention Program and Abstracts, p. 281.

Smith, A.G., Hurley, A.M. and Briden, J.C.
1981: Phanerozoic Continental World Maps; Cambridge University Press, Cambridge, 102 p.

Spaw, J.M.
1977: Paleo-environments of Middle Pennsylvanian *Chaetetes* lithotype, Texas and New Mexico; Unpublished M.Sc. thesis, Rice University, unknown p.

Stanley, D.J. and Moore, G.T. (eds.)
1983: The Shelfbreak: Critical Interface on Continental Shelf Margins; Society of Economic Paleontologists and Mineralogists, Special Publication No. 33, 467 p.

Stemmerik, L.
1988: Chaetetid bioherm, Upper Carboniferous, Holm Land, eastern north Greenland; *in* Geldsetzer, H.H.J., James, N.P. and Tebbutt, G.E. (eds.); Reefs, Canada and Adjacent Areas, Canadian Society of Petroleum Geologists, Memoir 13, p. 688-689.

Stemmerik, L. and Worsley, D.
1989: Late Palaeozoic sequence correlations, North Greenland, Svalbard and the Barents Shelf; *in* Collinson, J.D. (ed.); Correlation in hydrocarbon exploration, p. 99-111.

Suchy, D.R. and West, R.R.
1988: A Pennsylvanian cryptic community associated with laminar chaetetid colonies; Palaios, vol. 3, p. 404-412.

Thériault, P.
1991: Synrift sedimentation in the Upper Carboniferous Canyon Fiord Formation, SW Ellesmere Island, Canadian Arctic; Unpublished M.Sc. thesis, University of Ottawa, 210 p.

Thériault, P. and Desrochers, A.
1993: Carboniferous calcretes in the Canadian Arctic; Sedimentology, vol. 40, p. 449-465.

Thompson, M.L.
1964: Fusulinacea; *in* Moore, R.C. (ed.); Treatise on Invertebrate Paleontology Part C Protista 2 vol. 1, The Geological Society of America and the University of Kansas Press, Lawrence, p. c358-c436.

Thorsteinsson, R.
1974: Carboniferous and Permian stratigraphy of Axel Heiberg Island and western Ellesmere Island, Canadian Arctic Archipelago; Geological Survey of Canada, Bulletin 224, 115 p.

Thorsteinsson, R. and Tozer, E.T.
1957: Geological investigations in Ellesmere and Axel Heiberg Islands, 1956; Arctic, vol. 10, p. 3-31.

1970: Geology of the Arctic Archipelago; *in* Douglas, R.J.W. (ed.); Geology and economic minerals of Canada, Geological Survey of Canada, Economic Geological Report no. 1, p. 548-590.

Trettin, H.P.
1989: The Arctic Islands; *in* Bally, A.W. and Palmer, A.R. (eds.); The Geology of North America - An overview, Boulder, Colorado, Geological Society of America, The Geology of North America, Volume A, p. 349-370.

Troelsen, J.C.
1950: Contributions to the geology of northwest Greenland, Ellesmere Island and Axel Heiberg Island; Meddelelser Om Grønland, Bd. 149, Nr. 7, p. 1-86.

1952: Geological investigations in Ellesmere Island, 1952; Arctic, vol. 5, p. 39-50.

Tucker, M.E. and Wright, V.P.
1990: Carbonate Sedimentology; Blackwell Scientific Publication, Oxford, 482p.

Ustritsky, V.I.
1973: Permian climate; *in* Logan, A. and Hills, L.V. (eds.); The Permian and Triassic systems and their mutual boundaries, Canadian Society of Petroleum Geologists, Memoir 2, p. 733-744.

Utting, J., Goodarzi, F., Dougherty, B.J. and Henderson, C.M.
1989: Thermal maturity of Carboniferous and Permian rocks of the Sverdrup Basin, Canadian Arctic Archipelago; Geological Survey of Canada, Paper 89-19, 20 p.

West, R.W. and Clark, G.R.
1983: Chaetetids; *in* Broadhead, T.W. (ed.); Sponges and Spongiomorphs: notes for a short course, University of Tennessee, Knoxville Publication, p. 130-140.

Whalman, G.P.
1985: Lower Permian (Wolfcampian) *Archaeolithoporella-Tubiphytes*-sponge boundstones from the subsurface of West Texas; *in* Toomey, D.F. and Nitecki, M.H. (eds.); Paleoalgology: contemporary research and applications, Springer-Verlag, Berlin, p. 208-215.

Wilson, J.L.
1975: Carbonate Facies in Geologic History; Springer-Verlag, New York, 471 p.

Ziegler, P.A.
1988: Evolution of the Arctic - North Atlantic and the Western Tethys; American Association of Petroleum Geologists, Memoir 43, 198 p.

PLATES

PLATE 1

Exposures of the Nansen and Hare Fiord formations

a. Panorama of the Nansen Formation (section 5), Girty Glacier, at the head of Hare Fiord (adjacent to the type section). The succession includes the Borup Fiord (BF; conglomerates and sandstones), Otto Fiord (OF; evaporites), Hare Fiord (HF; mixed carbonates and siliciclastics) and Nansen (NA; carbonates) formations. The massive shelf edge Nansen buildups (NAm) are overlain by Essayoo volcanics. Stratigraphic thickness of the combined Otto Fiord - Nansen succession is approximately 2300 m.

b. Cliff exposure of facies change from Nansen (NA) shelf edge carbonates to Hare Fiord (HF) mixed slope to basin sediments along the north shore of Hare Fiord. The height of the cliff is approximately 1000 m. Note the steeply dipping clinoforms extending from the massive Nansen shelf edge onto the Hare Fiord slope.

c. Nansen Formation shelf and shelf edge deposits (section 1, 843 m thick). Massive shelf edge phylloid algal buildups occur at the base of the cliff (outlined) while cyclic shelf carbonate extends away from the buildups. Terra rosa paleoexposure surfaces (arrows) occur near the top of the cliff. Tertiary thrusting resulted in the dip observed at this outcrop.

d. Panorama of representative cyclic shelf deposits of the Nansen Formation within the northern portion of the study area (at a distance from the shelf edge). Each individual cycle is tens of metres in thickness. Dip is structurally controlled.

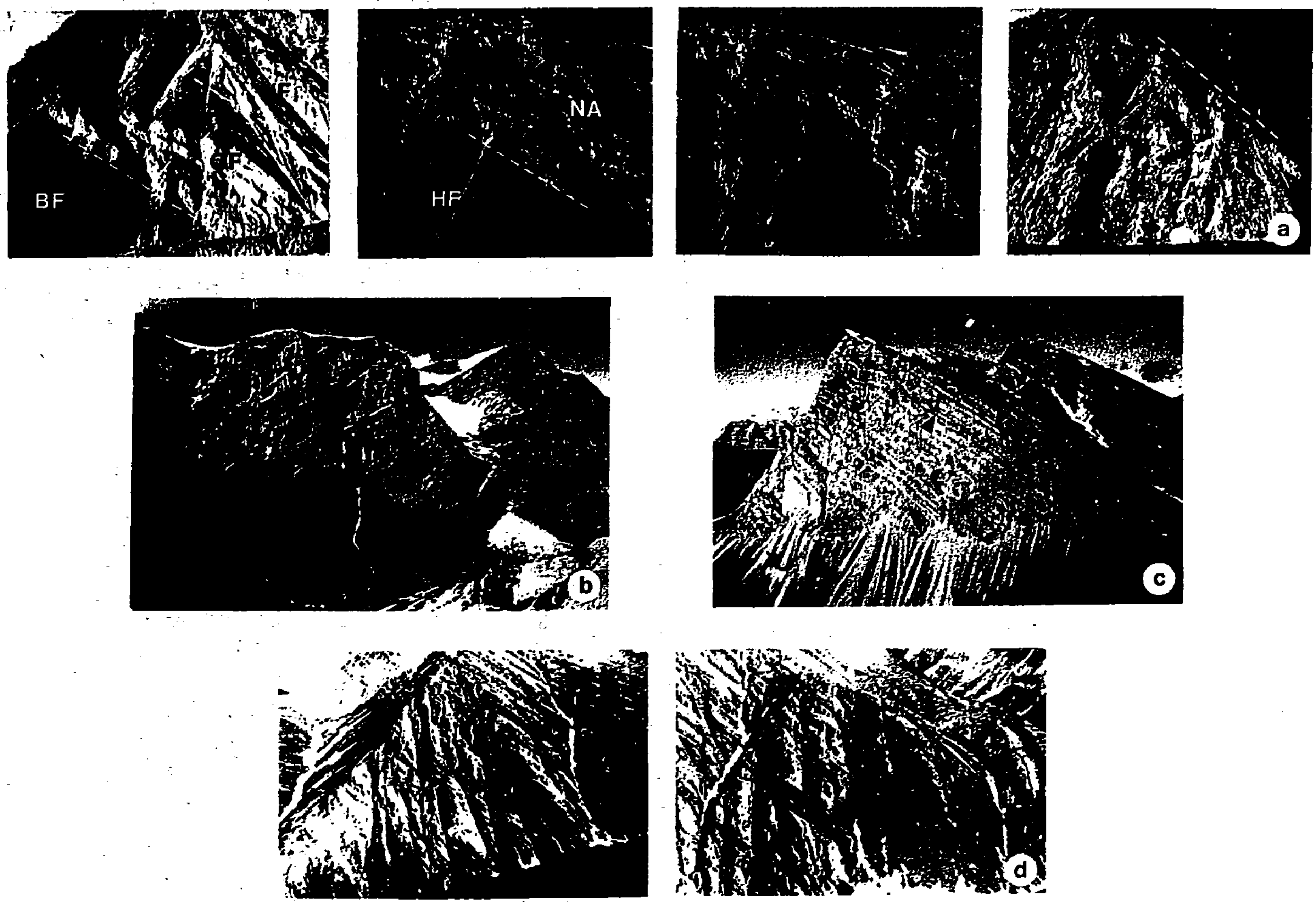
BF
NA
HF
a
b
c
d

PLATE 2

Exposures of the Hare Fiord Formation

a. Panorama of lower slope deposits of the Hare Fiord Formation (section 3, 693 m thick). Note cyclic recessive and resistant units. Debris flows appear as massive, laterally discontinuous lenses (arrows). The Hare Fiord Formation is overlain by the Trappers Cove Formation (TC).

b. Upper slope Hare Fiord facies assemblage in an outcrop adjacent to section 2. Alternating recessive and resistant packages visible at outcrop scale. Individual cycle thickness is tens of metres.

c. Cyclic nature of upper slope deposits visible in Hare Fiord Formation (section 2, 660-764 m).

d. Lower slope deposits of the Hare Fiord Formation at Stepanow Creek (section 7, 354 m thick). A bryozoan mud mound occurs at the base of the section (Televak limestone; arrow).

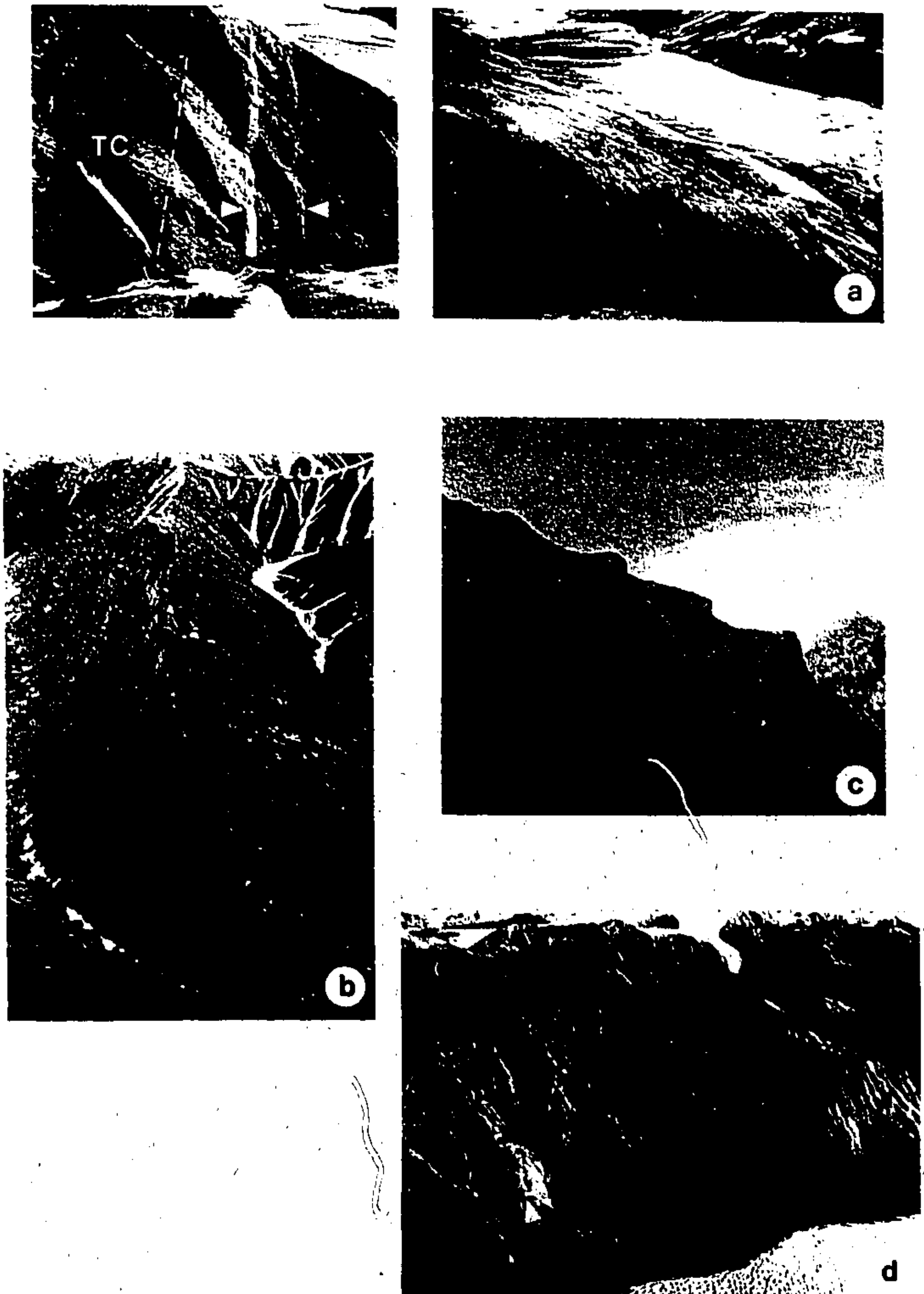
TC
a
b
c
d

PLATE 3

Shelf Facies

a. Photomicrograph of Crinoid-Bryozoan Facies in packstone. Crinoid (cr) and bryozoan (br) fragments are the most common framework elements with less abundant brachiopods and quartz silt (qs; section 1; C-240892). Scale bar is 1 mm.

b. Photomicrograph of Crinoid-Bryozoan Facies in grainstone/packstone. Crinoids (cr) and bryozoans (br) dominate with less abundant brachiopods (bp; section 1; C-240908). Scale bar is 1 mm.

c. Photomicrograph of Foraminiferal Facies in packstone. Small foraminifers (fo) and fusulinids (fu) are abundant along with ungdarellid algae (un; section 6; C-241210). Scale bar is 1 mm.

d. Photomicrograph of Foraminiferal Facies in grainstone. Small benthic (bf) and encrusting foraminifers (ef) dominate along with crinoids (cr), beresellid algae (ba) and minor brachiopods (bp; section 6; C-241213). Abundant encrusting foraminifers indicate relatively restricted marine conditions. Scale bar is 0.5 mm.

e. Photomicrograph of Foraminiferal Facies in grainstone. Small foraminifers (fo) and fusulinids (fu) are associated with ungdarellid algae and pervasively cemented by early isopachous fibrous cement (ic; section 1; C-240811). Scale bar is 1 mm.

f. Photomicrograph of Peloidal Facies in packstone. Peloids (pe) are the most common element along with small foraminifers and micritized grains (section 9; C-241302). Scale bar is 0.5 mm.

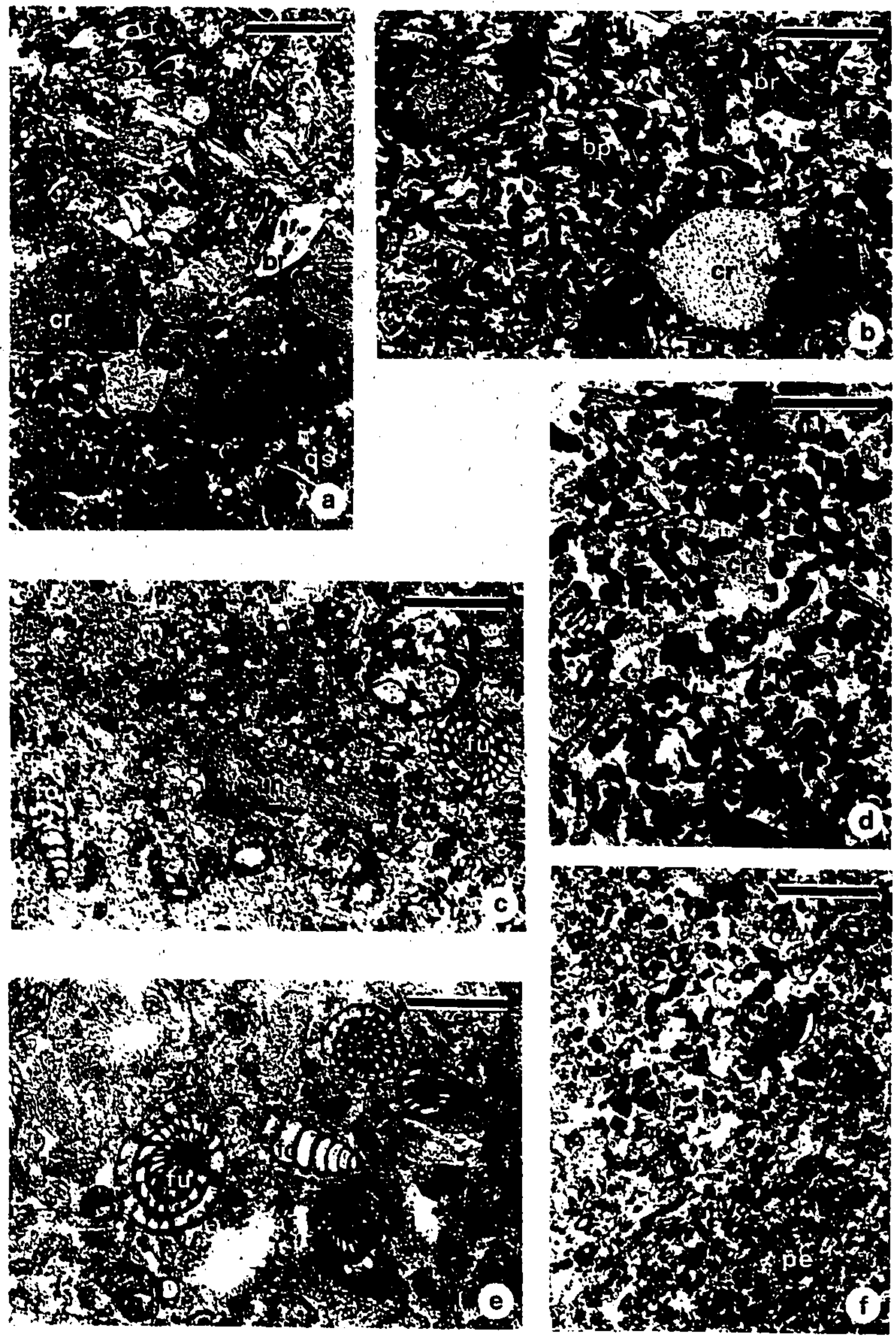

a
cr
br
qs
b
br
bp
cr
c
fu
d
cr
e
fu
f
pe

PLATE 4

Shelf Facies

a. Photomicrograph of Oolitic Facies in grainstone. Ooids are commonly dissolved or micritized. Coated fusulinid grains (fu) are abundant. Note early fibrous calcite cement (ic) surrounding grains (section 5; C-241120). Scale bar is 1 mm.

b. Photomicrograph of Oolitic Facies in grainstone. Ooids are well sorted and commonly display a concentric fabric. Nuclei consist of bioclasts and peloids. Associated bioclasts include benthic and encrusting foraminifers (fo), and phylloid algae (pa; section 5; C-241133). Scale bar is 1 mm.

c. Chaetetid colonies occur in thin biostromal units in outcrop. Note the silicification rims surrounding this specimen (section 6). Hammer for scale.

d. Polished slab of Oolitic Facies. The relatively well sorted, well rounded grains are easily distinguished in hand sample. Oolitic sands occur in close association with the shelf edge Phylloid Algal Facies (section 5; C-241116). Scale bar is 1 cm.

e. Photomicrograph of Beresellid Facies in grainstone. Beresellid algae (ba) are associated with small foraminifers and ungdarellid algae. Late calcite cement occludes much of the porosity (section 9; C-241304). Scale bar is 1 mm.

f. Photomicrograph of Dasycladacean Facies in grainstone. Fragmented dasyclad algae (da) dominate with less abundant phylloid algae (pa), fusulinids (fu), foraminifers, gastropods (ga) and intraclasts (in). Dasyclad skeletal pores are filled with micrite and the skeleton itself is infilled and surrounded with early marine fibrous calcite cement (section 1; C-240901). Scale bar is 1 mm.

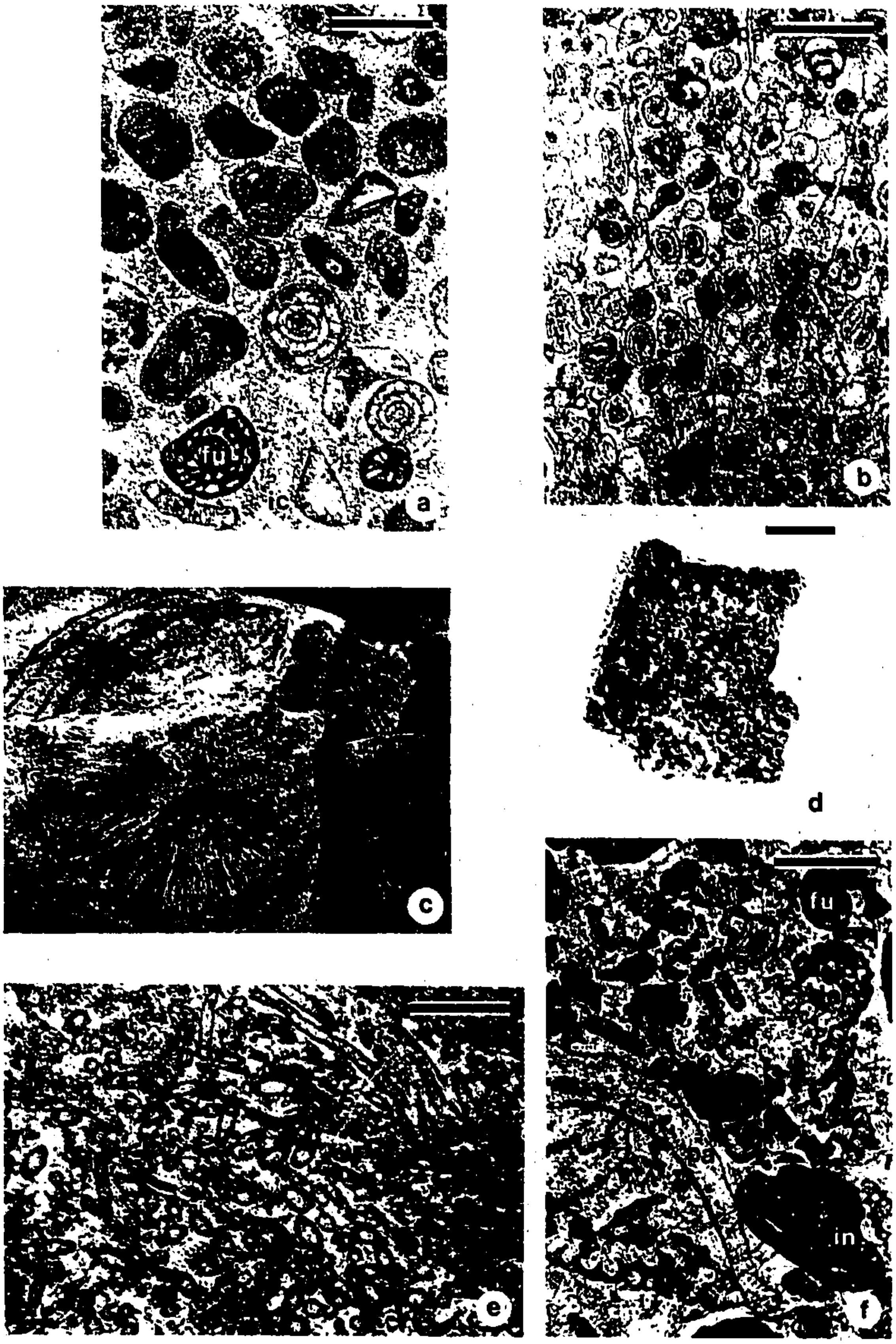
fu
ic
a
b
c
d
e
fu
in
f

PLATE 5

Shelf Edge Facies

a. Polished slab of phylloid algal boundstone. The boundstone texture displays a relatively open framework of phylloid algal plates (pa). Growth cavities are filled with alternating multiple layers of marine fibrous calcite cement (ic) and geopetal peloidal muds (gm; section 1; C-240862). Scale bar is 1 cm.

b. Photomicrograph of Phylloid Algal Facies in boundstone. Note the poor preservation of the formerly aragonitic phylloid plates (pa) now recognizable only from micritic rims surrounding submarine cement-filled cavities (section 1; C-240862). Scale bar is 0.5 mm.

c. Weathered surface of phylloid algal boundstone. Both the large scale massive appearance and the small scale cement layers make the Phylloid Algal Facies easily recognizable in outcrop (section 1). Lens cap for scale.

d. Polished slab of a cement-filled growth cavity within phylloid algal boundstone. The multiple layers of isopachous fibrous calcite cement are various shades of grey depending on the chemistry of the cement generation (section 5; C-241130). Scale bar is 1 cm.

e. Polished slab of cement-filled dyke cutting through Phylloid Algal Facies grainstone. The early marine isopachous fibrous calcite cement (ic) lining the fracture indicates its early development (section 1; C-240903). Scale bar is 1 cm.

f. Photomicrograph of Bryozoan Facies in grainstone. Bryozoan fragments (br) are the most common framework elements along with crinoids (cr) and brachiopods (bp). The open framework is largely infilled by cloudy isopachous fibrous calcite cement (section 1; C-240801). Scale bar is 1 mm.

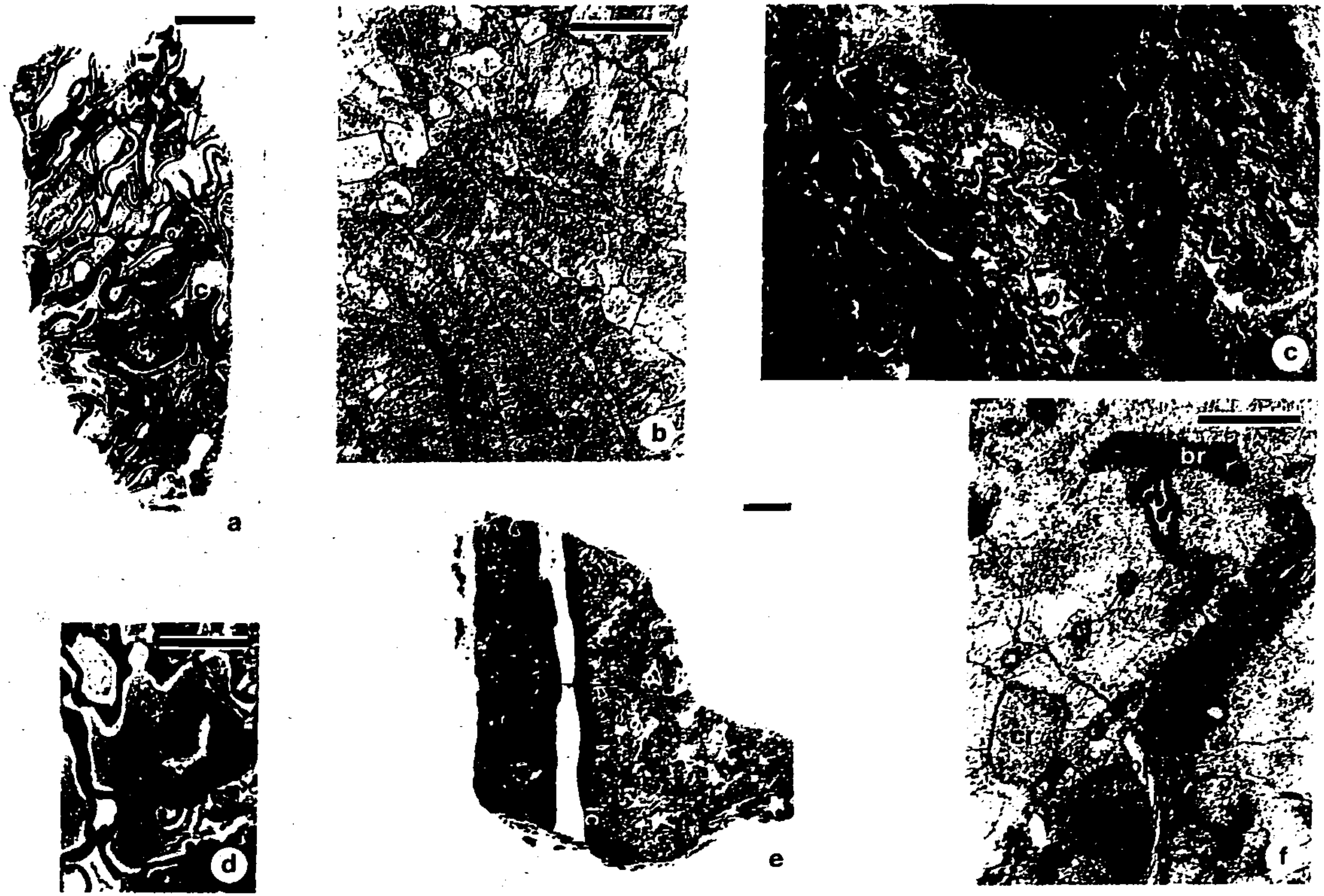
a
b
c
br
d
e
f

PLATE 6

Slope Facies

a. Photomicrograph of Calcisiltite Facies in wackestone. Abundant siliceous sponge spicules (ss) are associated with brachiopods and quartz silt (section 7; C-241247). Scale bar is 1 mm.

b. Photomicrograph of Calcisiltite Facies in wackestone. Abundant calcispheres (cs) are associated with quartz silt (section 7; C-241238). Scale bar is 0.5 mm.

c. Polished slab of mixed Calcisiltite and Siltstone Facies in wackestone. Well laminated sediments indicate quiet water deposition (section 5; C-241092). Scale bar is 1 cm.

d. Polished slab of mixed Calcisiltite and Siltstone Facies in wackestone. Well laminated sediments have been disrupted by slumping on the steep upper slope (section 5; C-241098). Scale bar is 1 cm.

e. Photomicrograph of Calcisiltite-Siltstone Facies in mudstone. This laminated, quartz silt-rich sample demonstrates the continuum which exists between these two facies (section 5; C-241091). Scale bar is 0.5 mm.

f. Photomicrograph of Siltstone Facies in wackestone. Abundant quartz silt occurs in a carbonate mud matrix with crinoid and brachiopod debris. Bioturbation has disrupted the deposit, obscuring any original sedimentary structures (section 7; C-241245). Scale bar is 1 mm.

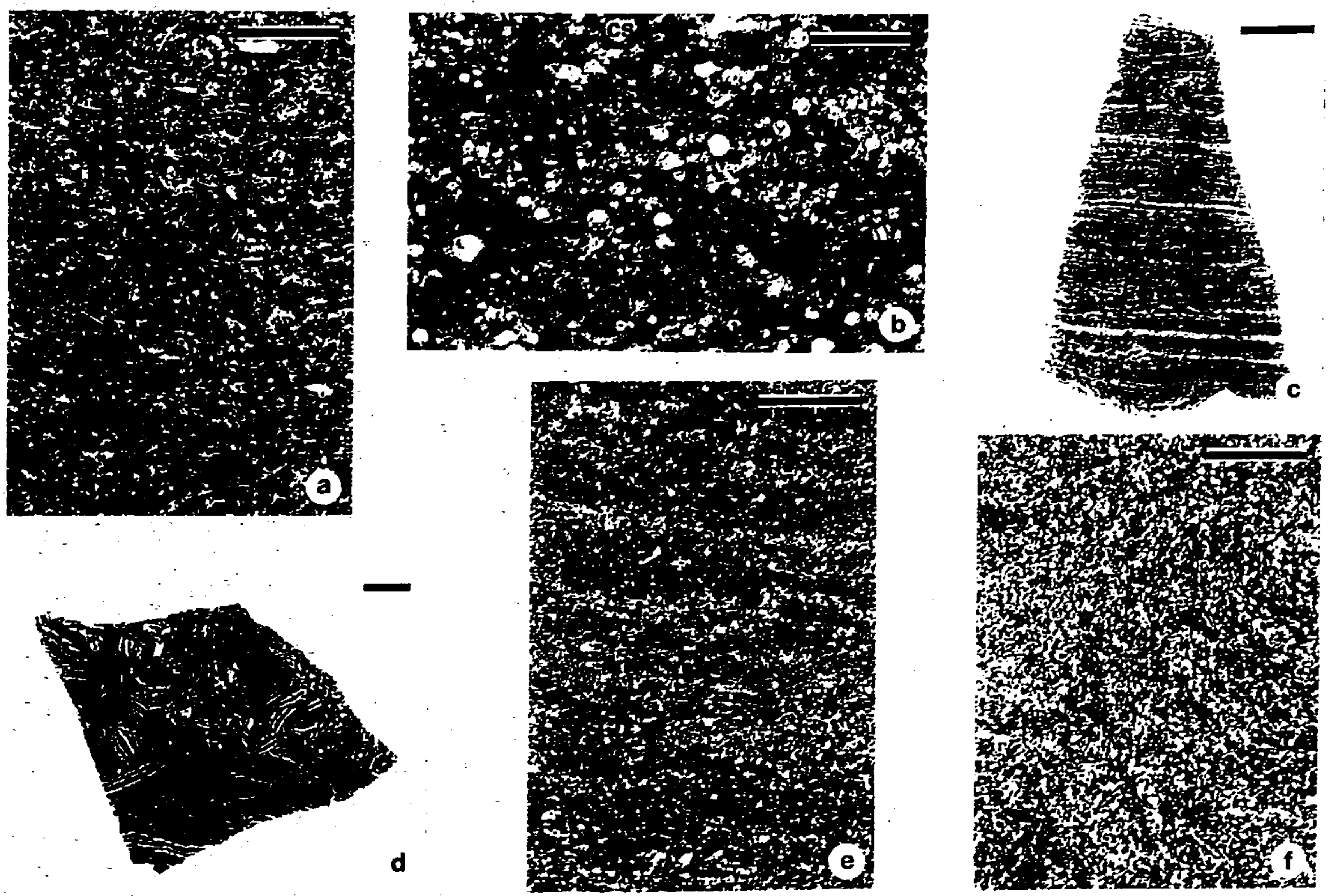
a
b
c
d
e
f

PLATE 7

Slope Facies

a. *Zoophycos* on bedding surface in lower slope facies, Hare Fiord Formation (section 3, at 330 m). Lens cap for scale.

b. Horizontal traces on bedding surface in lower slope facies, Hare Fiord Formation (section 3). Lens cap for scale.

c. Black shale overlying debris flow deposit in lower slope facies, Hare Fiord Formation (section 3, at 523 m). Hammer for scale.

d. Graded turbidite in upper slope environment, Hare Fiord Formation (section 2, at 475 m). Note sharp basal contact (arrow) with background sediments below. Note also the substantial grain size change across the boundary. Pen for scale.

e. Debris flows in outcrop. The deposits occur along distinct horizons in the Hare Fiord lower slope facies, on the north shore of Hare Fiord. Approximate outcrop thickness is 15 m.

f. Debris flow in outcrop (section 3, at 606 m). Note sharp basal contact as well as resistant and massive nature of deposit. Thickness is 12 m.

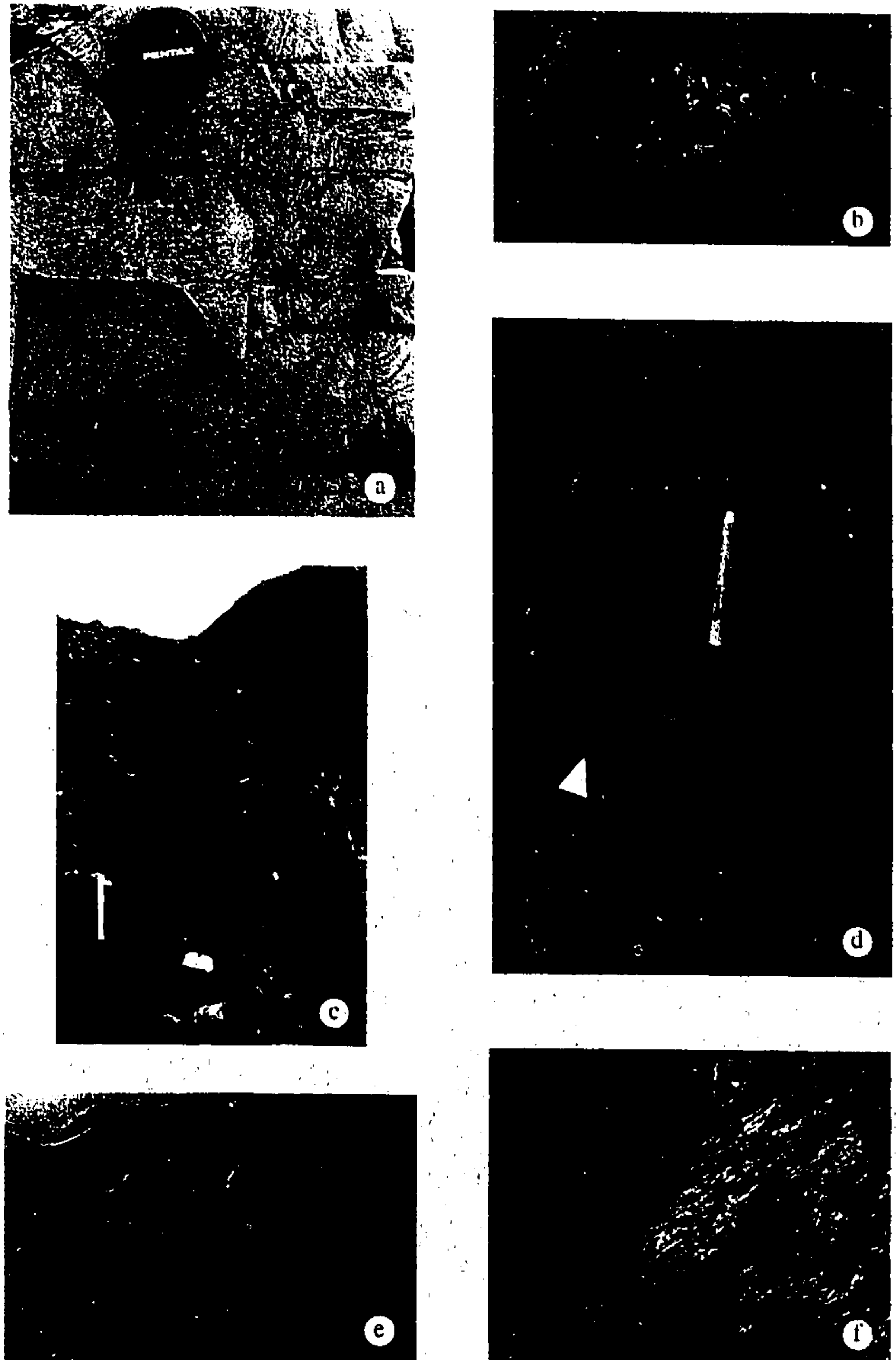
PENTAX
a
b
c
d
e
f

PLATE 8

Slope Facies and Diagenesis

a. Photomicrograph of Calcarenite Facies in packstone. Coarse fragments of ramose bryozoans (rb), brachiopods (bp), crinoids (cr) and fusulinids (fu) dominate in a fine matrix (section 7; C-241257). Scale bar is 0.5 cm.

b. Polished slab of Calcarenite Facies in packstone/grainstone. Crinoid debris dominates with ramose bryozoans. Sharp basal contact and normal grading define this as a carbonate turbidite (section 3; C-241017). Scale bar is 1 cm.

c. Photomicrograph of Calcarenite Facies in grainstone. Bryozoan fragments (br) dominate with crinoids (cr), small foraminifers (fo), brachiopods (bp), gastropods (ga) and *Tubiphytes* (Tu). Late sparry calcite (sc) occludes porosity (section 7; C-241249). Scale bar is 1 mm.

d. Photomicrograph of Calcarenite Facies in grainstone. Crinoid fragments (cr) dominate. Deposit has been extensively silicified (section 3; C-240987). Scale bar is 0.5 cm.

e. Photomicrograph of Debrite Facies in packstone. The presence of early marine fibrous calcite cement (ic) indicates that sediments were at least partially indurated before the time of the debris flow. Early marine cement development and the contained biotic assemblage verify that clasts occurring within debris flows on the lower slope originated in shallower water environments (section 3; C-241008B). Scale bar is 1 mm.

f. Photomicrograph of completely dolomitized sediment. Only ghosts of bioclasts (crinoids; cr) remain as evidence of the original rock composition. Dolomitization produces secondary porosity and could result in the development of a potential hydrocarbon reservoir (section 1; C-240826). Scale bar is 0.5 mm.

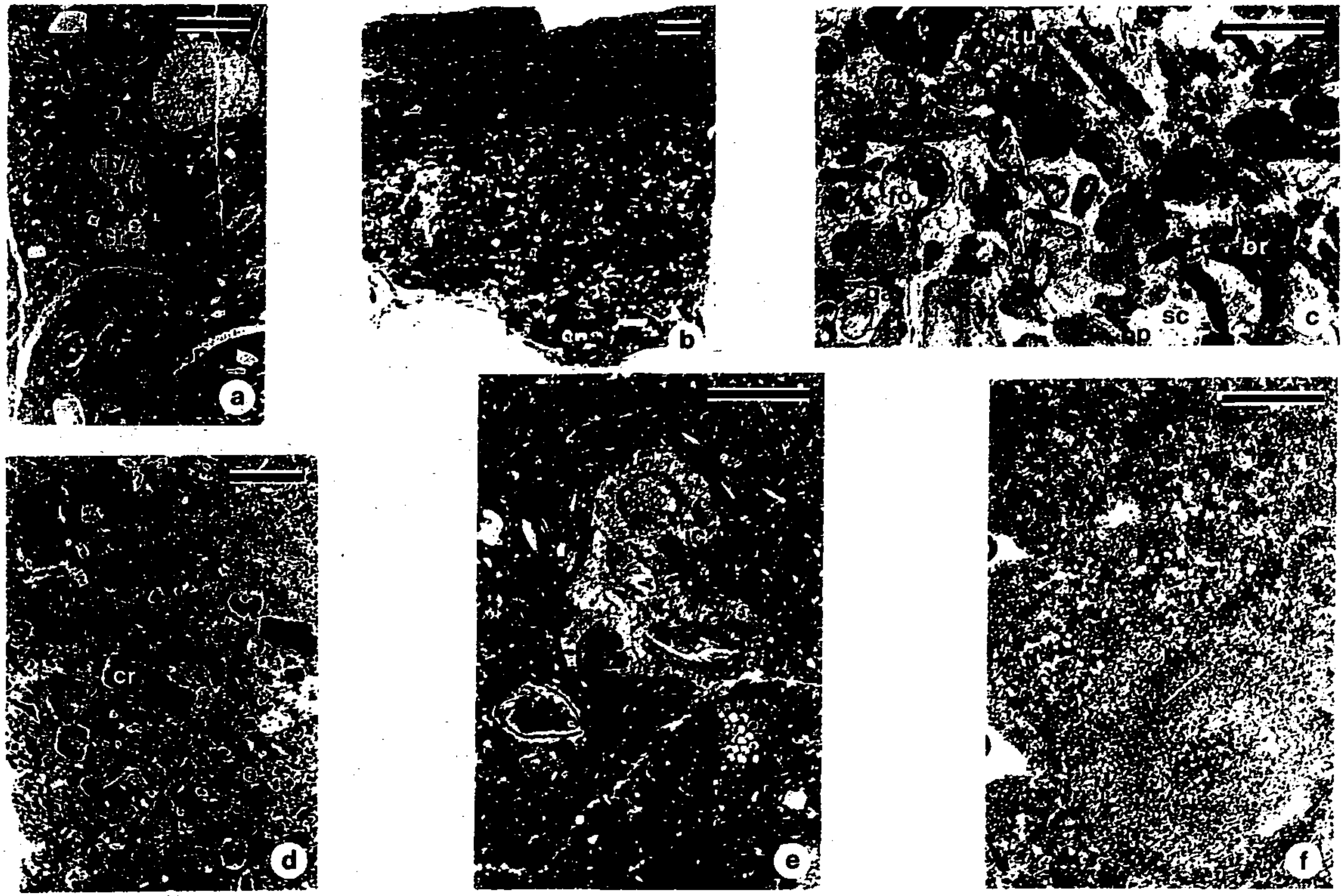

a
b
br
sc
c
cr
d
e
f

APPENDICES

APPENDIX 1: SECTION LOCALITIES

Localities of measured sections in the Otto Fiord-Hare Fiord region of northwestern Ellesmere Island. See Thorsteinsson (1974), Map 1309A, for complete geologic and topographic information.

Section	Latitude	Longitude
1	81° 17' N	85° 54' W
2	81° 19' N	85° 30' W
3	81° 06' N	85° 07' W
4	81° 18' N	86° 05' W
5	81° 13' N	82° 08' W
6	81° 24' N	85° 18' W
7	81° 07' N	84° 20' W
8	81° 22' N	84° 35' W
9	81° 32' N	86° 48' W

APPENDIX 2: STRATIGRAPHIC SECTIONS

Schematic stratigraphic columns of the measured sections. Units less than 1 m thick are not illustrated. Chronostratigraphic data are based on work by Dr. Sylvie Pinard (small foraminifera) and Dr. Rui Lin (fusulinaceans), both at the Institute of Sedimentary and Petroleum Geology (Calgary, Alberta). Symbols used for lithologies and lithofacies are listed on the following page. 'Cycle boundaries' marked in the Nansen Formation of section 5 indicate partings in the rock and are not necessarily indicative of true cyclicity.

LITHOLOGIES

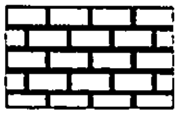 LIMESTONE

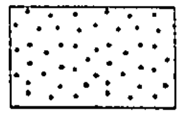 SILTSTONE

 DOLOSTONE

 SHALE

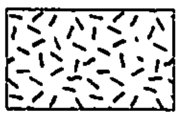 IGNEOUS INTRUSIVE (SILL)

LITHOFACIES

CB: CRINOID-BRYOZOAN
FO: FORAMINIFERAL
PL: PELOIDAL
OL: OOLITIC
CH: CHAETETID
BA: BERESELLID ALGAL
DA: DASYCLADACEAN
PA: PHYLLOID ALGAL
BR: BRYOZOAN
CS: CALCISILTITE
ST: SILTSTONE
SH: SHALE
CA: CALCARENITE
DE: DEBRITE
DO: DOLOMITIZED

MS: MUDSTONE
WS: WACKESTONE
PS: PACKSTONE
GS: GRAINSTONE
BS: BOUNDSTONE

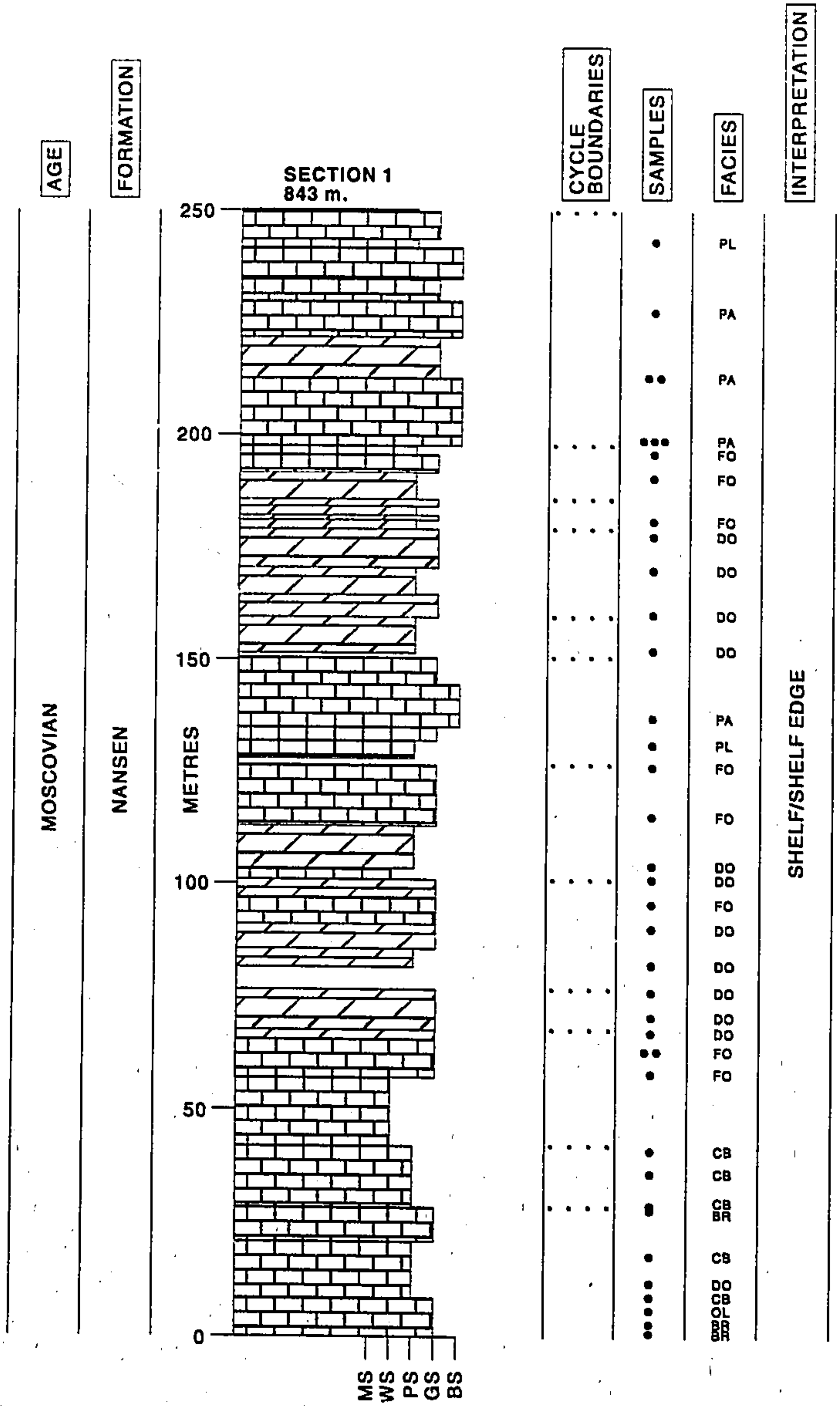
AGE
FORMATION
SECTION 1
843 m.
CYCLE BOUNDARIES
SAMPLES
FACIES
INTERPRETATION
MOSCOVIAN
NANSEN
METRES
250
200
150
100
50
0
PL
PA
PA
PA
FO
FO
FO
DO
DO
DO
DO
PA
PL
FO
FO
DO
DO
FO
DO
DO
DO
DO
DO
FO
FO
CB
CB
CB
BR
CB
DO
CB
OL
BR
BR
SHELF/SHELF EDGE
MS
WS
PS
GS
BS

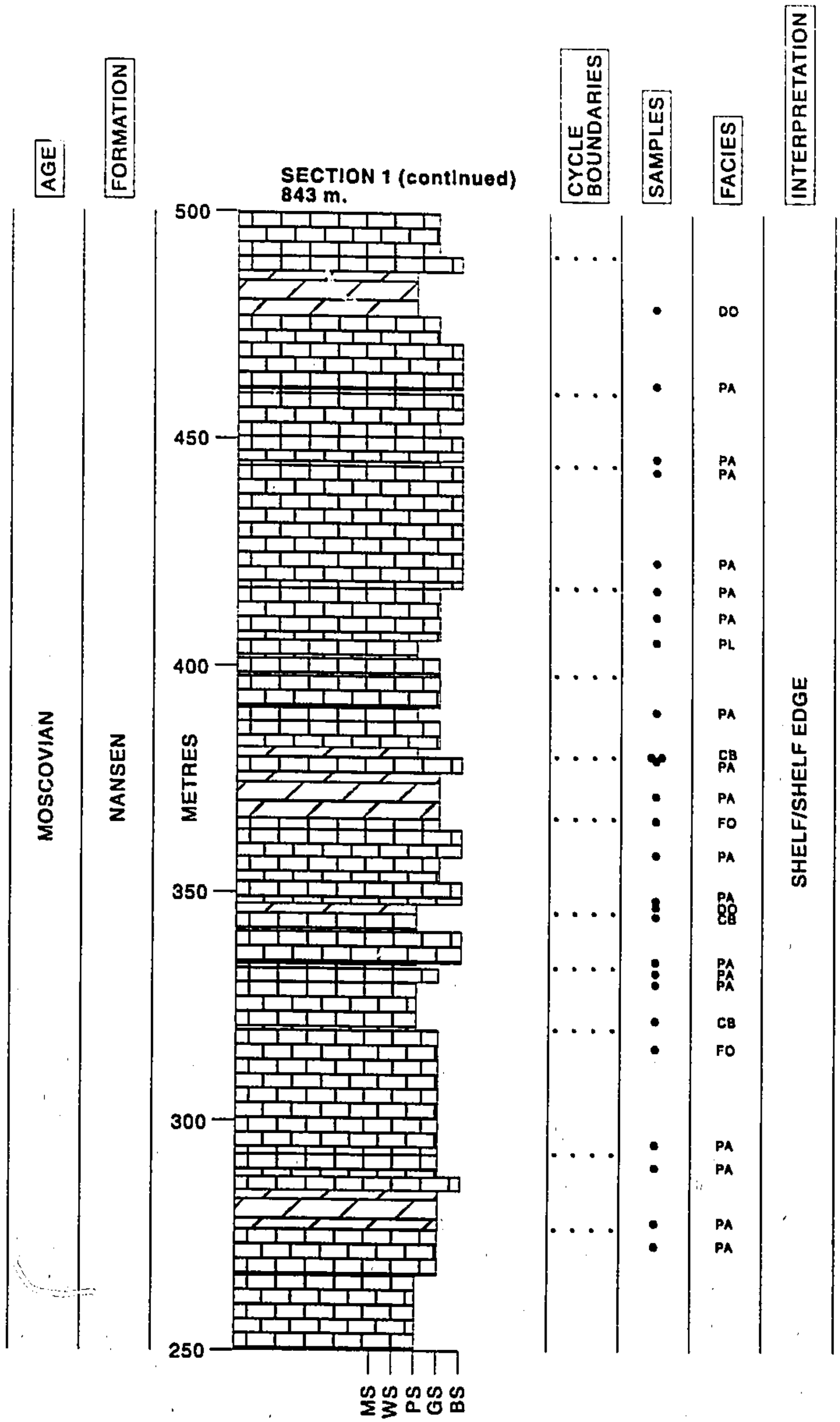
AGE
FORMATION
SECTION 1 (continued)
843 m.
CYCLE BOUNDARIES
SAMPLES
FACIES
INTERPRETATION
500
450
400
350
300
250
MOSCOVIAN
NANSEN
METRES
DO
PA
PA
PA
PA
PA
PA
PL
PA
CB
PA
PA
FO
PA
PA
DO
CB
PA
PA
PA
CB
FO
PA
PA
PA
PA
SHELF/SHELF EDGE
MS
WS
PS
GS
BS

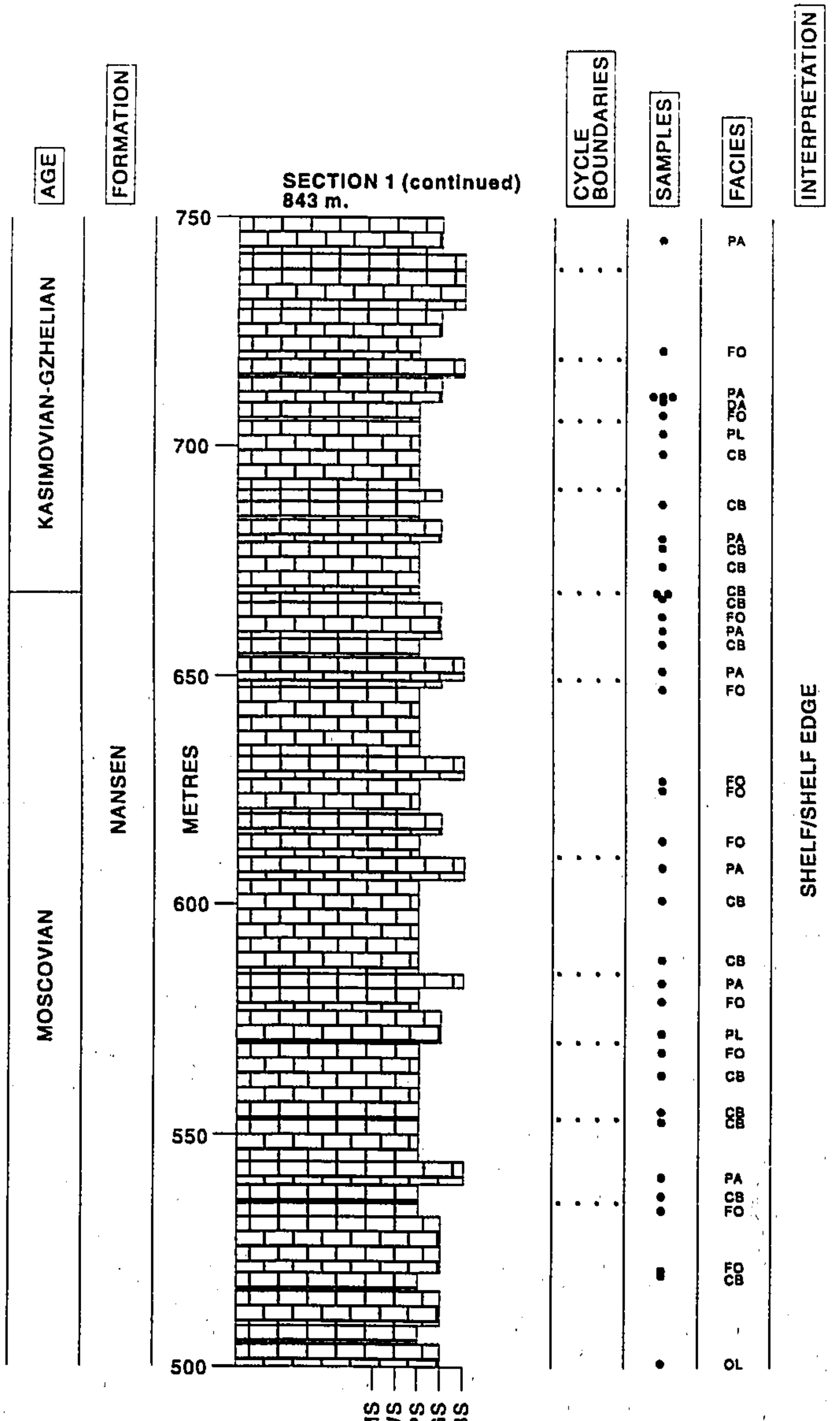

SECTION 1 (continued)
843 m.
AGE
FORMATION
CYCLE BOUNDARIES
SAMPLES
FACIES
INTERPRETATION
KASIMOVIAN-GZHELIAN
MOSCOVIAN
NANSEN
METRES
750
700
650
600
550
500
MS
WS
PS
GS
BS
PA
FO
PL
CB
OL
SHELF/SHELF EDGE

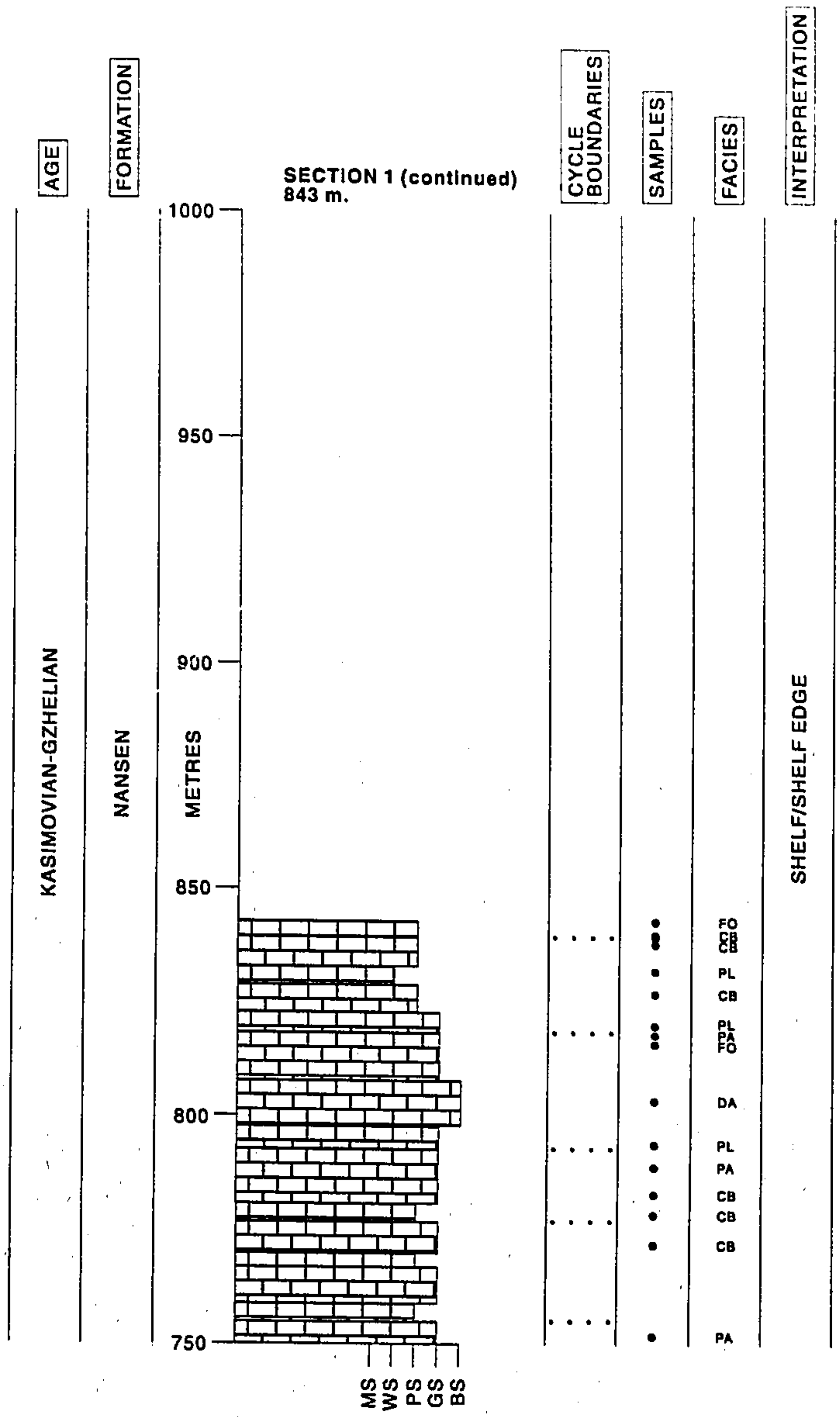
SECTION 1 (continued)
843 m.
AGE
FORMATION
CYCLE BOUNDARIES
SAMPLES
FACIES
INTERPRETATION
KASIMOVIAN-GZHELIAN
NANSEN
METRES
SHELF/SHELF EDGE
1000
950
900
850
800
750
FO
CB
CB
PL
CB
PL
PA
FO
DA
PL
PA
CB
CB
CB
PA
MS
WS
PS
GS
BS

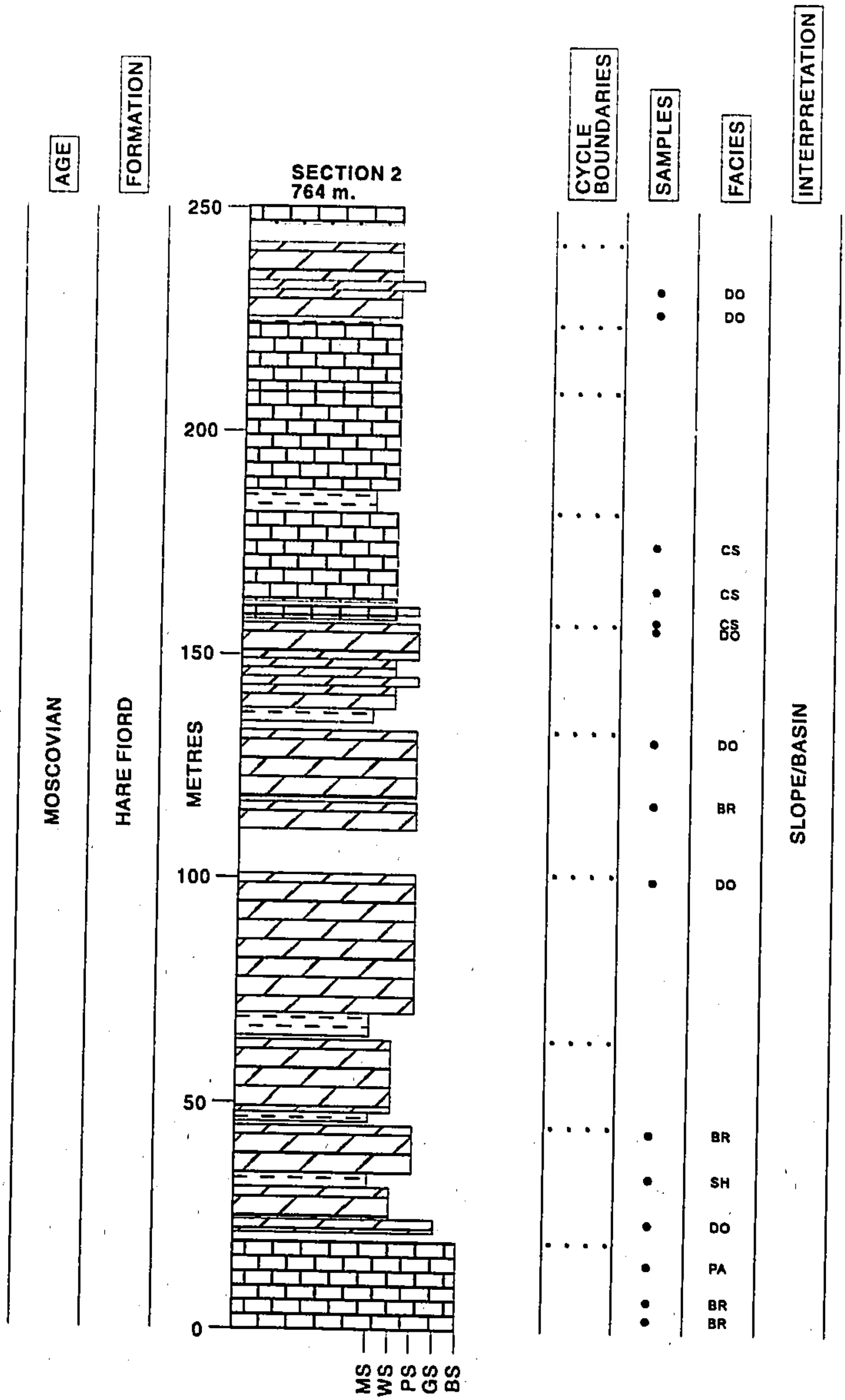
AGE
FORMATION
SECTION 2
764 m.
CYCLE BOUNDARIES
SAMPLES
FACIES
INTERPRETATION
MOSCOVIAN
HARE FIORD
METRES
250
200
150
100
50
0
MS
WS
PS
GS
BS
DO
DO
CS
CS
CS
DO
DO
BR
DO
BR
SH
DO
PA
BR
BR
SLOPE/BASIN

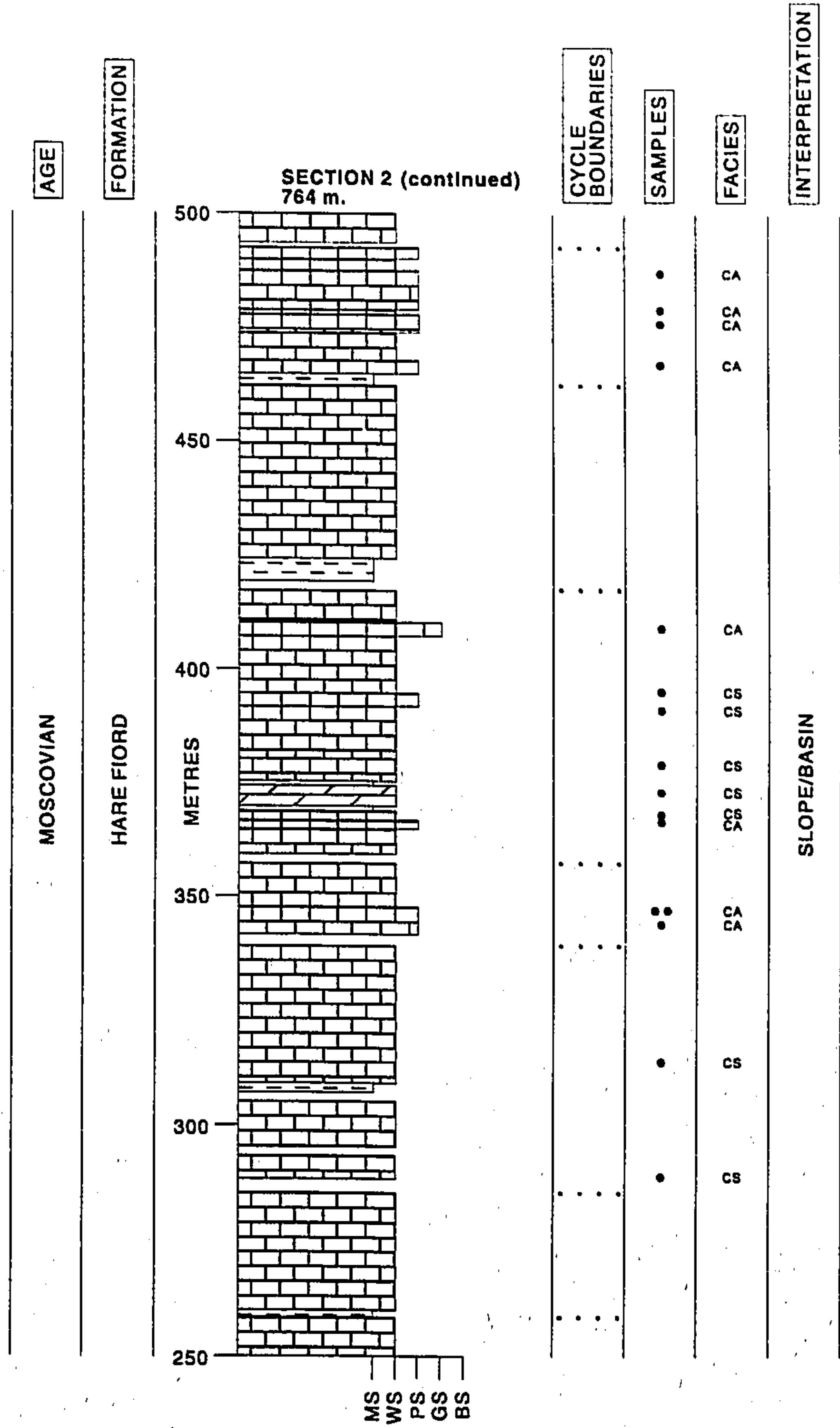
AGE
FORMATION
SECTION 2 (continued)
764 m.
CYCLE BOUNDARIES
SAMPLES
FACIES
INTERPRETATION
MOSCOVIAN
HARE FIORD
METRES
500
450
400
350
300
250
CA
CA
CA
CA
CA
CS
CS
CS
CS
CS
CA
CA
CA
CS
CS
SLOPE/BASIN
MS
WS
PS
GS
BS

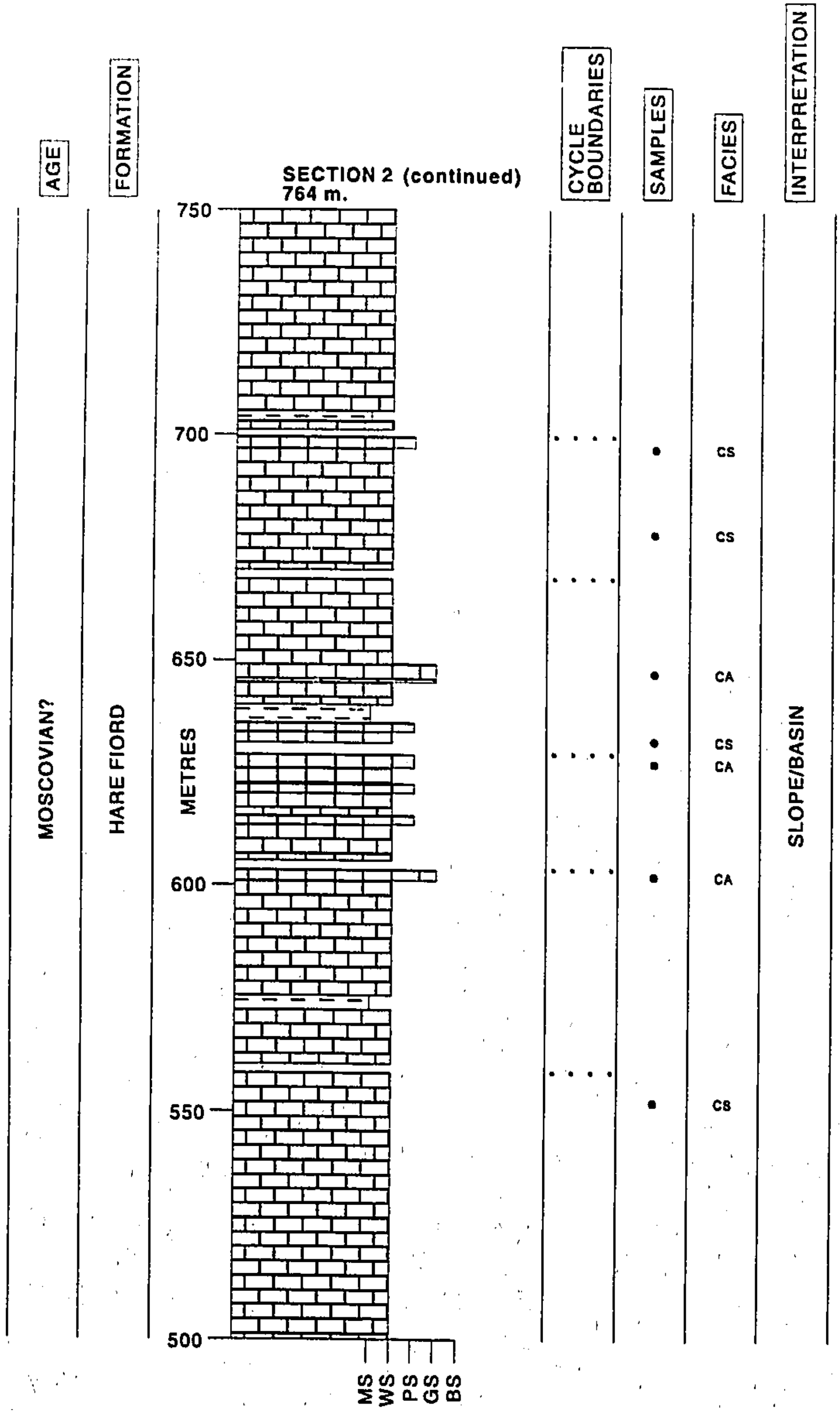
AGE
FORMATION
SECTION 2 (continued)
764 m.
CYCLE BOUNDARIES
SAMPLES
FACIES
INTERPRETATION
MOSCOVIAN?
HARE FIORD
METRES
750
700
650
600
550
500
CS
CS
CA
CS
CA
CA
CB
SLOPE/BASIN
MS
WS
PS
GS
BS

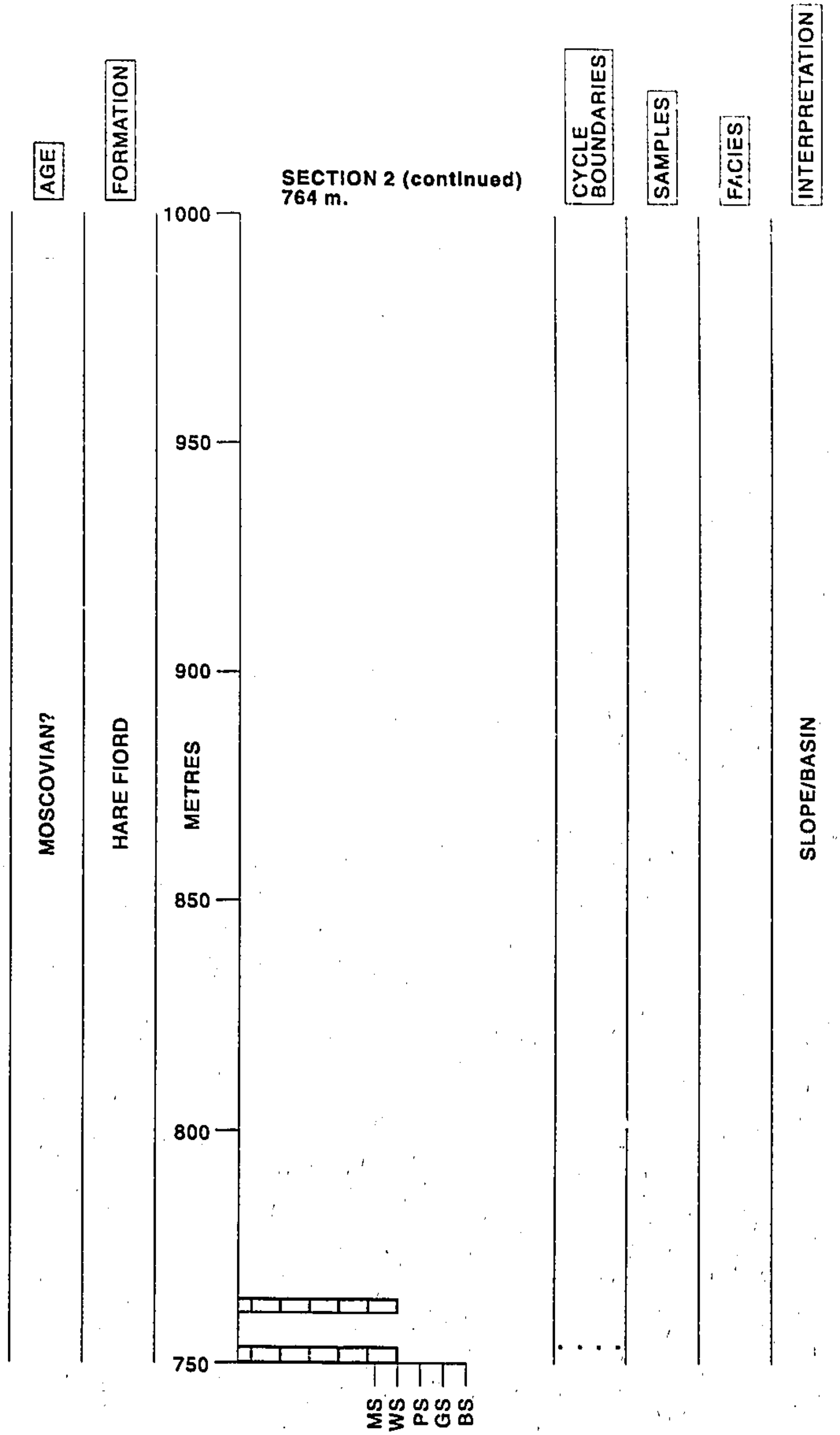
SECTION 2 (continued)
764 m.
AGE
FORMATION
CYCLE BOUNDARIES
SAMPLES
FACIES
INTERPRETATION
MOSCOVIAN?
HARE FIORD
METRES
1000
950
900
850
800
750
SLOPE/BASIN
MS
WS
PS
GS
BS

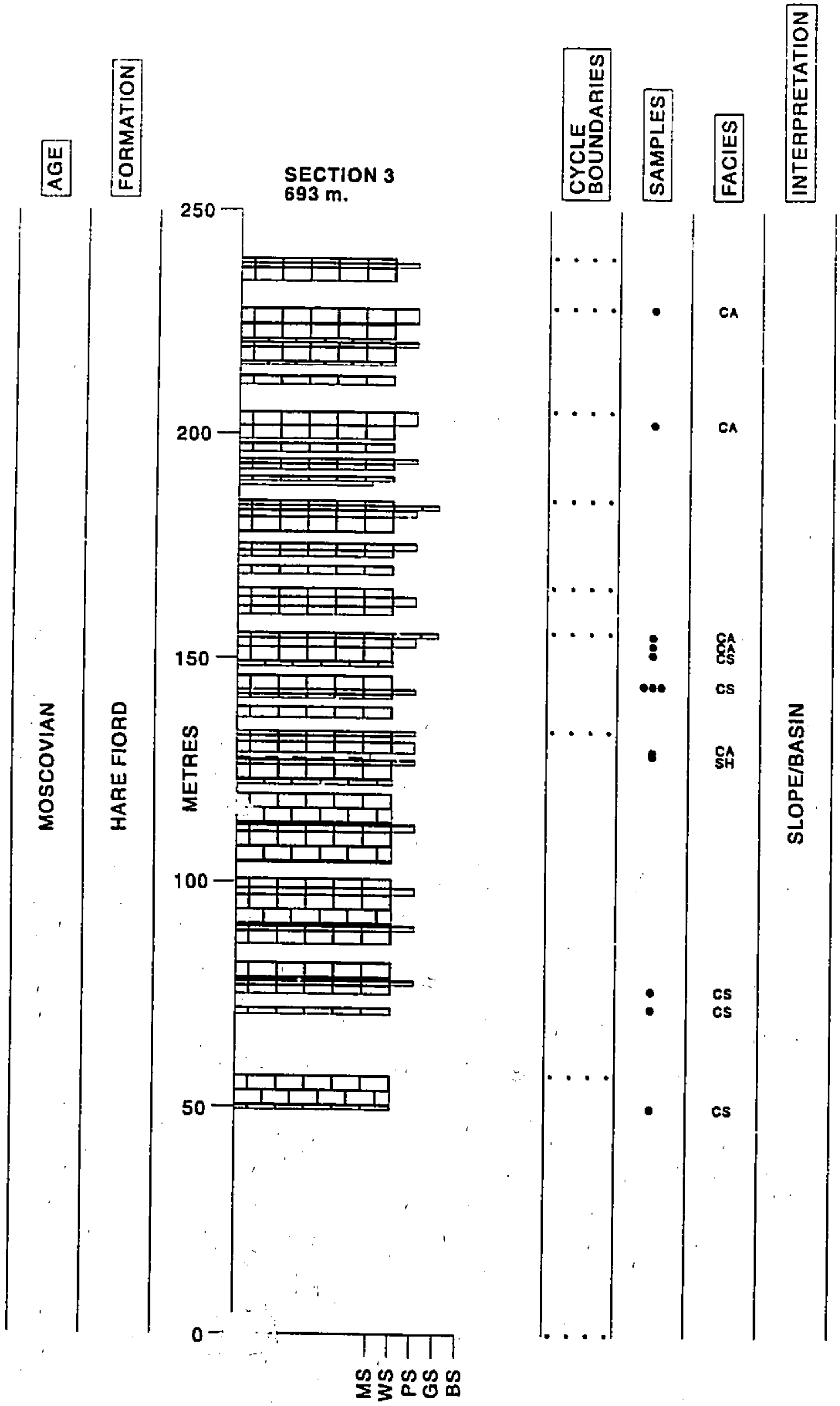
AGE
FORMATION
SECTION 3
693 m.
CYCLE BOUNDARIES
SAMPLES
FACIES
INTERPRETATION
MOSCOVIAN
HARE FIORD
METRES
250
200
150
100
50
0
CA
CA
CA
CA
CS
CS
CA
SH
CS
CS
CS
SLOPE/BASIN
MS
WS
PS
GS
BS

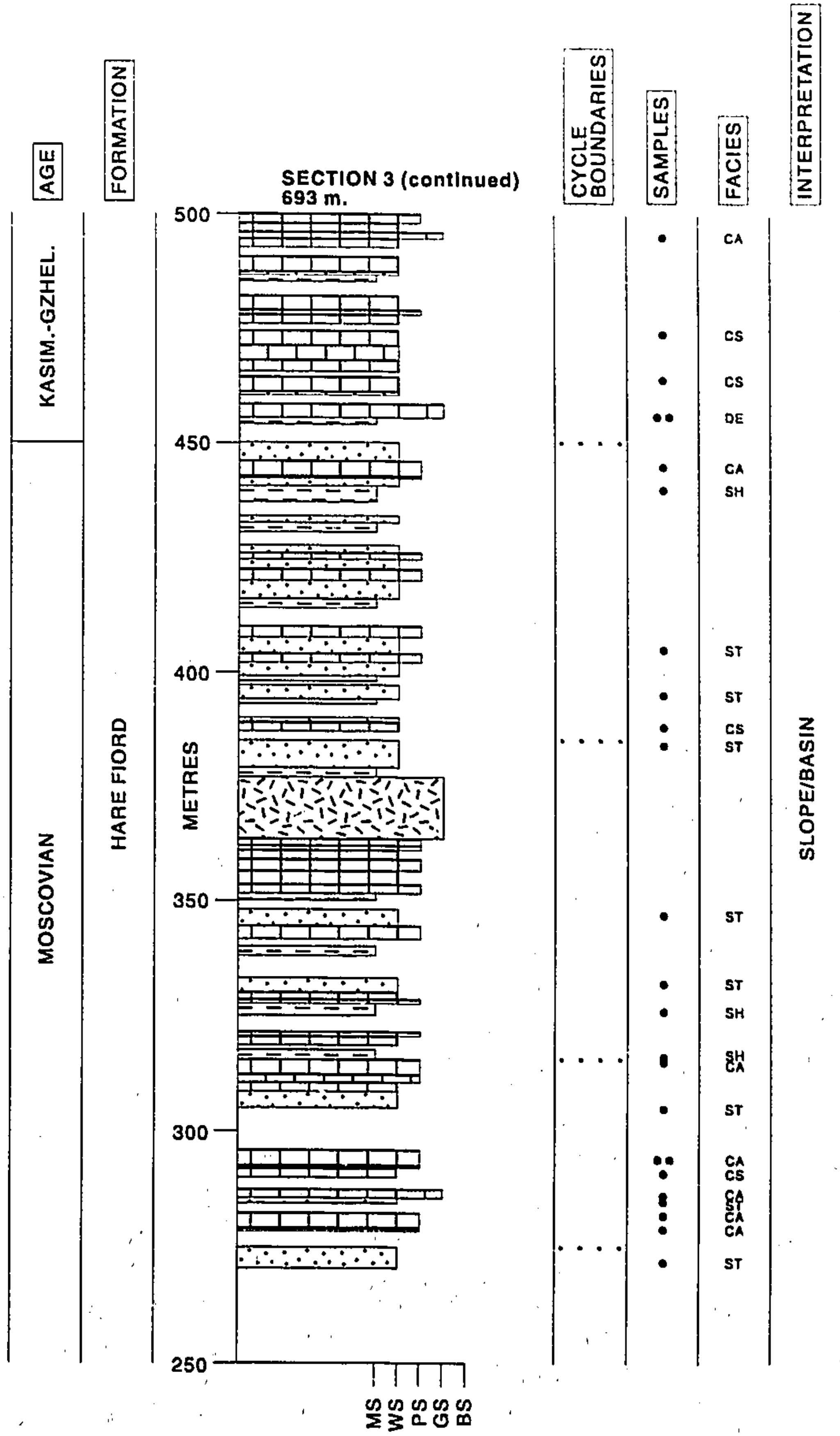

SECTION 3 (continued)
693 m.
AGE
FORMATION
CYCLE BOUNDARIES
SAMPLES
FACIES
INTERPRETATION
KASIM.-GZHEL.
MOSCOVIAN
HARE FIORD
METRES
500
450
400
350
300
250
CA
CS
CS
DE
CA
SH
ST
ST
CS
ST
ST
ST
SH
SH
CA
ST
CA
CS
CA
ST
CA
CA
ST
SLOPE/BASIN
MS
WS
PS
GS
BS

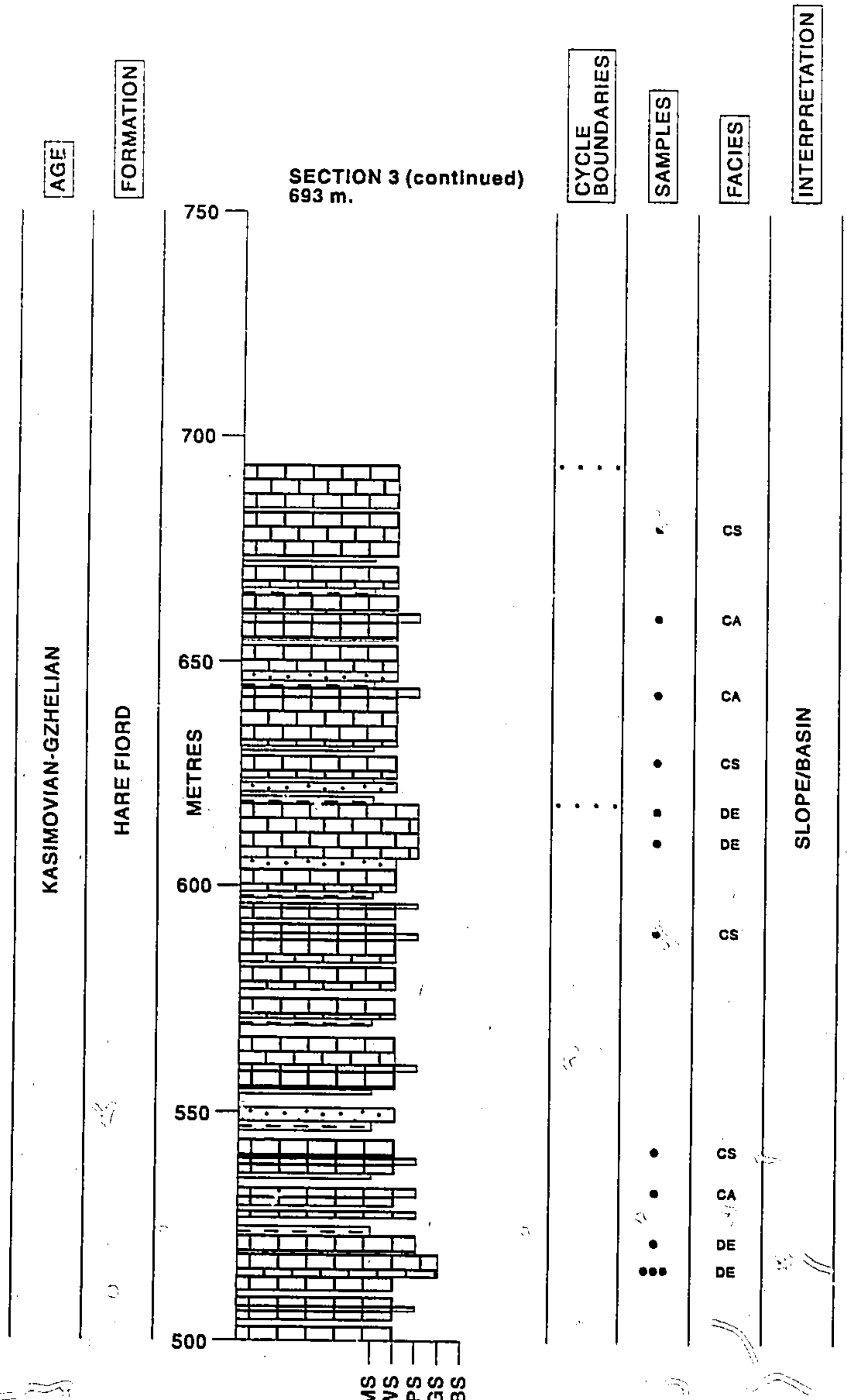
AGE
FORMATION
SECTION 3 (continued)
693 m.
CYCLE BOUNDARIES
SAMPLES
FACIES
INTERPRETATION
750
700
650
600
550
500
METRES
KASIMOVIAN-GZHELIAN
HARE FIORD
SLOPE/BASIN
CS
CA
CA
CS
DE
DE
CS
CS
CA
DE
DE
MS
WS
PS
GS
BS

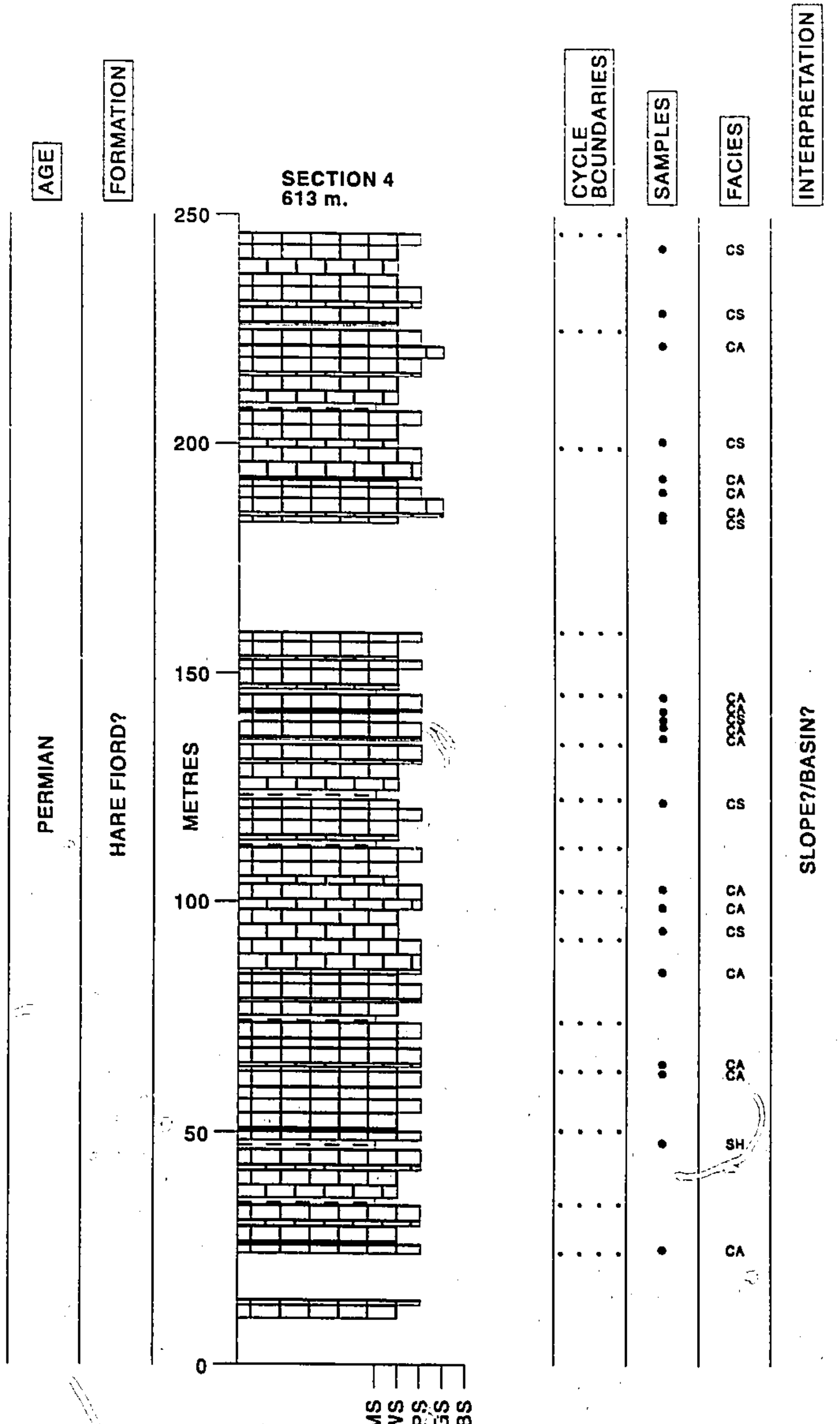
AGE
FORMATION
SECTION 4
613 m.
CYCLE BOUNDARIES
SAMPLES
FACIES
INTERPRETATION
250
200
150
100
50
0
METRES
PERMIAN
HARE FIORD?
SLOPE?/BASIN?
CS
CS
CA
CS
CA
CA
CA
CS
CS
CA
CA
CS
CA
CA
CA
SH
CA
MS
WS
PS
GS
BS

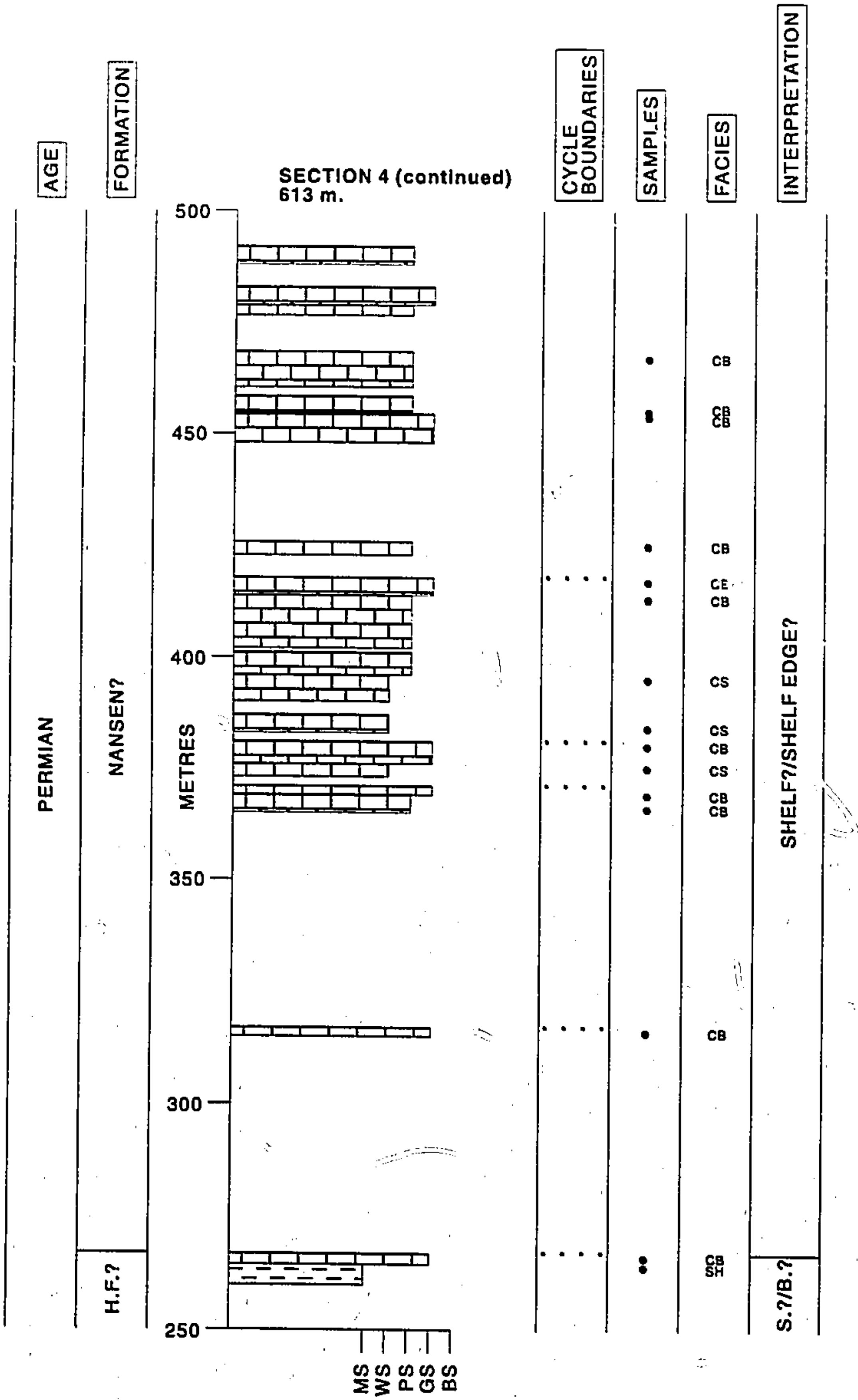

AGE
FORMATION
SECTION 4 (continued)
613 m.
CYCLE BOUNDARIES
SAMPLES
FACIES
INTERPRETATION
PERMIAN
NANSEN?
H.F.?
METRES
500
450
400
350
300
250
MS
WS
PS
GS
BS
CB
CB
CB
CB
CE
CB
CS
CS
CB
CS
CB
CB
CB
CB
SH
SHELF?/SHELF EDGE?
S.?/B.?

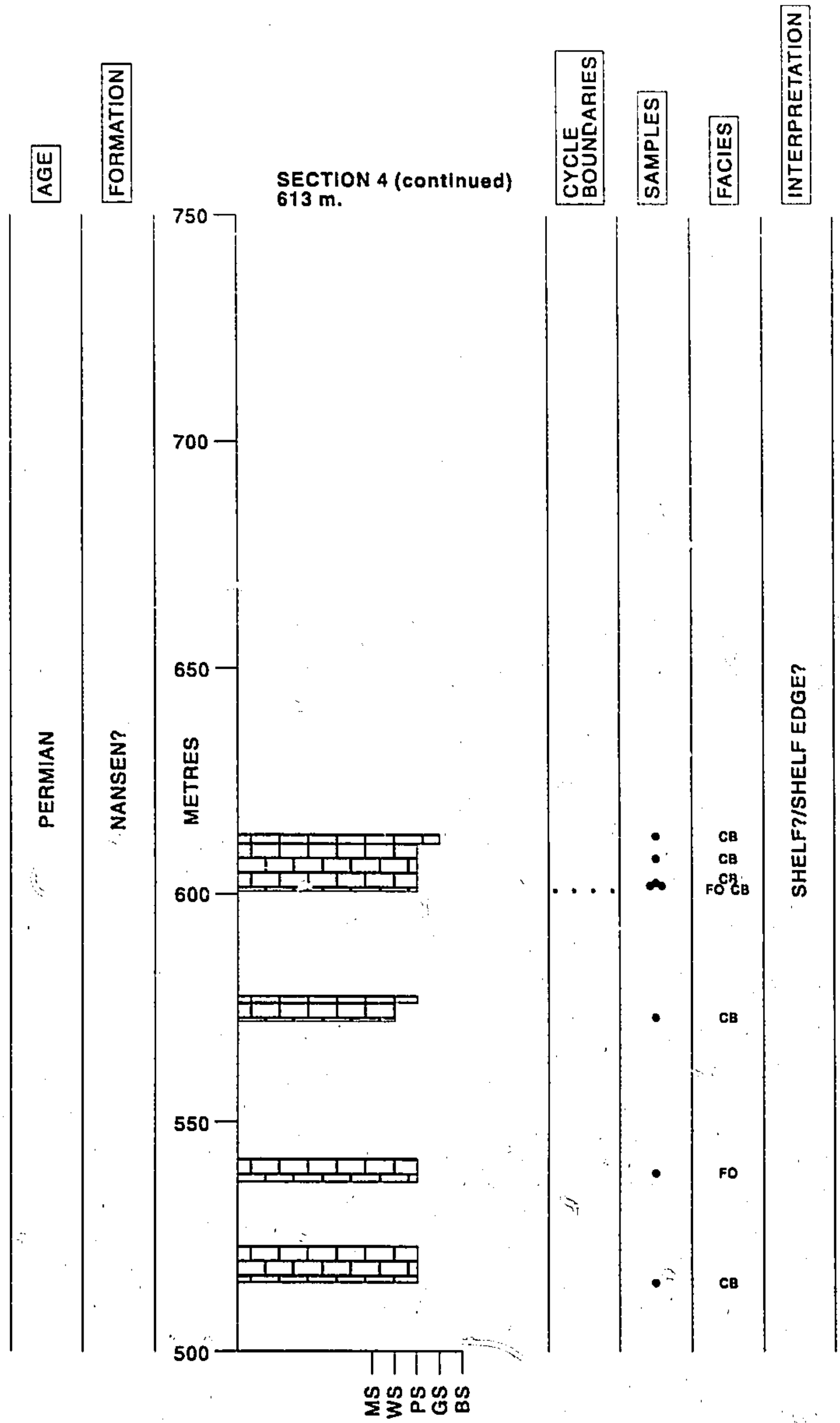
AGE
FORMATION
SECTION 4 (continued)
613 m.
CYCLE BOUNDARIES
SAMPLES
FACIES
INTERPRETATION
750
700
650
600
550
500
PERMIAN
NANSEN?
METRES
CB
CB
CB
FO CB
CB
FO
CB
SHELF?/SHELF EDGE?
MS
WS
PS
GS
BS

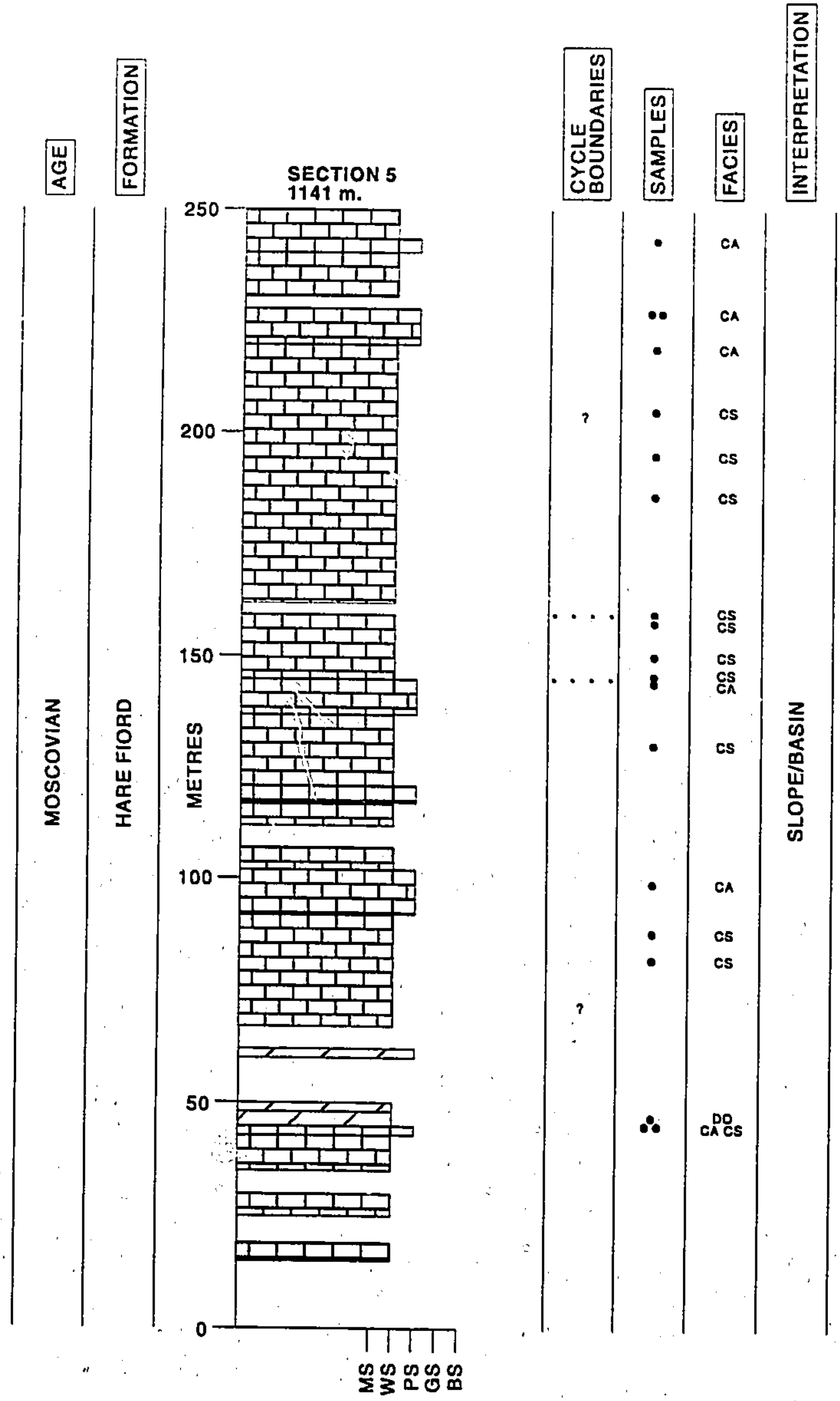
AGE
FORMATION
SECTION 5
1141 m.
CYCLE BOUNDARIES
SAMPLES
FACIES
INTERPRETATION
MOSCOVIAN
HARE FIORD
METRES
SLOPE/BASIN
250
200
150
100
50
0
CA
CA
CA
CS
CS
CS
CS
CS
CS
CS
CA
CS
CA
CS
CS
DO
CA CS
?
?
MS
WS
PS
GS
BS

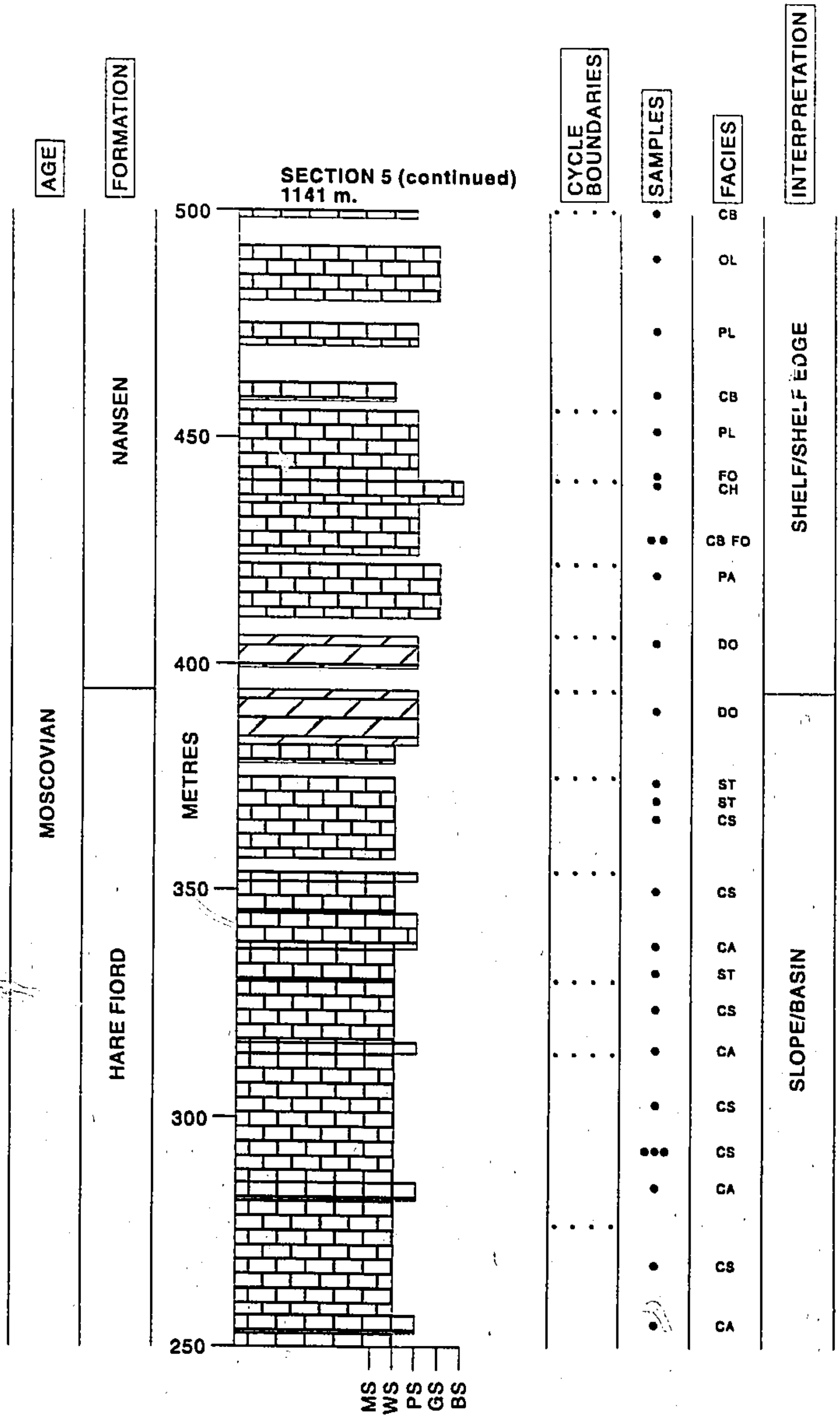
AGE
FORMATION
SECTION 5 (continued)
1141 m.
CYCLE BOUNDARIES
SAMPLES
FACIES
INTERPRETATION
MOSCOVIAN
NANSEN
HARE FIORD
METRES
500
450
400
350
300
250
CB
OL
PL
CB
PL
FO
CH
CB FO
PA
DO
DO
ST
ST
CS
CS
CA
ST
CS
CA
CS
CS
CA
CS
CA
SHELF/SHELF EDGE
SLOPE/BASIN
MS
WS
PS
GS
BS

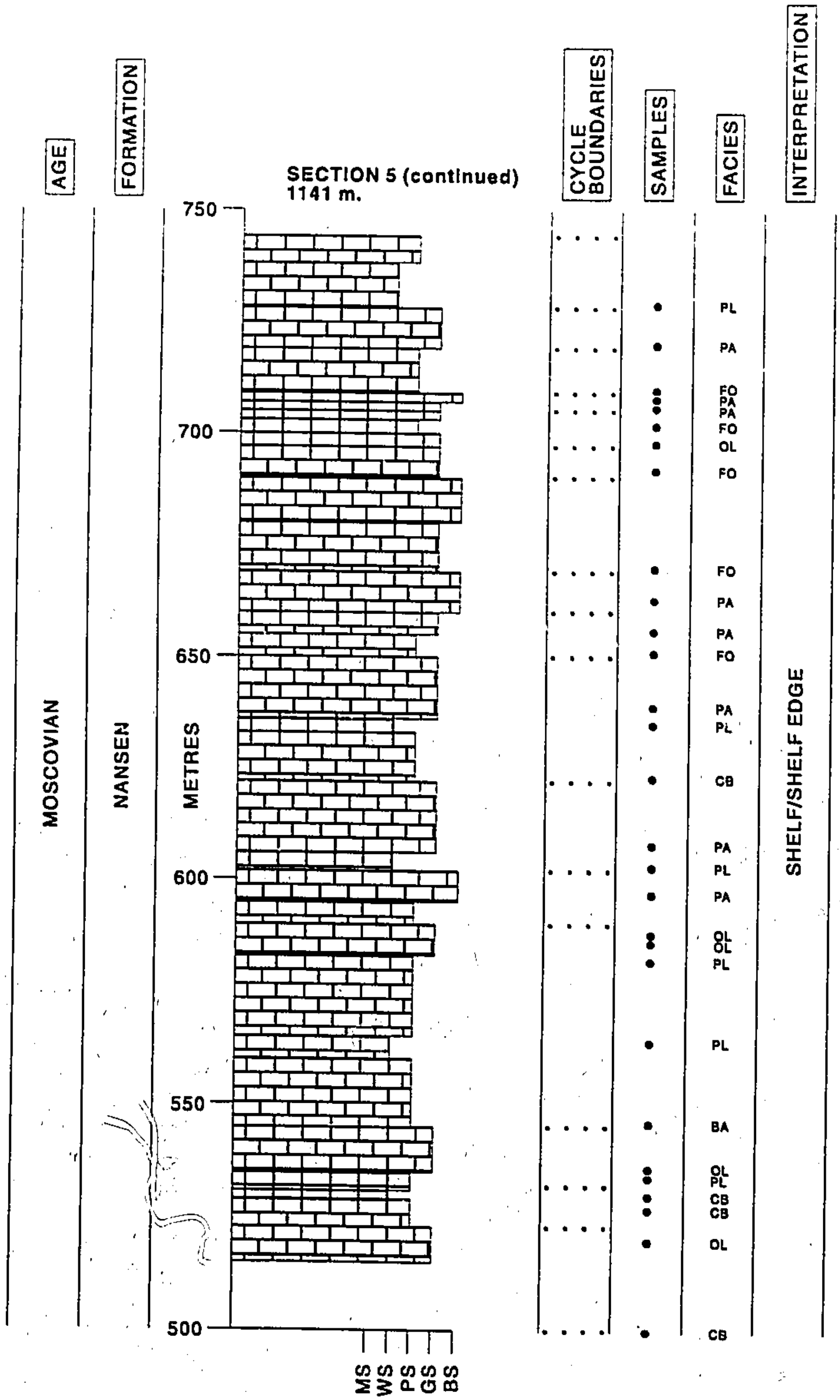
AGE
FORMATION
SECTION 5 (continued)
1141 m.
CYCLE BOUNDARIES
SAMPLES
FACIES
INTERPRETATION
MOSCOVIAN
NANSEN
METRES
750
700
650
600
550
500
MS
WS
PS
GS
BS
PL
PA
FO
PA
PA
FO
OL
FO
FO
PA
PA
FO
PA
PL
CB
PA
PL
PA
OL
OL
PL
PL
BA
OL
PL
CB
CB
OL
CB
SHELF/SHELF EDGE

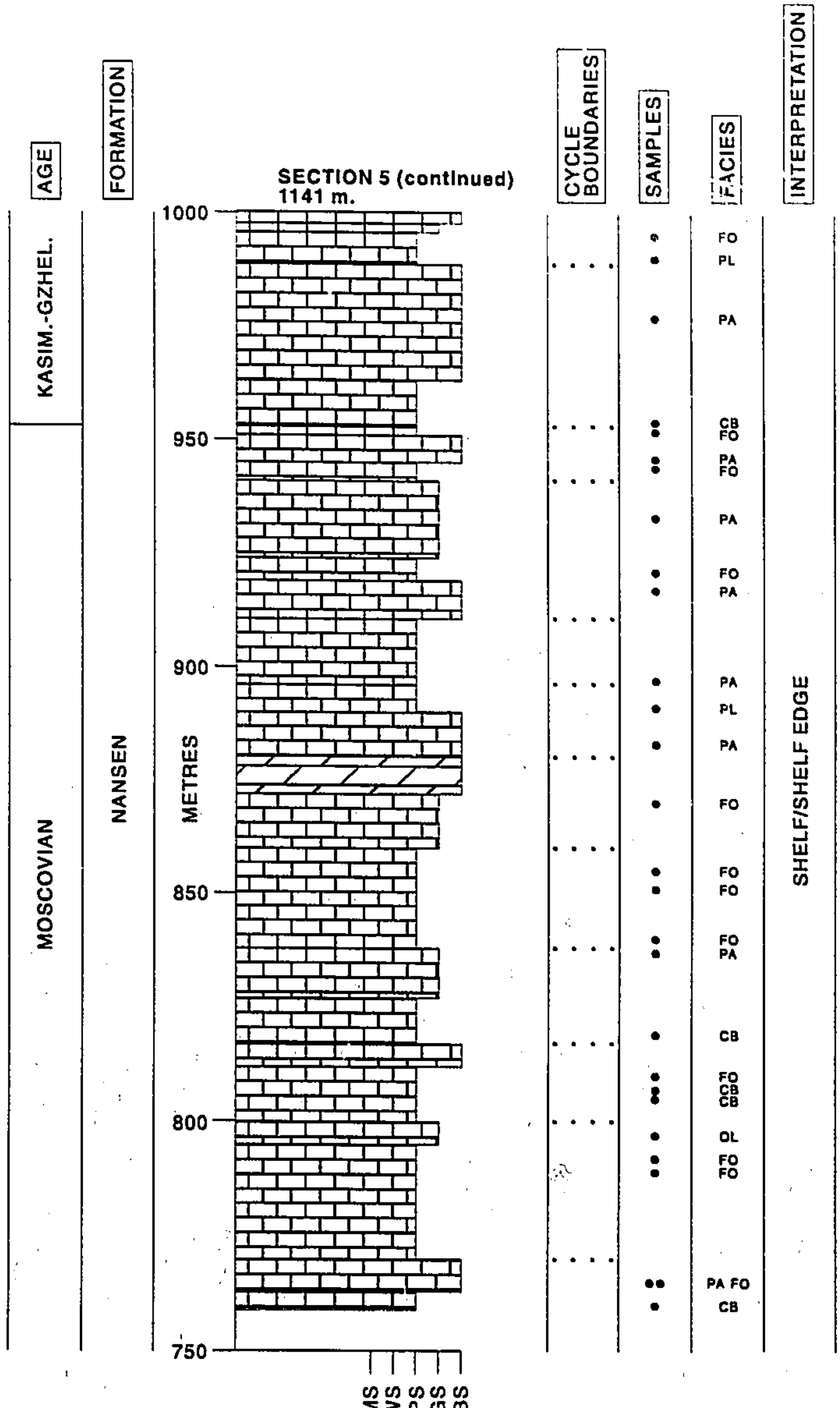

AGE
FORMATION
SECTION 5 (continued)
1141 m.
CYCLE BOUNDARIES
SAMPLES
FACIES
INTERPRETATION
KASIM.-GZHEL.
MOSCOVIAN
NANSEN
METRES
1000
950
900
850
800
750
FO
PL
PA
CB
FO
PA
FO
PA
FO
PA
PA
PL
PA
FO
FO
FO
FO
PA
CB
FO
CB
CB
OL
FO
FO
PA FO
CB
SHELF/SHELF EDGE
MS
WS
PS
GS
BS

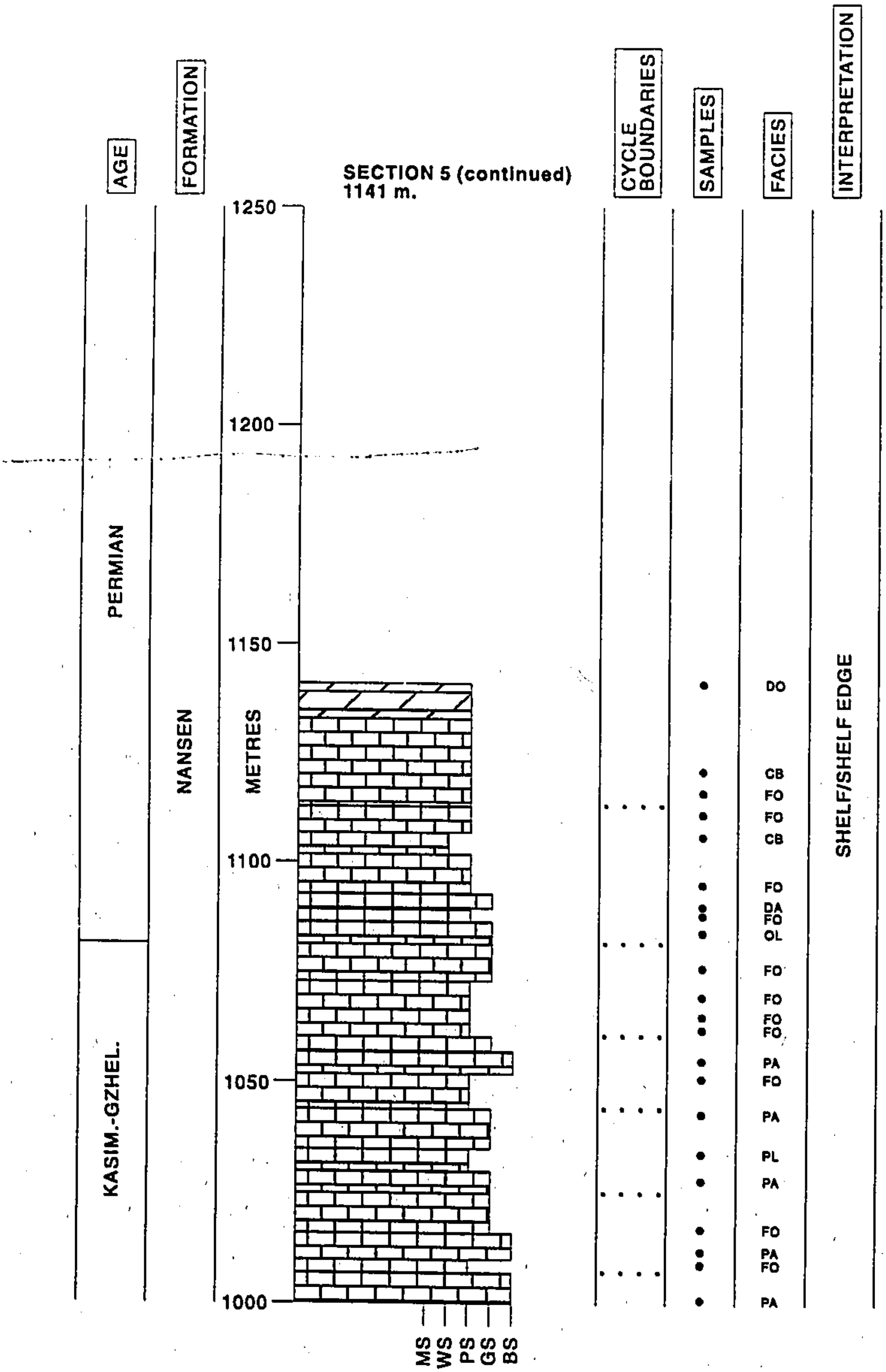
AGE
FORMATION
SECTION 5 (continued)
1141 m.
CYCLE BOUNDARIES
SAMPLES
FACIES
INTERPRETATION
1250
1200
1150
1100
1050
1000
METRES
PERMIAN
KASIM.-GZHEL.
NANSEN
DO
CB
FO
FO
CB
FO
DA
FO
OL
FO
FO
FO
FO
PA
FO
PA
PL
PA
FO
PA
FO
PA
SHELF/SHELF EDGE
MS
WS
PS
GS
BS

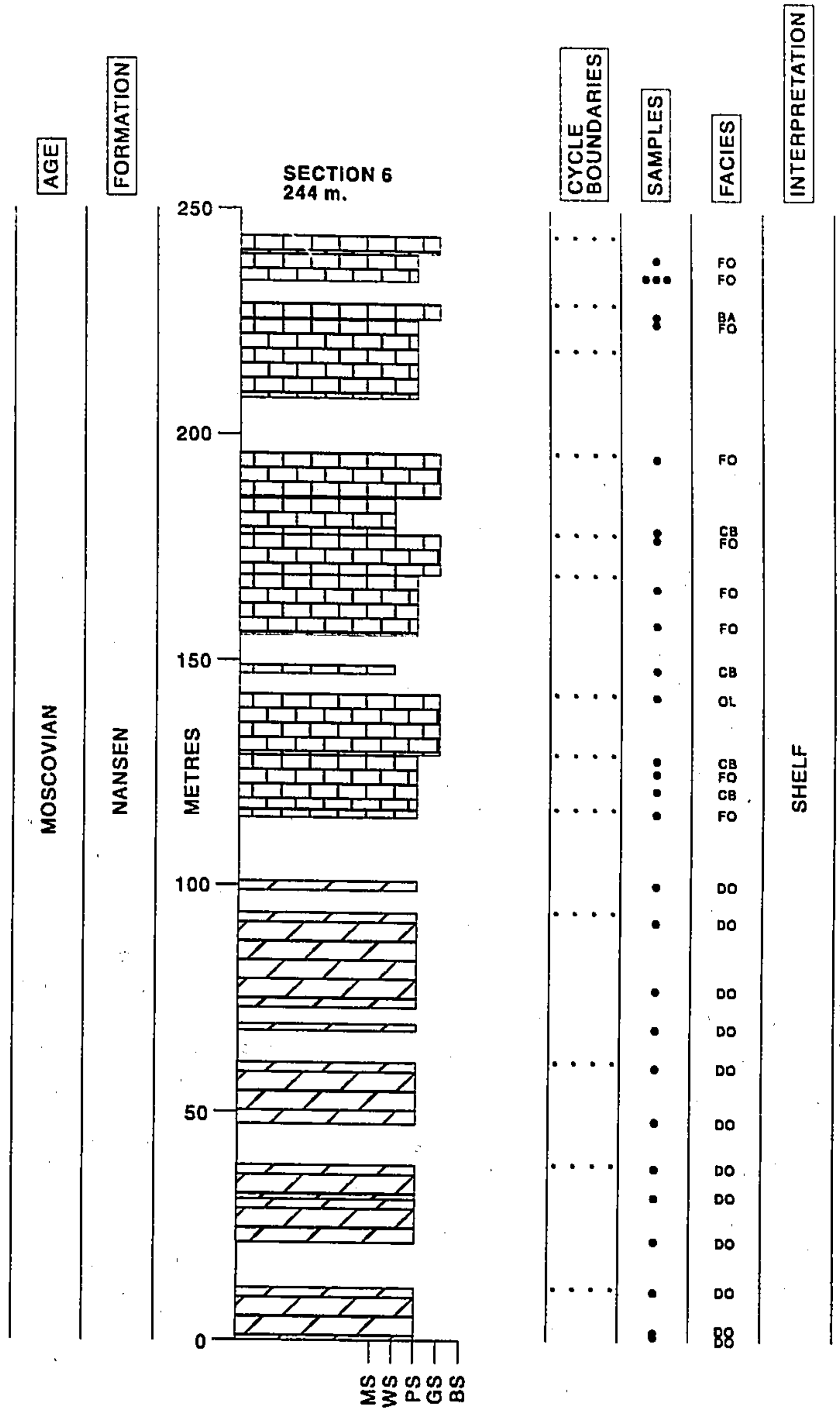
AGE
FORMATION
SECTION 6
244 m.
CYCLE BOUNDARIES
SAMPLES
FACIES
INTERPRETATION
MOSCOVIAN
NANSEN
METRES
SHELF
250
200
150
100
50
0
FO
FO
BA
FO
FO
CB
FO
FO
FO
CB
OL
CB
FO
CB
FO
DO
DO
DO
DO
DO
DO
DO
DO
DO
DO
DO
DO
MS
WS
PS
GS
BS

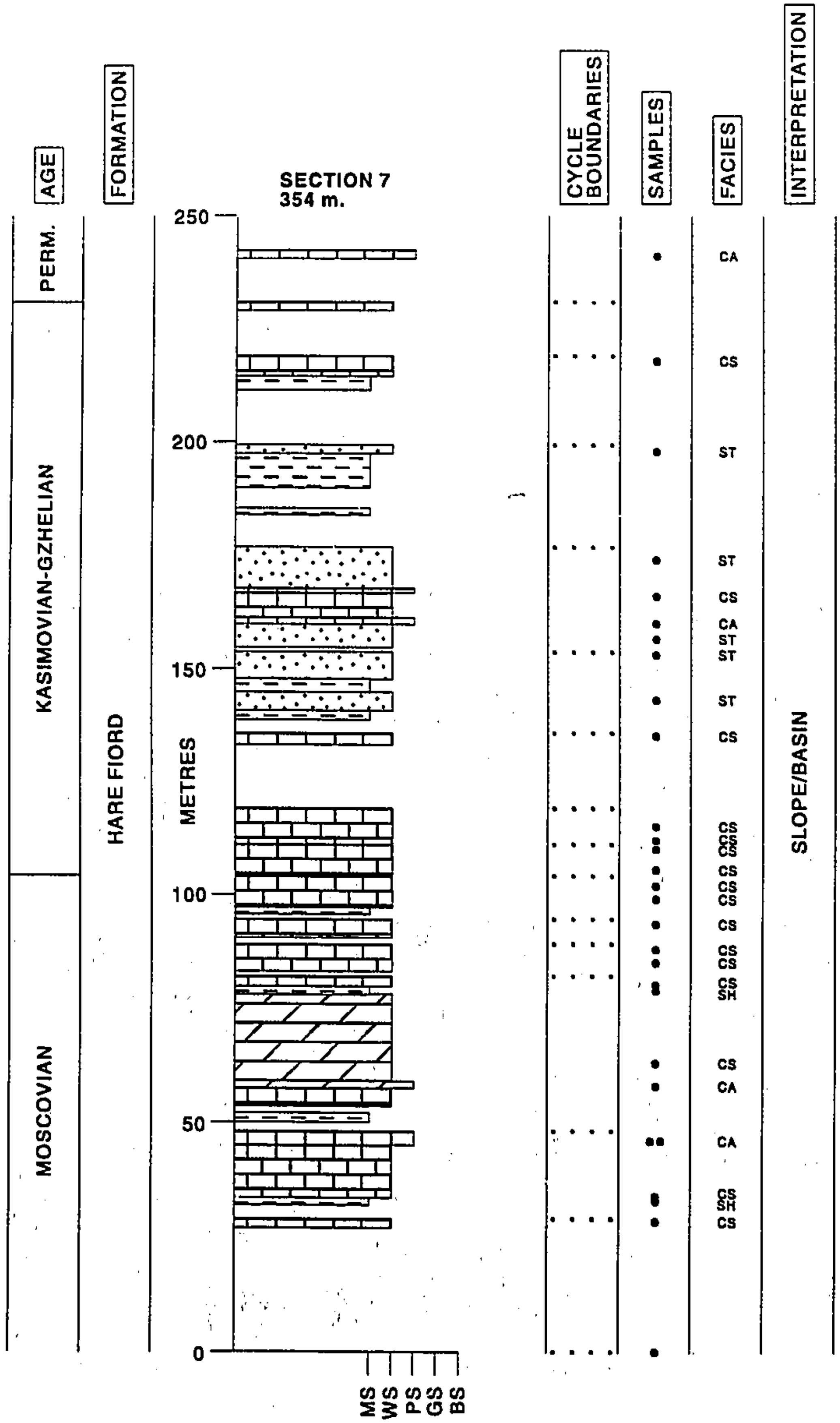
AGE
FORMATION
SECTION 7
354 m.
CYCLE BOUNDARIES
SAMPLES
FACIES
INTERPRETATION
PERM.
KASIMOVIAN-GZHELIAN
MOSCOVIAN
HARE FIORD
METRES
250
200
150
100
50
0
MS
WS
PS
GS
BS
CA
CS
ST
ST
CS
CA
ST
ST
ST
CS
CS
CS
CS
CS
CS
CS
CS
CS
CS
CS
SH
CS
CA
CA
CS
SH
CS
SLOPE/BASIN

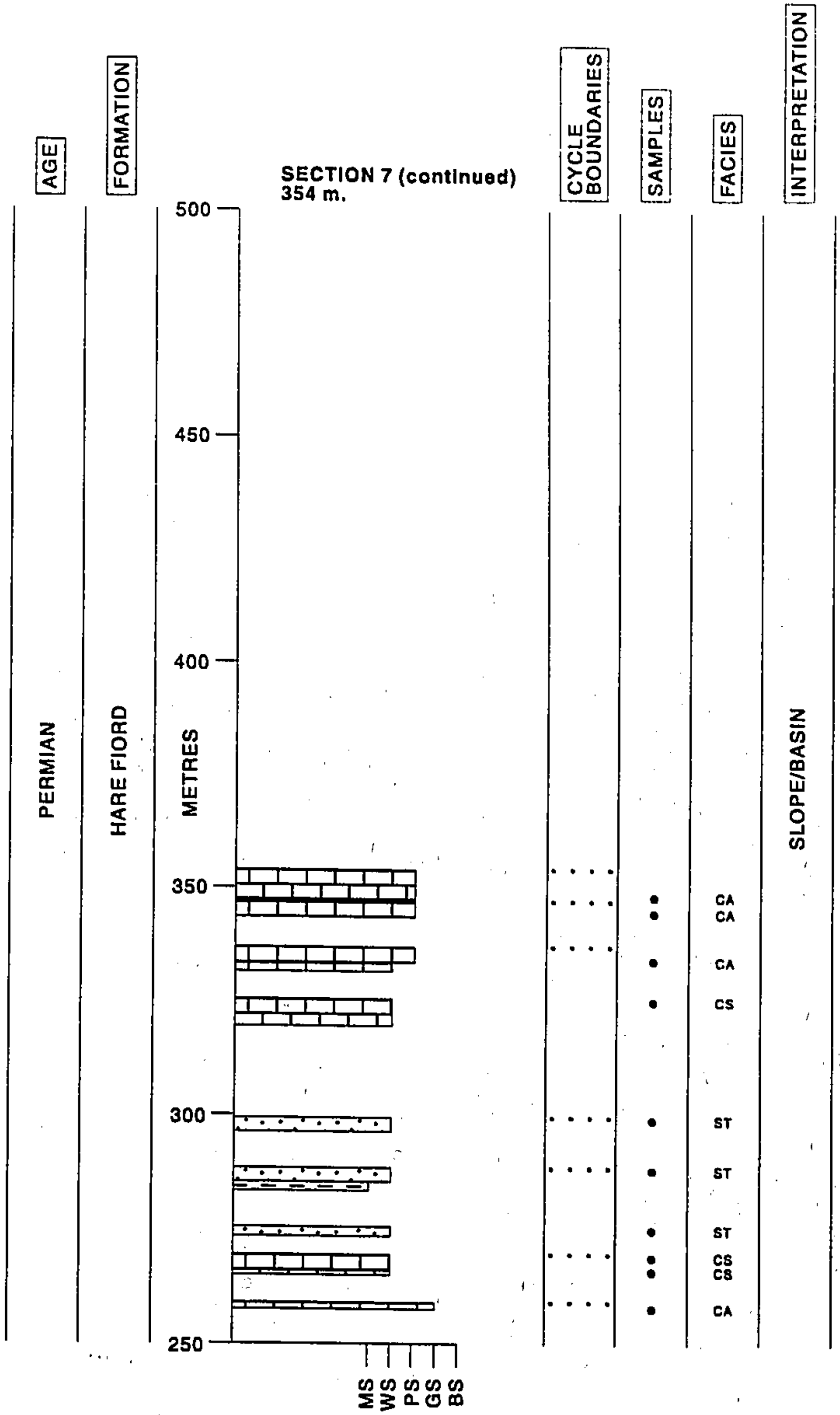
AGE
FORMATION
SECTION 7 (continued)
354 m.
CYCLE BOUNDARIES
SAMPLES
FACIES
INTERPRETATION
500
450
400
350
300
250
PERMIAN
HARE FIORD
METRES
SLOPE/BASIN
CA
CA
CA
CS
ST
ST
ST
CS
CS
CA
MS
WS
PS
GS
BS

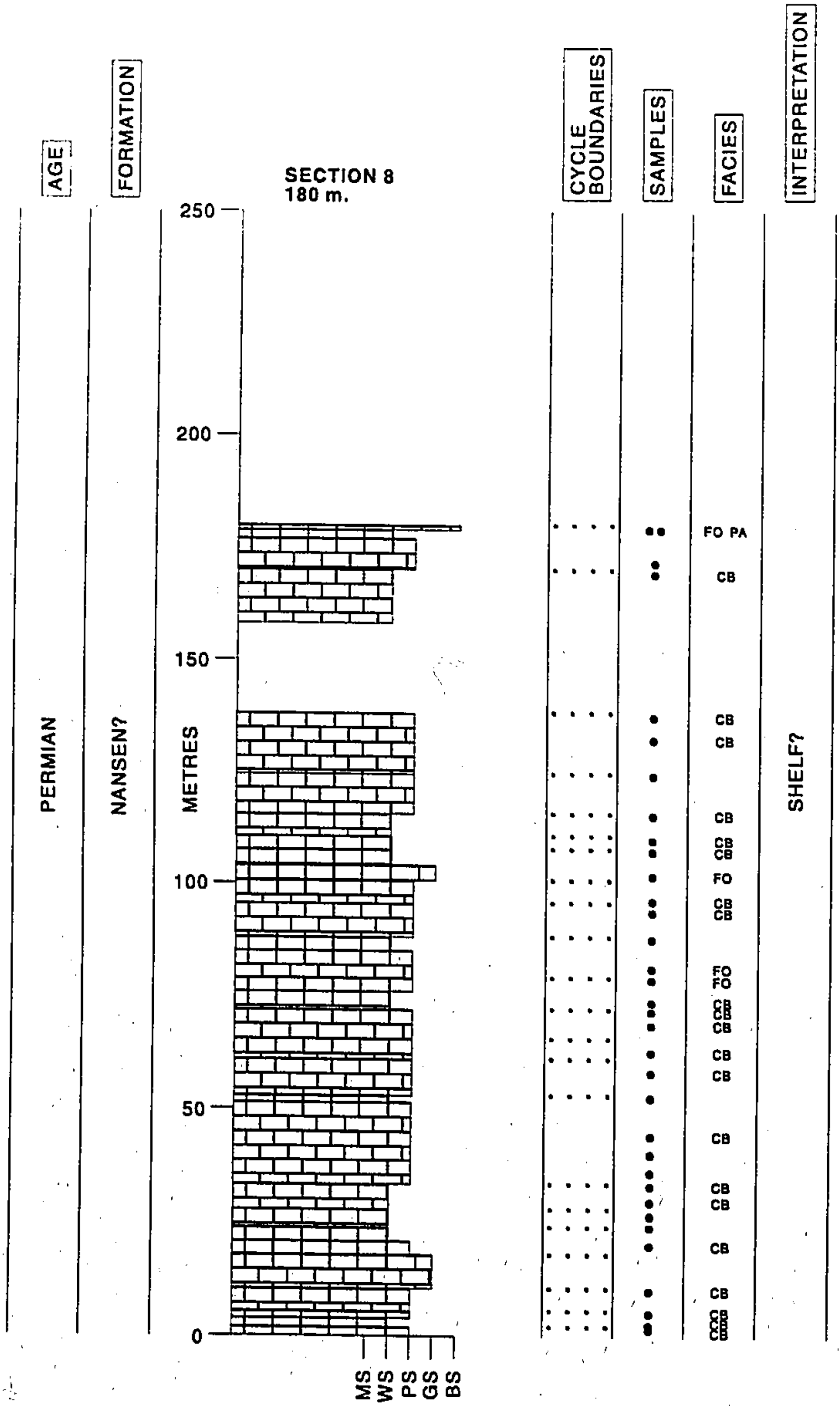
AGE
FORMATION
SECTION 8
180 m.
CYCLE BOUNDARIES
SAMPLES
FACIES
INTERPRETATION
250
200
150
100
50
0
PERMIAN
NANSEN?
METRES
SHELF?
FO PA
CB
CB
CB
CB
CB
CB
FO
CB
CB
FO
FO
CB
CB
CB
CB
CB
CB
CB
CB
CB
CB
CB
CB
CB
MS
WS
PS
GS
BS

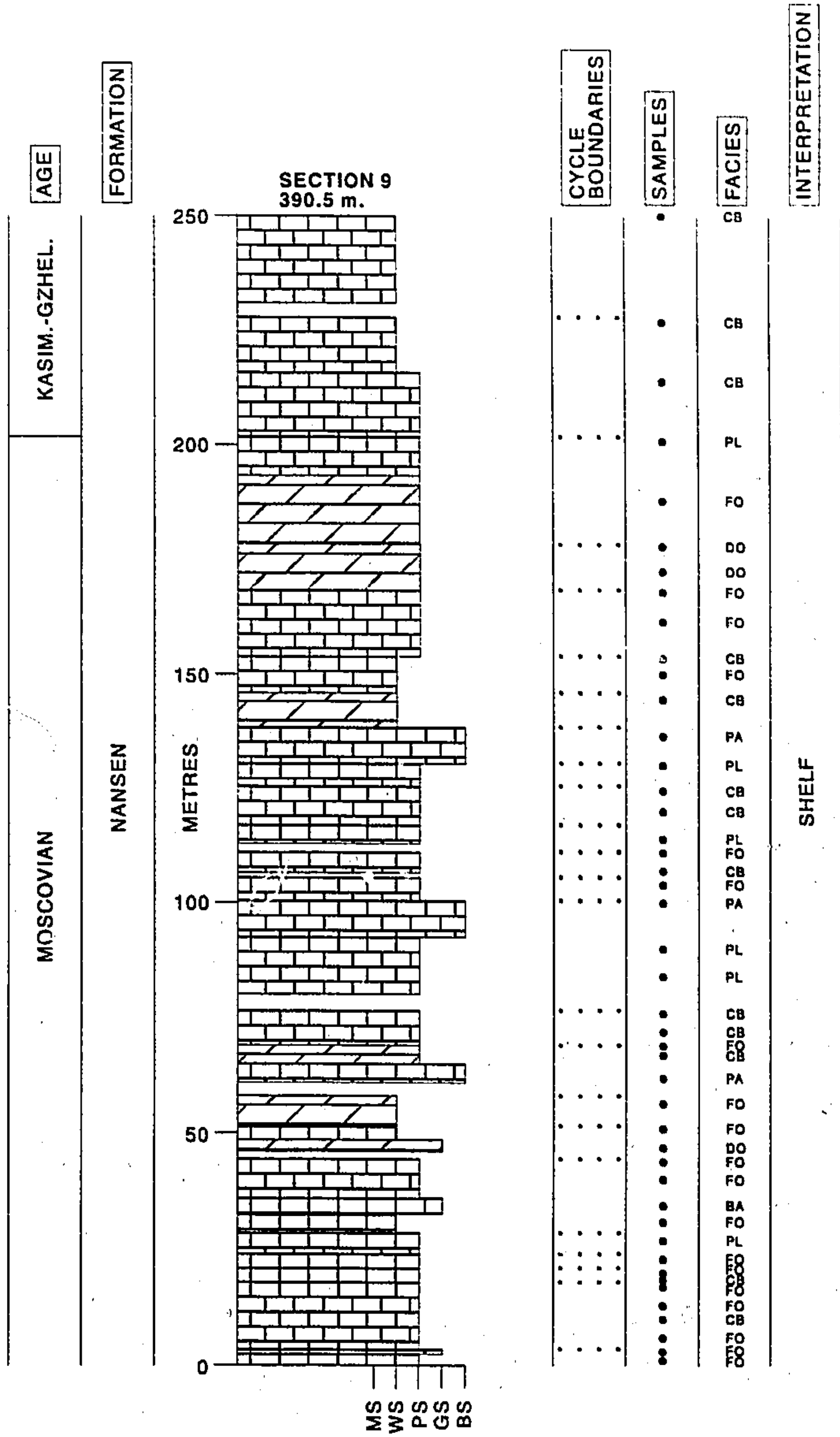
AGE
FORMATION
SECTION 9
390.5 m.
CYCLE BOUNDARIES
SAMPLES
FACIES
INTERPRETATION
KASIM.-GZHEL.
MOSCOVIAN
NANSEN
METRES
SHELF
250
200
150
100
50
0
MS
WS
PS
GS
BS

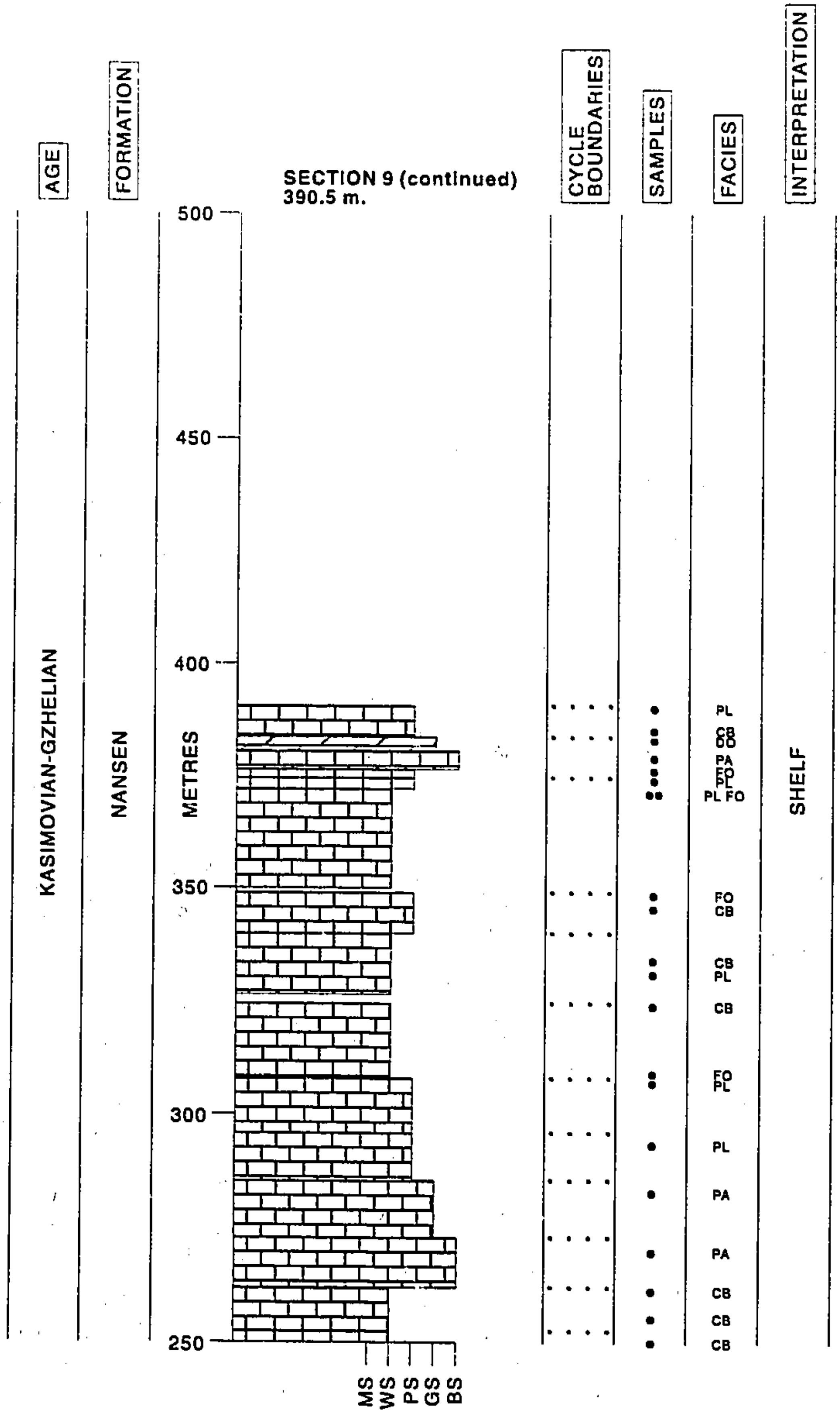

AGE
FORMATION
SECTION 9 (continued)
390.5 m.
CYCLE BOUNDARIES
SAMPLES
FACIES
INTERPRETATION
KASIMOVIAN-GZHELIAN
NANSEN
METRES
500
450
400
350
300
250
MS
WS
PS
GS
BS
PL
CB
OO
PA
FO
PL
PL FO
FO
CB
CB
PL
CB
FO
PL
PL
PA
PA
CB
CB
CB
SHELF

APPENDIX 3: ROCK SAMPLES

Location, stratigraphic level (above base of section), lithology (MS = mudstone; WS = wackestone; PS = packstone; GS = grainstone; BS = boundstone) and lithofacies of each hand sample (HS), thin section (TS), and/or polished slab (PS). Symbols for lithofacies are the same as in Appendix 2. Samples from sections 4 and 8 were not fully classified as they represent strata outside the realm of the current study.

SECTION 1

SAMPLE # Field #	(CTS-/C-) GSC #	LEVEL	LITH	FACIES	HS	TS	PS
01-01	240801	1.0 m	GS	BR	X	X	
01-02	240802	3.0 m	GS	BR	X	X	
01-03	240803	6.0 m	GS	OL	X	X	
01-04	240804	9.0 m	PS	CB	X		
01-05	240805	12.0 m	PS	DO	X		
01-06	240806	18.0 m	PS	CB	X		
01-07	240807	28.0 m	GS/BS	BR	X	X	
01-08	240808	29.0 m	PS	CB	X		
01-09	240809	36.0 m	PS	CB	X		
01-10	240810	41.0 m	PS	CB	X		
01-11	240811	58.0 m	GS	FO	X	X	
01-12	240812	63.0 m	GS	FO	X	X	
01-12	240813	63.0 m	cement		X		X
01-13	240814	67.0 m	GS/PS	DO	X	X	
01-14	240815	70.5 m	GS/PS	DO	X	X	
01-15	240816	76.0 m	GS/PS	DO	X	X	
01-16	240817	82.0 m	PS	DO	X		X
01-17	240818	90.0 m	GS/PS	DO	X	X	
01-18	240819	95.5 m	GS	FO	X	X	
01-19	240820	101.0 m	GS/PS	DO	X	X	
01-20	240821	104.0 m	PS/GS	DO	X	X	
01-21	240822	115.0 m	GS	FO	X	X	
01-22	240823	126.0 m	GS	FO	X	X	
01-23	240824	131.0 m	PS	PL	X	X	
01-24	240825	137.0 m	BS	PA	X		X
01-25	240826	152.0 m	PS/GS	DO	X	X	
01-26	240827	160.0 m	GS/PS	DO	X	X	
01-27	240828	170.0 m	PS/GS	DO	X	X	
01-28	240829	177.5 m	GS	DO	X	X	
01-29	240830	181.0 m	PS	FO	X	X	X
01-30	240831	190.5 m	PS	FO/BR	X	X	
01-31	240832	196.0 m	PS	FO	X	X	

01-32	240833	199.0 m	PS/GS	DO	X	X	
01-32A	240834	199.0 m	GS	PA/OL	X	X	
01-32B	240835	199.0 m	BS	PA	X		
01-33	240836	213.0 m	PS/GS	DO	X	X	
01-33A	240837	213.0 m	GS/BS	PA	X	X	
01-34	240838	227.5 m	BS	PA	X	X	
01-35	240839	243.0 m	PS	PL	X	X	
01-36	240840	273.0 m	GS	PA	X	X	
01-37	240841	278.0 m	GS	PA/DO	X	X	
01-38	240842	290.0 m	GS/BS	PA/OL	X	X	
01-39	240843	295.0 m	GS	PA	X	X	
01-40	240844	316.0 m	GS	FO/PA	X	X	
01-41	240845	322.0 m	PS	CB	X	X	
01-42	240846	330.0 m	PS/GS	PA	X		
01-43	240847	332.5 m	GS	PA	X	X	
01-44	240848	335.0 m	BS	PA	X		
01-45	240849	345.0 m	PS	CB	X		
01-46	240850	347.0 m	PS	DO	X	X	
01-47	240851	348.5 m	BS	PA	X		
01-48	240852	358.5 m	BS	PA	X	X	
01-49	240853	367.0 m	GS	FO	X	X	
01-50	240854	371.5 m	GS/BS	PA	X	X	
01-51	240855	379.5 m	BS/GS	PA	X	X	
01-52	240856	380.0 m	PS/GS	CB	X	X	
01-53	240857	380.2 m	PS	CB	X	X	
01-54	240858	390.0 m	PS/GS	PA/FO	X		
01-55	240859	405.5 m	PS/WS	PL	X		
01-56	240860	411.0 m	GS	PA	X	X	
01-57	240861	417.0 m	GS	PA	X	X	X
01-58	240862	423.0 m	BS	PA	X	X	X
01-59	240863	443.0 m	BS	PA	X	X	
01-60	240864	446.0 m	BS	PA	X	X	
01-61	240865	462.0 m	BS	PA	X	X	
01-62	240866	479.0 m	PS/GS	DO	X	X	
01-63	240867	501.0 m	GS	OL/FO	X	X	
01-64	240868	520.0 m	PS	CB	X		
01-65	240869	521.0 m	GS	FO/OL	X	X	X
01-66	240870	534.0 m	PS	FO	X	X	
01-67	240871	537.0 m	PS	CB	X	X	
01-68	240872	541.0 m	BS	PA	X	X	
01-69	240873	553.0 m	PS	CB	X		
01-70	240874	555.0 m	PS	CB/FO	X		
01-71	240875	563.0 m	PS	CB	X	X	
01-72	240876	568.0 m	PS	FO	X	X	
01-73	240877	572.0 m	GS	PL/FO	X	X	
01-74	240878	579.0 m	PS	FO	X		
01-75	240879	583.0 m	BS	PA	X		
01-76	240880	588.0 m	PS	CB	X	X	
01-77	240881	601.0 m	PS	CB/FO	X		
01-78	240882	608.0 m	BS	PA	X	X	
01-79	240883	614.0 m	PS	FO	X	X	
01-80	240884	625.0 m	PS	FO	X		
01-81	240885	627.0 m	PS	FO	X		
01-82	240886	647.0 m	PS	FO	X		

01-83	240887	651.0 m	BS	PA	X		
01-84	240888	657.0 m	PS	CB	X		
01-85	240889	660.0 m	GS/BS	PA	X	X	
01-86	240890	663.0 m	GS	FO/PA	X	X	X
01-87	240891	667.0 m	PS	CB	X	X	
01-88	240892	668.0 m	PS	CB	X	X	X
01-88	240893	668.0 m	PS	CB	X	X	
01-89	240894	674.0 m	PS	CB	X	X	
01-90	240895	678.0 m	PS	CB/FO	X	X	
01-91	240896	680.0 m	GS	PA	X		
01-92	240897	687.5 m	PS/GS	CB	X	X	
01-93	240898	698.5 m	PS	CB	X	X	
01-94	240899	703.0 m	PS/WS	PL/FO	X	X	
01-95	240900	707.0 m	PS/GS	FO	X		
01-96	240901	710.0 m	GS	DA	X	X	X
01-97A	240902	711.0 m	GS	PA	X	X	
01-97B	240903	711.0 m	GS/BS	PA	X	X	X
01-97C	240904	711.0 m	GS	PA	X	X	X
01-98	240905	721.0 m	PS/GS	FO	X		
01-99	240906	745.0 m	GS/BS	PA	X		
01-100	240907	752.0 m	GS	PA	X	X	
01-101	240908	772.0 m	GS	CB	X	X	
01-102	240909	778.5 m	PS	CB	X	X	
01-103	240910	783.0 m	GS	CB	X		
01-104	240911	789.0 m	GS	PA	X	X	
01-105	240912	794.0 m	GS	PL/FO	X	X	
01-106	240913	803.5 m	BS	DA	X	X	
01-107	240914	816.0 m	GS	FO	X		
01-108	240915	818.0 m	GS	PA	X	X	
01-109	240916	820.0 m	GS	PL	X	X	
01-110	240917	827.0 m	PS	CB	X		
01-111	240918	832.0 m	WS	PL	X	X	
01-112	240919	838.0 m	PS	CB/FO	X		
01-113	240920	839.6 m	PS	CB	X	X	
01-114	240921	840.0 m	PS	CB	X	X	
01-115	240922	843.0 m	PS	FO	X	X	
01 A-E	240923	talus	BS	PA	X		X
01 F-H	240924	talus	BS	PA	X		X
01 I	240925	talus	GS/BS	PA	X		
01 J	240926	talus	GS	PA	X		X
01 K-L	240927	talus	GS	PA	X		
01 M-O	240928	talus	PS	CB	X		
01 P-W	240929	talus	PS/BS	CB/FO/PA	X		
01 X	240930	talus	BS	PA	X		

SECTION 2

SAMPLE # Field #	(CTS-/C-) GSC #	LEVEL	LITH	FACIES	HS	TS	PS
02-01	240931	3.0 m	BS	BR	X	X	
02-02	240932	7.0 m	BS	BR	X	X	

02-03	240933	15.0 m	BS	PA	X	X	
02-04	240934	24.0 m	GS	DO	X	X	
02-05	240935	34.0 m	MS	SH	X		
02-06	240936	44.0 m	PS	BR	X	X	
02-07	240937	100.0 m	PS/GS	DO	X	X	
02-08	240938	117.0 m	PS	BR	X	X	
02-09	240939	131.0 m	PS/WS	DO	X	X	
02-10	240940	156.0 m	PS	DO	X	X	
02-11	240941	158.0 m	WS/MS	CS	X		
02-12	240942	165.0 m	WS/MS	CS	X		
02-13	240943	175.0 m	WS	CS	X	X	
02-14	240944	227.0 m	WS/PS	DO	X	X	
02-15	240945	232.0 m	PS	DO	X	X	
02-16	240946	289.0 m	WS	CS	X	X	
02-17	240947	314.0 m	WS/MS	CS	X	X	
02-18	240948	344.0 m	PS	CA	X	X	
02-19A	240949	347.0 m	PS	CA	X	X	
02-19B	240950	347.0 m	PS	CA	X	X	
02-20	240951	366.5 m	PS/WS	CA	X	X	
02-21	240952	368.0 m	WS	CS	X		
02-22	240953	373.0 m	WS	CS	X	X	
02-23	240954	379.0 m	WS	CS	X	X	
02-24	240955	391.0 m	WS	CS	X		
02-25	240956	395.0 m	WS	CS	X	X	X
02-26	240957	409.0 m	PS	CA	X	X	
02-27	240958	467.0 m	PS	CA	X		
02-28	240959	476.0 m	PS	CA	X	X	
02-29	240960	479.0 m	PS	CA	X		
02-30	240961	487.0 m	PS	CA	X	X	
02-31	240962	552.0 m	WS/MS	CS	X	X	
02-32	240963	602.0 m	GS	CA	X	X	
02-33	240964	627.0 m	PS	CA	X	X	
02-34	240965	632.0 m	WS	CS	X		
02-35	240966	647.0 m	GS	CA	X	X	
02-36	240967	678.0 m	WS	CS	X	X	
02-37	240968	697.0 m	WS	CS	X	X	
02 A	240969	talus	GS	BR	X		
02 B	240970	talus	GS/PS		X		X
02 C	240971	talus	WS	CS	X		

SECTION 3

SAMPLE # Field #	(CTS-/C-) GSC #	LEVEL	LITH	FACIES	HS	TS	PS
03-01	240972	50.0 m	WS	CS	X	X	
03-02	240973	72.0 m	WS	CS	X	X	
03-02A	240974	76.0 m	WS	CS	X	X	
03-03	240975	128.5 m	MS	SH	X		
03-04	240976	129.0 m	PS	CA	X	X	
03-05A	240977A	144.0 m	WS	CS	X	X	
03-05B	240977B	144.0 m	WS	CS	X	X	

03-05C	240977C	144.0 m	WS	CS	X	X	
03-06	240978	151.0 m	WS	CS	X	X	
03-07	240979	153.0 m	PS	CA	X	X	
03-08	240980	155.0 m	GS	CA	X	X	
03-09	240981	202.5 m	PS/GS	CA	X	X	
03-10	240982	228.0 m	PS	CA	X	X	X
03-11	240983	272.0 m	WS	ST	X	X	
03-12	240984	279.0 m	PS/GS	CA	X	X	
03-13	240985	282.0 m	PS	CA	X	X	X
03-14	240986	285.0 m	WS	ST	X	X	
03-15	240987	286.0 m	GS	CA	X	X	
03-16	240988	291.0 m	WS	CS	X	X	
03-17	240989	294.0 m	PS/GS	CA	X	X	X
03-17A	240989A	294.0 m	PS	CA	X	X	
03-18	240990	305.0 m	WS	ST	X	X	
03-19	240991	315.0 m	PS	CA	X	X	
03-20	240992	316.0 m	MS	SH/CS	X		
03-21	240993	326.0 m	MS	SH/CS	X		
03-22	240994	332.0 m	WS	ST	X	X	
03-23	240995	347.0 m	WS	ST	X	X	
03-24	240996	384.0 m	WS	ST	X	X	
03-25	240997	388.0 m	WS	CS	X		
03-26	240998	395.0 m	WS	ST	X	X	
03-27	240999	405.0 m	WS	ST	X	X	
03-28	241000	440.0 m	MS	SH	X		
03-29	241001	445.0 m	PS	CA	X	X	
03-30A,B	241002	456.0 m	GS	DE	X	X	
03-30C	241003	456.0 m	PS	DE	X	X	
03-31	241004	464.0 m	WS	CS	X	X	
03-32	241005	474.0 m	WS	CS	X	X	
03-33	241006	495.0 m	GS	CA	X	X	
03-34A	241007	516.0 m	MS	DE	X		
03-34B-D	241008	516.0 m	GS/PS	DE	X	X	X
03-34	241008A	516.0 m	PS	DE	X	X	
03-35	241009	522.0 m	PS	DE	X		
03-36	241010	533.0 m	PS	CA	X		X
03-36A	241010A	533.0 m	PS	CA	X	X	
03-37	241011	542.0 m	WS	CS	X	X	
03-38	241012	590.0 m	WS	CS	X	X	
03-39	241013	610.0 m	PS/GS	DE	X		
03-40	241014	617.0 m	PS	DE	X	X	
03-41	241015	628.0 m	WS	CS	X	X	
03-42	241016	643.0 m	PS	CA	X	X	
03-43	241017	660.0 m	PS/GS	CA	X		X
03-44	241018	680.0 m	WS	CS	X	X	
03 A-E,Z	241019	talus	PS/GS	CA	X		X
03 F	241020	talus	GS	CA	X		
03 G	241021	talus	GS/PS	CA	X		
03 H	241022	talus	PS	CA	X		
03 I	241023	talus	WS	CS	X		

SECTION 4

SAMPLE # Field #	(CTS-/C-) GSC #	LEVEL	LITH	FACIES	HS	TS	PS
04-01	241024	25.0 m	PS	CA	X	X	
04-02	241025	48.0 m	MS	SH	X		
04-03	241026	63.0 m	PS	CA	X	X	
04-04	241027	65.0 m	PS	CA	X		
04-05	241028	85.0 m	PS	CA	X		
04-06	241029	94.0 m	WS/MS	CS	X		
04-07	241030	99.0 m	PS	CA	X	X	
04-08	241031	103.0 m	PS/GS	CA	X		
04-09	241032	122.0 m	WS/MS	CS	X		
04-10	241033	266.0 m	GS	CB	X	X	
04-11	241034	138.5 m	PS	CA	X		
04-12	241035	140.0 m	WS	CS	X		
04-13	241036	142.0 m	PS	CA	X	X	
04-14	241037	145.0 m	PS	CA	X	X	
04-15	241038	184.0 m	WS/MS	CS	X		
04-16	241039	185.0 m	GS	CA	X	X	
04-17	241040	190.0 m	PS	CA	X	X	
04-18	241041	193.0 m	PS	CA	X	X	
04-19	241042	201.0 m	WS	CS	X	X	
04-19A	241043	222.0 m	PS	CA	X		
04-20	241044	229.0 m	WS	CS/CA	X	X	
04-21	241045	243.0 m	WS	CS	X		
04-22A	241046	264.0 m	MS	SH	X		
04-22	241047	266.0 m	GS	CB	X	X	
04-23	241048	316.0 m	GS	CB	X	X	
04-24	241049	369.0 m	PS	CB	X		
04-24A	241050	366.0 m	PS	CB	X		
04-25	241051	375.0 m	WS	CS	X	X	
04-26	241052	380.0 m	GS	CB	X	X	
04-27	241053	384.0 m.	WS	CS	X	X	
04-28	241054	395.0 m	WS	CS	X		
04-29	241055	413.0 m	PS	CB	X		
04-30	241056	417.0 m	GS	CB	X	X	
04-31	241057	425.0 m	PS	CB	X	X	
04-32	241058	454.0 m	GS	CB	X	X	
04-32A	241059	455.0 m	PS	CB	X		
04-33	241060	467.0 m	PS	CB	X		
04-34	241061	515.0 m	PS/WS	CB	X		
04-35	241062	539.0 m	PS	FO/CB	X		
04-36	241358	573.0 m	WS	CB	X		
04-37A	241063	602.0 m	PS	FO	X	X	
04-37B	241064	602.0 m	PS	CB/FO	X	X	
04-38	241065	602.5 m	PS	CB	X	X	
04-39	241066	608.0 m	PS	CB	X		
04-40	241067	613.0 m	GS	CB	X	X	

SECTION 5

SAMPLE # Field #	(CTS-/C-) GSC #	LEVEL	LITH	FACIES	HS	TS	PS
05-01	241068	45.0 m	PS/WS	CA/CS	X	X	
05-01A	241069	45.0 m	WS	DO/CS	X	X	
05-02	241070	47.0 m	WS/PS	DO	X	X	
05-03	241071	82.0 m	WS/MS	CS	X		
05-04	241072	88.0 m	WS	CS	X	X	
05-05	241073	99.0 m	PS/WS	CA	X	X	
05-06	241074	130.0 m	WS	CS	X		
05-07	241075	144.0 m	PS/WS	CA	X		
05-08	241076	145.5 m	WS	CS	X	X	
05-09	241077	150.0 m	WS	CS	X		
05-10	241078	157.5 m	WS	CS	X		
05-11	241079	159.5 m	WS	CS	X	X	
05-12	241080	186.0 m	WS	CS	X	X	
05-13	241081	195.0 m	WS	CS	X		
05-14	241082	205.0 m	WS	CS	X	X	
05-15	241083	219.0 m	WS/PS	CA/CS	X	X	
05-16	241084	227.0 m	PS	CA	X	X	
05-16A	241085	227.0 m	PS	CA	X		
05-17	241086	243.0 m	PS/GS	CA	X	X	
05-18	241087	255.0 m	PS/WS	CA	X	X	
05-19	241088	268.0 m	WS	CS	X	X	
05-20	241089	285.0 m	PS	CA	X	X	
05-21	241090	293.0 m	WS	CS/ST	X	X	X
05-21A	241091	293.0 m	MS/WS	CS/ST	X	X	X
05-21B	241092	293.0 m	WS/MS	CS/ST	X	X	X
05-22	241093	303.0 m	WS	CS	X	X	
05-23	241094	315.0 m	PS/WS	CA	X	X	
05-24	241095	324.0 m	WS/MS	CS	X	X	
05-25	241096	332.0 m	WS/MS	ST	X	X	
05-26	241097	338.0 m	PS	CA	X	X	
05-27	241098	350.0 m	WS	CS/ST	X		
05-28	241359	366.0 m	WS	CS	X	X	
05-29	241360	370.0 m	WS	ST	X	X	X
05-30	241099	374.0 m	WS	ST	X	X	
05-31	241100	390.0 m	PS	DO	X	X	
05-32	241101	405.0 m	PS/GS	DO	X	X	
05-33	241102	420.0 m	GS/PS	PA/FO	X	X	
05-34	241103	428.0 m	PS	CB	X		
05-34A	241104	428.0 m	PS	FO	X	X	
05-35	241105	440.0 m	BS	CH	X	X	
05-36	241106	442.0 m	PS	FO/PL	X	X	
05-37	241107	452.0 m	PS/WS	PL	X	X	
05-38	241108	460.0 m	WS/PS	CB	X		
05-39	241109	474.0 m	PS	PL/FO	X	X	
05-40	241110	490.0 m	GS	OL	X	X	
05-41	241111	500.0 m	PS	CB/FO	X	X	
05-42	241112	520.0 m	GS	OL	X	X	
05-43	241113	527.0 m	WS/PS	CB	X		

05-44	241114	530.0 m	WS	CB	X		
05-45	241115	534.0 m	PS/WS	PL	X	X	
05-46	241116	536.0 m	GS	OL	X	X	X
05-47	241117	546.0 m	PS	BA/FO	X	X	
05-48	241118	564.0 m	WS	PL	X		
05-49	241119	582.0 m	PS	PL	X	X	
05-50	241120	586.0 m	GS	OL	X	X	
05-51	241121	588.0 m	GS	OL/PA	X	X	
05-52	241122	597.0 m	BS	PA	X		
05-53	241123	603.0 m	WS	PL/FO	X		
05-54	241124	608.0 m	GS/BS	PA	X	X	
05-55	241125	623.0 m	PS	CB	X	X	
05-56	241126	635.0 m	WS	PL	X		
05-57	241127	639.0 m	GS	PA/FO	X	X	
05-58	241128	651.0 m	PS	FO	X		
05-59	241129	656.0 m	GS	PA	X	X	
05-60	241130	663.0 m	BS	PA	X	X	X
05-61	241131	670.0 m	GS	FO	X	X	
05-62	241132	692.0 m	GS	FO	X	X	
05-63	241133	698.0 m	GS	OL/PA	X	X	X
05-64	241134	702.0 m	PS	FO/PA	X	X	
05-65	241135	706.0 m	GS	PA	X	X	
05-65A	241136	708.0 m	BS	PA	X	X	
05-66	241137	710.0 m	PS	FO	X	X	
05-67	241138	720.0 m	GS	PA	X	X	
05-68	241139	729.0 m	WS	PL/FO		X	
05-69	241140	760.0 m	PS	CB	X	X	
05-70A	241141	765.0 m	BS/GS	PA	X	X	
05-70B	241142	765.0 m	PS	FO	X		
05-71	241143	789.0 m	PS/GS	FO	X	X	
05-72	241144	792.0 m	PS	FO	X	X	
05-73	241145	797.0 m	GS/PS	OL/FO	X		
05-74	241146	805.0 m	PS	CB	X	X	
05-75	241147	807.0 m	PS	CB	X	X	
05-76	241148	810.0 m	PS	FO	X	X	
05-77	241149	819.0 m	PS/WS	CB	X	X	
05-78	241150	837.0 m	GS	PA	X		
05-79	241151	840.0 m	PS	FO	X		
05-80	241152	851.0 m	PS	FO/CB	X		
05-81	241153	855.0 m	PS/WS	FO	X	X	
05-82	241154	870.0 m	GS	FO	X		
05-83	241155	883.0 m	BS	PA	X	X	
05-84	241156	891.0 m	PS	PL	X	X	
05-85	241157	897.0 m	PS/GS	PA/FO	X	X	
05-86	241158	917.0 m	BS	PA	X	X	
05-87	241159	921.0 m	PS	FO/CB	X	X	
05-88	241160	933.0 m	GS	PA	X	X	
05-89	241161	944.0 m	PS	FO	X	X	
05-90	241162	946.0 m	BS	PA	X		X
05-91	241163	952.0 m	PS	FO	X	X	
05-92	241164	954.0 m	PS	CB/FO	X	X	
05-93	241165	977.0 m	BS	PA	X	X	X
05-94	241166	990.0 m	PS	PL	X	X	
05-95	241167	995.0 m	PS/GS	FO	X		

05-96	241168	1001.0 m	BS	PA	X		
05-97	241169	1009.0 m	PS	FO	X	X	
05-98	241170	1012.0 m	BS	PA	X		
05-99	241171	1017.0 m	GS	FO	X	X	
05-100	241172	1028.0 m	GS	PA	X	X	
05-101	241173	1034.0 m	PS	PL	X	X	
05-102	241174	1043.0 m	GS	PA/FO	X		
05-103	241175	1051.0 m	PS	FO	X		
05-104	241176	1055.0 m	BS	PA	X		
05-105	241177	1062.0 m	PS/WS	FO/CB	X	X	
05-106	241178	1065.0 m	PS	FO	X	X	
05-107	241179	1069.5 m	PS	FO	X		
05-108	241180	1076.0 m	GS	FO/PA	X	X	
05-109	241181	1084.0 m	GS	OL	X	X	
05-110	241182	1088.0 m	PS/GS	FO	X		
05-111	241183	1090.0 m	GS	DA	X	X	
05-112	241184	1095.0 m	PS	FO	X	X	
05-113	241185	1106.0 m	WS	CB	X	X	
05-114	241186	1111.0 m	PS/GS	FO	X		
05-115	241187	1116.0 m	PS	FO/CB	X	X	
05-116	241188	1121.0 m	PS	CB	X		
05-117	241189	1141.0 m	PS	DO	X	X	
05 A	241190	talus	WS	CA/CS	X		

SECTION 6

SAMPLE # Field #	(CTS-/C-) GSC #	LEVEL	LITH	FACIES	HS	TS	PS
06-01	241191	1.0 m	PS	DO	X		
06-02	241192	1.5 m	PS	DO	X	X	
06-03	241193	11.0 m	PS/GS	DO	X	X	
06-04	241194	22.0 m	PS	DO	X	X	
06-05	241195	31.5 m	PS	DO	X	X	
06-06	241196	38.0 m	PS	DO	X	X	
06-07	241197	48.0 m	PS	DO	X	X	
06-08	241198	60.0 m	PS/WS	DO	X	X	
06-09	241199	68.5 m	PS/GS	DO	X	X	
06-10	241200	77.0 m	PS/WS	DO	X	X	
06-11	241201	92.0 m	PS/GS	DO	X	X	
06-12	241202	100.0 m	PS/GS	DO	X	X	
06-13	241203	116.0 m	PS	FO	X		
06-14	241204	121.0 m	PS/WS	CB	X	X	
06-15	241205	125.0 m	PS/GS	FO	X	X	
06-15A	241206	128.0 m	PS/WS	CB	X		
06-16	241207	142.0 m	GS	OL	X	X	
06-17	241208	148.0 m	WS/PS	CB	X	X	
06-18	241209	158.0 m	PS	FO	X	X	
06-19	241210	166.0 m	PS/GS	FO	X	X	
06-20	241211	177.0 m	GS	FO	X	X	
06-21	241212	179.0 m	WS/PS	CB	X	X	
06-22	241213	195.0 m	GS	FO	X	X	

06-23	241214	225.0 m	PS	FO	X	X	
06-24	241215	226.5 m	GS	BA	X	X	
06-25A	241216	235.0 m	GS	FO	X	X	X
06-25B	241217	235.0 m	GS	FO	X	X	
06-25C	241218	235.0 m	PS/GS	FO	X	X	
06-26	241219	239.0 m	GS	FO	X	X	

SECTION 7

SAMPLE # Field #	(CTS-/C-) GSC #	LEVEL	LITH	FACIES	HS	TS	PS
07-01	241220	0.0 m	WS		X	X	
07-02	241221	28.5m	WS/MS	CS	X	X	
07-03	241222	33.0 m	MS	SH	X		
07-04	241223	34.0 m	WS/MS	CS	X	X	
07-05	241224	46.0 m	PS	CA	X	X	
07-05A	241225	46.0 m	PS	CA	X	X	
07-06	241226	58.0 m	PS	CA	X	X	
07-07	241227	63.0 m	WS	CS	X	X	
07-08	241228	79.0 m	MS	SH	X		
07-09	241229	80.0 m	WS	CS	X		
07-10	241230	85.0 m	WS	CS	X	X	
07-11	241231	88.0 m	WS	CS	X		
07-12	241232	93.5 m	WS	CS	X	X	
07-13	241233	99.0 m	WS/MS	CS	X	X	
07-14	241234	102.0 m	WS/MS	CS	X	X	
07-15	241235	105.5 m	WS	CS	X	X	
07-16	241236	110.0 m	WS/MS	CS	X	X	
07-17	241237	112.0 m	WS	CS	X	X	
07-18	241238	115.0 m	WS	CS	X	X	
07-19	241239	135.0 m	WS	CS	X	X	
07-20	241240	143.0 m	WS	ST	X	X	
07-21	241241	153.0 m	WS	ST	X	X	
07-22	241242	156.5 m	WS	ST	X	X	
07-23	241243	160.0 m	PS	CA	X	X	
07-24	241244	166.0 m	WS	CS	X		
07-25	241245	174.0 m	WS	ST	X	X	
07-26	241246	198.0 m	WS	ST	X	X	X
07-27	241247	218.0 m	WS/PS	CS	X	X	
07-28	241248	241.0 m	PS	CA	X	X	
07-29	241249	258.0 m	GS	CA	X	X	
07-30	241250	266.0 m	WS	CS	X	X	
07-31	241251	269.0 m	WS/PS	CS	X	X	
07-32	241252	275.0 m	WS	ST	X	X	
07-33	241253	288.0 m	WS	ST	X	X	
07-34	241254	299.0 m	WS	ST	X	X	
07-35	241255	325.0 m	WS/MS	CS	X	X	
07-36	241256	334.0 m	PS	CA	X	X	
07-37	241257	344.5 m	PS	CA	X	X	
07-38	241258	348.0 m	PS	CA	X	X	

SECTION 8

SAMPLE # Field #	(CTS-/C-) GSC #	LEVEL	LITH	FACIES	HS	TS	PS
08-01	241259	1.5 m	PS	CB	X	X	
08-02	241260	2.5 m	WS	CB	X		
08-03	241261	5.0 m	PS/WS	CB	X		
08-04	241262	10.0 m	PS/WS	CB	X		
08-05	241263	20.0 m	PS	CB	X		
08-06	241264	24.0 m	WS		X		
08-07	241265	26.5 m	WS		X		
08-08	241266	29.5 m	WS	CB	X		
08-09	241267	33.0 m	WS	CB	X		
08-10	241268	36.0 m	PS		X		
08-11	241269	40.0 m	PS		X		
08-12	241270	44.0 m	PS	CB	X		
08-13	241271	52.5 m	WS		X		
08-14	241272	58.0 m	PS/WS	CB	X		
08-15	241273	62.5 m	PS	CB	X		
08-16	241274	68.5 m	PS	CB	X		
08-17	241275	71.5 m	PS/WS	CB	X		
08-18	241276	73.5 m	WS	CB	X		
08-19	241277	78.5 m	PS	FO	X		
08-20	241278	81.0 m	PS	FO	X	X	
08-21	241279	87.5 m	WS/MS		X		
08-22	241280	93.5 m	PS	CB	X		
08-23	241281	96.0 m	PS	CB	X		
08-24	241282	101.5 m	GS	FO	X		
08-25	241283	107.0 m	WS	CB	X		
08-26	241284	109.5 m	WS	CB	X		
08-27	241285	115.0 m	WS/PS	CB	X		
08-28	241286	124.0 m	PS		X		
08-29	241287	132.0 m	PS	CB	X		
08-30	241288	137.0 m	PS	CB	X		
08-31	241289	169.0 m	WS	CB	X		
08-32	241290	171.5 m	PS		X		
08-33	241291	179.0 m	WS	FO	X		
08-33A	241292	179.0 m	BS	PA	X	X	

SECTION 9

SAMPLE # Field #	(CTS-/C-) GSC #	LEVEL	LITH	FACIES	HS	TS	PS
09-01	241293	1.0 m	PS	FO	X	X	
09-02	241294	3.0 m	GS/PS	FO	X	X	
09-03	241295	6.0 m	PS/GS	FO	X	X	
09-04	241296	10.0 m	PS	CB	X	X	
09-05	241297	13.0 m	PS/WS	FO	X		
09-06	241298	17.0 m	PS	FO	X	X	
09-07	241299	18.5 m	PS	CB	X	X	

09-08	241300	20.0 m	PS	FO	X	X
09-09	241301	23.0 m	PS/GS	FO	X	X
09-10	241302	27.0 m	PS	PL	X	X
09-11	241303	31.0 m	WS/PS	FO	X	X
09-12	241304	34.5 m	GS	BA	X	X
09-13	241305	40.0 m	PS	FO	X	X
09-14	241306	44.0 m	PS	FO	X	X
09-15	241307	47.0 m	GS/PS	DO	X	X
09-16	241308	51.0 m	WS/PS	FO	X	X
09-17	241309	56.5 m	WS/PS	FO	X	X
09-18	241310	62.0 m	BS	PA	X	X
09-19	241311	67.0 m	PS	CB	X	X
09-20	241312	69.0 m	PS	FO	X	X
09-21	241313	72.0 m	PS	CB	X	X
09-22	241314	76.0 m	PS/WS	CB	X	X
09-23	241315	84.0 m	PS/WS	PL	X	X
09-24	241316	90.0 m	PS	PL	X	X
09-25	241317	100.0 m	BS	PA	X	
09-26	241318	104.0 m	PS/WS	FO	X	X
09-27	241319	107.0 m	PS	CB	X	X
09-28	241320	111.0 m	PS	FO	X	X
09-29	241321	114.0 m	PS	PL	X	X
09-30	241322	120.0 m	PS	CB	X	X
09-31	241323	124.5 m	PS	CB	X	X
09-32	241324	130.0 m	PS	PL	X	X
09-33	241325	136.5 m	BS	PA	X	
09-34	241326	144.5 m	WS	CB	X	X
09-35	241327	150.0 m	WS/PS	FO	X	X
09-36	241328	153.5 m	WS/PS	CB	X	X
09-37	241329	161.5 m	PS/WS	FO	X	X
09-38	241330	168.0 m	PS	FO	X	X
09-39	241331	172.5 m	PS/GS	DO	X	X
09-40	241332	178.0 m	PS/GS	DO	X	X
09-41	241333	188.0 m	PS	FO	X	X
09-42	241334	201.0 m	PS/WS	PL	X	X
09-43	241335	214.0 m	PS	CB	X	X
09-44	241336	227.0 m	WS	CB	X	X
09-45	241337	250.0 m	WS	CB	X	
09-46	241338	255.5 m	WS/PS	CB	X	X
09-47	241339	261.5 m	WS	CB	X	X
09-48	241340	270.0 m	BS	PA	X	X
09-49	241341	283.0 m	GS	PA	X	X
09-50	241342	293.5 m	PS	PL	X	X
09-51	241343	307.0 m	PS/WS	PL	X	X
09-52	241344	309.0 m	WS/PS	FO	X	X
09-53	241345	324.0 m	WS/PS	CB	X	X
09-54	241346	331.0 m	WS/PS	PL	X	X
09-55	241347	334.0 m	WS	CB	X	X
09-56	241348	345.5 m	PS	CB	X	X
09-57	241349	348.5 m	PS	FO	X	X
09-58	241350	371.0 m	WS	PL/FO	X	X
09-58A	241351	371.0 m	WS/PS	FO	X	X
09-59	241352	374.0 m	PS/WS	PL	X	X
09-60	241353	376.0 m	PS/WS	FO	X	X

09-61	241354	379.0 m	BS	PA	X	X
09-62	241355	383.0 m	GS/PS	DO	X	X
09-63	241356	385.0 m	PS/GS	CB	X	X
09-64	241357	390.0 m	PS/WS	PL	X	X

APPENDIX 4: FORAMINIFERAL DATA

Locality, stratigraphic level (above base of section), and age (E. = Early; L. = Late; Carb. = Carboniferous; Bashk. = Bashkirian; Mosc. = Moscovian; Kasim. = Kasimovian; Gzhel. = Gzhelian; Perm. = Permian; Assel. = Asselian; Sakmar. = Sakmarian) of samples containing identifiable small foraminifera and fusulinaceans. Small foraminiferal ages were determined by Dr. Sylvie Pinard. Fusulinacean ages were determined by Dr. Rui Lin. Both scientists are associated with the Institute of Sedimentary and Petroleum Geology (Geological Survey of Canada), Calgary, Alberta.

SECTION 1

SAMPLE # Field #	(CTS-/C-) GSC #	LEVEL	FORAM	FUSULINID
01-03	240803	6.0 m		E. Mosc.
01-11	240811	58.0 m	Mosc?	E. Mosc.
01-12	240812	63.0 m	Mosc?	?E. Mosc.
01-13	240814	67.0 m	Mosc?	
01-18	240819	95.5 m	Mosc.	L. Mosc.
01-21	240822	115.0 m	Mosc.	L. Mosc.
01-22	240823	126.0 m	L. Mosc.	L. Mosc.
01-23	240824	131.0 m	L. Mosc.	
01-29	240830	181.0 m	L. Mosc.	L. Mosc.
01-30	240831	190.5 m	L. Mosc.	L. Mosc.
01-31	240832	196.0 m	L. Mosc.	L. Mosc.
01-32	240833	199.0 m	L. Mosc.	
01-32A	240834	199.0 m	L. Mosc.	?L. Mosc.
01-33	240836	213.0 m	L. Mosc.	
01-33A	240837	213.0 m	L. Mosc.	
01-35	240839	243.0 m	L. Mosc.	
01-36	240840	273.0 m	L. Mosc.	L. Mosc.
01-38	240842	290.0 m		L. Mosc.
01-39	240843	295.0 m	L. Mosc.	L. Mosc.
01-40	240844	316.0 m	L. Mosc.	L. Mosc.
01-43	240847	332.5 m	L. Mosc.	L. Mosc.
01-46	240850	347.0 m	L. Mosc.	
01-48	240852	358.5 m	L. Mosc.	L. Mosc.
01-49	240853	367.0 m	L. Mosc.	L. Mosc.
01-50	240854	371.5 m	L. Mosc.	L. Mosc.
01-51	240855	379.5 m	L. Mosc.	L. Mosc.
01-52	240856	380.0 m	L. Mosc.	
01-53	240857	380.2 m	L. Mosc.	
01-56	240860	411.0 m	L. Mosc.	

01-57	240861	417.0 m	Mosc.	?L. Mosc.
01-58	240862	423.0 m	L. Mosc.	
01-59	240863	443.0 m	L. Mosc.	
01-60	240864	446.0 m	L. Mosc.	
01-61	240865	462.0 m	L. Mosc.	
01-63	240867	501.0 m	L. Mosc.	
01-65	240869	521.0 m	L. Mosc.	?L. Mosc.
01-66	240870	534.0 m	I. L. Mosc. (Myachkovian?)	?L. Mosc.
01-67	240871	537.0 m	L. Mosc.	?L. Mosc.
01-71	240875	563.0 m	L. Mosc.	?L. Mosc.
01-72	240876	568.0 m	L. Mosc.	?L. Mosc.
01-73	240877	572.0 m	L. Mosc.	
01-76	240880	588.0 m	L. Mosc?	
01-78	240882	608.0 m	L. Mosc.	
01-79	240883	614.0 m	L. Mosc.	?L. Mosc.
01-85	240889	660.0 m	L. Mosc? or younger (Kasim?)	
01-86	240890	663.0 m	L. Mosc. or Kasim.	?L. Mosc.
01-87	240891	667.0 m	Kasim.	
01-88	240892	668.0 m	Kasim?	
01-88	240893	668.0 m	Kasim.	
01-89	240894	674.0 m	Kasim.	
01-90	240895	678.0 m	Kasim.	
01-92	240897	687.5 m	Kasim.	
01-93	240898	698.5 m	Kasim.	
01-94	240899	703.0 m	Kasim.	
01-96	240901	710.0 m	Kasim.	
01-97B	240903	711.0 m	Kasim.	
01-97C	240904	711.0 m	Kasim.	
01-100	240907	752.0 m	Kasim.	?Kasim.
01-101	240908	772.0 m	Kasim. or younger	
01-102	240909	778.5 m	Kasim.	
01-104	240911	789.0 m	Kasim.	?Kasim.
01-105	240912	794.0 m	Kasim.	
01-106	240913	803.5 m	Kasim.	
01-108	240915	818.0 m	Kasim.	
01-109	240916	820.0 m	Kasim.	
01-111	240918	832.0 m	Kasim.	
01-113	240920	839.6 m	Kasim. or younger	
01-114	240921	840.0 m	Kasim? or Gzhel?	?Kasim.

SECTION 2

SAMPLE # Field #	(CTS-/C-) GSC #	LEVEL	FORAM	FUSULINID
02-03	240933	15.0 m	Mosc.	
02-13	240943	175.0 m	L. Mosc?	
02-26	240957	409.0 m	L. Mosc. or younger	
02-28	240959	476.0 m	L. Mosc. or younger	
02-33	240964	627.0 m	L. Mosc. or younger	

02-36	240967	678.0 m	Mosc?, Kasim? or younger
02-37	240968	697.0 m	Mosc? or younger

SECTION 3

SAMPLE # Field #	(CTS-/C-) GSC #	LEVEL	FORAM	FUSULINID
03-02A	240974	76.0 m	Carb.	
03-05B	240977B	144.0 m	Mosc? or older	
03-05C	240977C	144.0 m	Mosc. or younger?	
03-06	240978	151.0 m	Mosc?	
03-07	240979	153.0 m	Mosc.	
03-08	240980	155.0 m	Mosc.	
03-09	240981	202.5 m	L. Mosc.	
03-10	240982	228.0 m	Mosc.	
03-11	240983	272.0 m	Mosc.	
03-12	240984	279.0 m	Mosc.	
03-13	240985	282.0 m	L. Mosc.	
03-14	240986	285.0 m	L. Mosc.	
03-15	240987	286.0 m	L. Mosc.	
03-17	240989	294.0 m	L. Mosc.	
03-32	241005	474.0 m	Kasim. or younger (Gzhel?)	
03-33	241006	495.0 m	Kasim. or younger	
03-34B-D	241008	516.0 m	Kasim. or younger	
03-36	241010	533.0 m	Kasim. or younger	
03-42	241016	643.0 m	Kasim. or younger	

SECTION 4

SAMPLE # Field #	(CTS-/C-) GSC #	LEVEL	FORAM	FUSULINID
04-01	241024	25.0 m	Mosc. or younger	
04-03	241026	63.0 m	Mosc. or younger	
04-07	241030	99.0 m	Gzhel. or younger (Assel?)	
04-10	241033	136.0 m	Kasim. - Sakmar.	
04-13	241036	142.0 m	Assel? or Sakmar?	
04-14 to 04-40	241037 to 241067	145.0 m to 613.0 m	Assel? to Sakmar.	

SECTION 5

SAMPLE # (CTS-/C-) Field #	GSC #	LEVEL	FORAM	FUSULINID
05-05	241073	99.0 m		E. Mosc.
05-15	241083	219.0 m	Mosc? or older?	
05-20	241089	285.0 m		E. Mosc.
05-26	241097	338.0 m		E. Mosc.
05-33	241102	420.0 m		E. Mosc.
05-34A	241104	428.0 m	L? Mosc. (Podolian?)	L. Mosc.
05-39	241109	474.0 m		L. Mosc.
05-45	241115	534.0 m		L. Mosc.
05-47	241117	546.0 m		L. Mosc.
05-69	241140	760.0 m		L. Mosc.
05-71	241143	789.0 m		L. Mosc.
05-81	241153	855.0 m		L. Mosc.
05-85	241157	897.0 m		L. Mosc.
05-97	241169	1009.0 m		?Kasim. to ?Gzhel.
05-106	241178	1065.0 m		?Kasim. to ?Gzhel.
05-108	241180	1076.0 m	Gzhel. or younger (Assel.)	
05-111	241183	1090.0 m		Assel.
05-115	241187	1116.0 m		Assel.

SECTION 6

SAMPLE # (CTS-/C-) Field #	GSC #	LEVEL	FORAM	FUSULINID
06-14	241204	121.0 m	L. Bashk. or E. Mosc.	
06-15	241205	125.0 m	E. Mosc.	
06-16	241207	142.0 m	E. Mosc.	
06-17	241208	148.0 m	E. Mosc.	
06-18	241209	158.0 m	E. Mosc.	
06-19	241210	166.0 m		
	to		Mosc.	
06-26	241219	239.0 m		

SECTION 7

SAMPLE # (CTS-/C-) Field #	GSC #	LEVEL	FORAM	FUSULINID
07-01	241220	0.0 m	?L. Mosc.	
07-02	241221	28.5m	Mosc.	
07-07	241227	63.0 m	Mosc.	
07-15	241235	105.5 m	Kasim? or younger (Perm.)	

07-29	241249	258.0 m	Gzhel. to Sakmar.	Assel.
07-37	241257	344.5 m		?Assel.
07-38	241258	348.0 m	Perm. (Sakmar?)	

SECTION 8

SAMPLE # Field #	(CTS-/C-) GSC #	LEVEL	FORAM	FUSULINID
08-01	241259	1.5 m	Kasim. or younger	
08-20	241278	81.0 m	Assel?	

SECTION 9

SAMPLE # Field #	(CTS-/C-) GSC #	LEVEL	FORAM	FUSULINID
09-01	241293	1.0 m	L. Mosc. (Podolian?)	
09-02	241294	3.0 m	Mosc.	L. Mosc.
09-03	241295	6.0 m	Mosc.	L. Mosc.
09-04	241296	10.0 m	Mosc.	
09-06	241298	17.0 m	Mosc.	L. Mosc.
09-07	241299	18.5 m	Mosc.	
09-08	241300	20.0 m	Mosc.	
09-09	241301	23.0 m	Mosc.	
09-10	241302	27.0 m	Mosc.	
09-11	241303	31.0 m	Mosc.	
09-12	241304	34.5 m	Mosc.	
09-13	241305	40.0 m	Mosc.	
09-14	241306	44.0 m	Mosc.	
09-15	241307	47.0 m	Mosc.	
09-16	241308	51.0 m	Mosc.	L. Mosc.
09-17	241309	56.5 m	Mosc.	
09-18	241310	62.0 m	Mosc.	
09-19	241311	67.0 m	Mosc.	
09-20	241312	69.0 m	Mosc.	
09-21	241313	72.0 m	Mosc.	
09-22	241314	76.0 m	Mosc.	
09-23	241315	84.0 m	Mosc.	
09-24	241316	90.0 m	Mosc.	
09-26	241318	104.0 m	Mosc.	
09-27	241319	107.0 m	Mosc.	L. Mosc.
09-28	241320	111.0 m	Mosc.	L. Mosc.
09-29	241321	114.0 m	Mosc.	
09-30	241322	120.0 m	Mosc.	
09-31	241323	124.5 m	Mosc.	
09-38	241330	168.0 m		L. Mosc.
09-43	241335	214.0 m	Kasim?	
09-46	241338	255.5 m	Kasim. or younger (Gzhel. to Perm.)	

09-51	241343	307.0 m	Kasim? or younger
09-56	241348	345.5 m	Kasim. or younger
09-58	241350	371.0 m	Gzhel. or younger

APPENDIX 5: CONODONT SAMPLES

Locality and stratigraphic level (above base of section) of samples collected to be processed for conodont identification. Conodont zones and ages to be determined by Dr. Charles Henderson at the University of Calgary, Calgary, Alberta.

SECTION 1

Sample # (C-)	Level
241367	0.0-1.0 m
241368	272.0-274.0 m
241369	379.0-380.0 m
241370	380.0-381.0 m
241371	667.0-668.0 m
241372	668.5-670.0 m
241373	838.0-839.5 m
241374	839.5-841.0 m

SECTION 2

Sample # (C-)	Level
241375	1.0-3.0 m
241376	221.0-223.0 m
241377	449.0-451.0 m
241378	697.0-699.0 m
241379	751.0-753.0 m
241380	762.0-764.0 m

SECTION 3

Sample # (C-)	Level
241381	49.0-51.0 m
241382	201.0-203.0 m
241383	325.0-326.0 m
241384	691.0-693.0 m

SECTION 4

Sample # (C-)	Level
241385	24.0-26.0 m
241386	143.0-145.0 m
241387	146.0-147.0 m
241388	388.0-390.0 m
241389	600.0-602.0 m

SECTION 5

none collected

SECTION 6

Sample # (C-)	Level
241390	0.0-2.0 m
241391	220.0-222.0 m

SECTION 7

Sample # (C-)	Level
241392	0.0 m
241393	166.0-167.0 m
241394	344.0-345.0 m

SECTION 8

Sample # (C-)	Level
241395	0.0-2.0 m
241396	178.5-180.0 m

SECTION 9

Sample # (C-)	Level
241397	0.0-1.5 m
241398	150.0-151.0 m
241399	308.0-309.0 m
241400	389.0-390.5 m